

We greatly value the careful reading and the detailed comments provided by the referees. The responses to the comments of the referees in our direct reply (shown below) and within the revised manuscript (see marked copy) are provided below. The pages and lines indicated below correspond to those in the marked copy.

Response to Referee 1 (Referees' comments are italicized)

1. Referee comment: *“Many experimental details and clarifications are needed to explain and justify this new technique. The discussion of the contribution of these organic acid contributions to WSOC and the many figures that detail organic acid mixing ratios should be pared down, since the species identification here are speculative, and there may be many interferences that have not been adequately considered.”*

Author response: We agree that the assignment of some of the organic acids, with the exception of formic and acetic acids, are speculative. As such, we have revised the manuscript to be more circumspect about the organic acid contribution to WSOC_g. Please refer to our response to comment 7.

We have also added more experimental details and discussions on interferences in the revised manuscript. Please refer to our responses to comments on experimental details and interferences below.

2. Referee comment: *“Previous reports have noted that SF₆⁻ is a viable reagent ion only for dewpoints below -20 C. The flow tube is at lower pressure here, and that is said to minimize interferences with water vapor (line 167). This needs to be explained much more thoroughly. The very high dilution with dry nitrogen likely does much more to reduce the water vapor interferences, but this is never discussed. This high dilution must reduce sensitivity. Please discuss the trade-off between reduced sensitivity and increased selectivity. Does the high dilution compromise time response, since there is a very small flow of ambient air into the flow tube? Does the large flow of N₂ through the ion source increase reagent ion signal?”*

Author response: The referee is correct in stating that there are tradeoffs between reduced sensitivity and increased selectivity when the sampled air is diluted by a large volume of N₂/SF₆ in the CIMS flow tube. The high flow (3.7 slpm) of N₂/SF₆ passed through the ion source increased the SF₆⁻ reagent ion signal. This does increase sensitivity but the N₂ flow also dilutes the sampled air flow in the flow tube which reduces the sensitivity. We chose these conditions to bring the water interferences to an acceptable level. We don't see significant differences in the time response for sample air flow flows $\geq 2 \text{ L min}^{-1}$ introduced into the flow tube because a large flow (7 L min^{-1}) is maintained in the sample inlet right up to the CIMS flow tube (Fig. 1). As requested, we have added more discussion on the tradeoffs between reduced sensitivity and increased selectivity when the sampled air is diluted by a large volume of N₂ in the CIMS flow tube and how the high dilution impacts time response in the revised manuscript:

Page 13 line 389: **“The 0.3 L min⁻¹ sampled air flow is diluted by 3.7 slpm of N₂/SF₆ flow in the flow tube. The ratio of the sampled air flow to the N₂/SF₆ flow introduced into the flow tube is approximately 1:13. While the high N₂/SF₆ flow (3.7 slpm) passed through the radioactive source into the flow tube increased the SF₆⁻ reagent ion signal, the high dilution**

of the sampled air flow in the flow tube reduced the CIMS instrument sensitivity by decreasing the number density of the analytes.”

3. Referee comment: “The flows as shown don’t make sense, and volume flow and mass flow don’t appear to be correctly distinguished. Accurately describing and discussing the flows is critical, since it is the altered gas flows that have made SF₆- viable in a humid environment. Line 154 gives the sampled air flow as a volume flow, but the orifice is said to maintain a constant mass flow. A 220 l/min scroll pump is used to pump a very small flow of 4 L/min through the flow tube, as shown in Figure 1. I suspect that the N₂ flow should be written as 3.7 slpm, rather than L/min. But even that doesn’t make sense, since it would be ~300 L/min volume flow, and greater than the pump speed. The instrument is said to be similar to Liao et al 2011, but the flows are very different, and these should be discussed completely.”

Author response: The referee is correct in pointing out that our previously stated flows and pump rates were incorrect. A 367 L min⁻¹ scroll pump (Edward nXDS 20i) was used. The N₂/SF₆ flow was 3.7 slpm. These corrections have been made to the revised manuscript:

Page 6 line 166: “The CIMS instrument was comprised of a series of differentially pumped regions: a flow tube, a collisional dissociation chamber, an octopole ion guide, a quadrupole mass filter and an ion detector. These sections were evacuated by a scroll pump (Edward nXDS 20i), a drag pump (Adixen MDP 5011) and two turbo pumps (Varian Turbo-V301), respectively. Ambient air was drawn continuously into the flow tube. A flow of 3.7 slpm of N₂ containing a few ppm of SF₆ (Scott-Marrin Inc.) was passed through a ²¹⁰Po ion source into the flow tube. SF₆⁻ anions, which were produced via associative electron attachment in the ²¹⁰Po ion source, reacted with the sampled ambient air in the flow tube to generate analyte ions.”

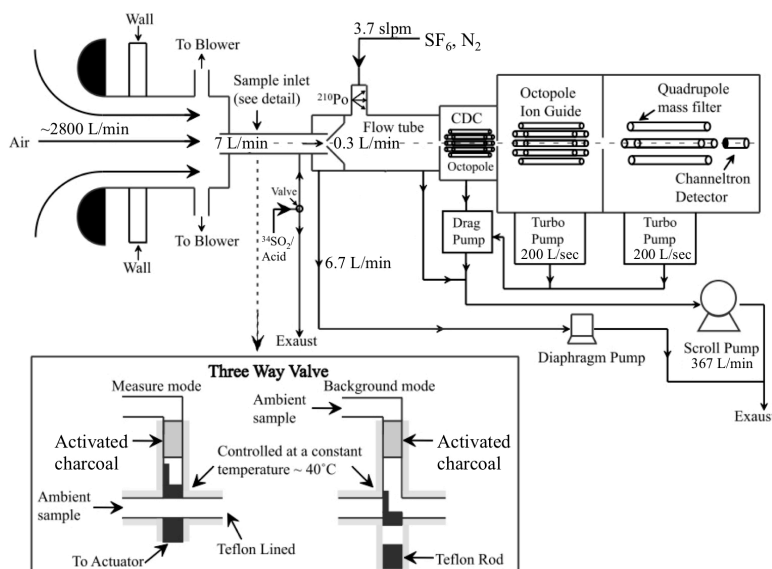


Figure 1: The CIMS instrument and inlet configuration used in the field study. The automated three-way sampling valve is shown in the inset. The figure was adapted from Liao et al. (2011).

4. Referee comment: “Please state and demonstrate time response, and preferably show a

calibration and a zero. Detection limits are given for 2.5 min. I don't understand the relation between the 2.5 min back- ground and the 0.04 s duty cycle for each mass (line 946). Please describe the measurement frequency - how often is a measurement made? I'm confused as to whether these are 0.04 s measurements, 2.5 min measurements, or 1 hr measurements (as used in the figures). And please be specific about the integration time for the mixing ratios. For example, are the range of mixing ratios in the abstract (line 22) for 1 hr averages?"

Author response: The dwell time for each m/z ion was set to 0.5 s and measurements of these ions were obtained every ~13 s. These measurements were averaged to generate 1-hour averaged mixing ratios of the various gases. Mixing ratios presented in this paper are the 1-hour averaged mixing ratios. We have added details on the frequency of measurements and stated explicitly that the data reported are 1-hour averages in the revised manuscript:

Page 7 line 192: "Ions monitored during the field study included m/z 45, 59, 65, 73, 75, 79, 82, 87, 89, 101, 102, 103, 108, 117, 131 and 148. The assignment of these ions will be discussed in section 3. The dwell time for each m/z ion was set to 0.5 s and measurements of these ions were obtained every ~13 s, which resulted in a ~4 % (= 0.5/13 x 100 %) duty cycle for each ion monitored. The data presented in this paper was averaged to 1-hour intervals unless stated otherwise."

The author is correct in stating that the range of mixing ratios reported in the abstract are the 1-hour averaged values. This is clarified in the revised manuscript:

Page 1 line 21: "1-hour averaged ambient concentrations of organic acids ranged from a few parts per trillion by volume (ppt) to several parts per billion by volume (ppb)."

Each background measurement period lasted ~4 min. However, ion signals for the different organic acids took up to 1.5 min to stabilize during the switch between ambient, calibration and background measurements during the field study. Hence, ion signals obtained during the first 1.5 min were not included in the calculation of the average and standard deviation of ion signals measured during background mode. This resulted in a 2.5 min (= 4 min – 1.5 min) integration time period for background measurements. The duty cycle (0.04 or 4 %) was calculated from the dwell time of each m/z ion monitored (0.5 s) and the measurement frequency (13 s). We clarified how detection limits were calculated from the background measurements in the revised manuscript:

Page 9 line 257: "The detection limits of the organic acids were estimated as 3 times the standard deviation values (3σ) of the ion signals measured during background mode. Although each background measurement period lasted ~4 min, ion signals of the different organic acids took up to 1.5 min to stabilize during the switch between ambient, calibration and background measurements during the field study. Thus, ion signals measured during the first 1.5 min were not included in the calculation of the average and standard deviation of ion signals measured during background mode. Table 1 summarizes the average detection limits of the organic acids for 2.5 min averaging periods which corresponds to the length of a background measurement with a 4 % duty cycle for each m/z."

As requested, we have added a section discussing the CIMS instrument time response and a figure showing a calibration and background measurement in the revised manuscript:

Page 14 line 426: "3.1.3. Background and calibration measurements"

Figure S4 shows an example of the CIMS instrument response during the switch between background, calibration and ambient measurements of formic and acetic acids during the field study. The 13 s time resolution data was used to determine the CIMS instrument time response. Formic (m/z 45, 65 and 108) and acetic (m/z 79) acid ion signals took ~ 1.5 min to reach a steady state after switches between ambient, calibration and background measurements (Figs. S4a and S4c).

The decays in the formic and acetic acid ion signals and times required for them to reach steady state after the removal of calibration gases during the switch from standard addition calibration to ambient sampling were used to determine the CIMS response time. The signal decays were fitted using double exponential functions. For formic acid, the m/z 45, 65 and 108 ion signals decayed to $1/e^2$ in 37 ± 2 , 33 ± 2 and 32 ± 2 s, respectively (Fig. S4b). For acetic acid, the m/z 79 ion signal decayed to $1/e^2$ in 42 ± 2 s (Fig. S4d)."

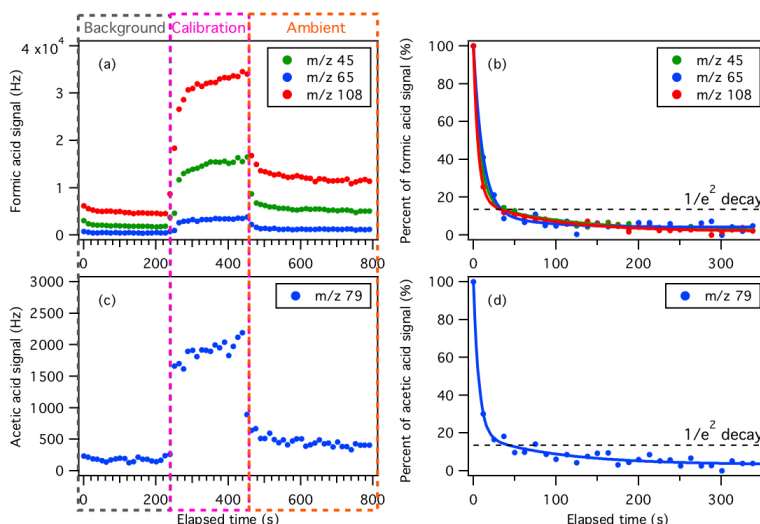


Figure S4: Example of the CIMS instrument response during switches between background, calibration and ambient measurements of (a) formic, and (c) acetic acids. Panels (b) and (d) show the percent of formic and acetic acid ion signals after the removal of a 6.75 ppb of formic acid and 5.87 ppb of acetic acid standard addition calibration as a function of time. All the data shown here are 13 s time resolution data. Double exponential fits to each m/z ion are shown as colored solid lines. Black dashed lines show the times for the ions to decay to $1/e^2$.

5. Referee comment: “Detection limits and abundances in the figures are written in ppb, but for most cases, ppt would be a more appropriate unit and much easier to read.”

Author response: We have made the requested changes in the revised manuscript.

6. Referee comment: “Giving sensitivities relative to $34SO_2$ is confusing and seems unnecessary, especially since that is a different ion-molecule reaction than all the organic acid reactions studied here and it has a water dependence. Providing absolute sensitivities will be much more useful for anyone who wants to compare this ion chemistry with others. And please discuss how these sensitivities compare to other techniques.”

Author response: As requested, we have provided the absolute sensitivities of organic acids and discussed how these sensitivities compare with other CIMS techniques in the revised manuscript:

Page 12 line 363: “Table 1 shows a summary of the sensitivities of X⁻ and X⁻•HF ions of organic acids. The average sensitivities of the HCOO⁻ (m/z 45) and HCOO⁻•HF (m/z 65) ions of formic acid were 1.29 ± 0.22 and 0.29 ± 0.05 Hz ppt⁻¹, respectively, while the average sensitivities of the CH₃COO⁻ (m/z 59) and CH₃COO⁻•HF (m/z 79) ions of acetic acid were 1.46 ± 0.29 and 0.30 ± 0.06 Hz ppt⁻¹, respectively. A weak ²¹⁰Po ion source (< 1 mCi) was used by SF₆-CIMS instrument during the field study, hence these sensitivities will be substantially higher if a stronger radioactive source is used. Nevertheless, these sensitivities are compared to formic and acetic acid sensitivities measured by a high-resolution time-of-flight chemical ionization mass spectrometer (Aerodyne Research Inc.) that utilized I⁻ reagent ions during the field study. Although the formic acid sensitivity measured by I-CIMS (1.33 ± 0.28 Hz ppt⁻¹) was comparable to that measured by SF₆-CIMS, the acetic acid sensitivity measured by I-CIMS (< 0.1 Hz ppt⁻¹) was substantially lower than that measured by SF₆-CIMS. Previous studies have similarly reported low acetic acid sensitivity measured by I-CIMS (Aljawhary et al., 2013; Lee et al., 2014).”

References:

Aljawhary, D., Lee, A. K. Y., and Abbatt, J. P. D.: High-resolution chemical ionization mass spectrometry (ToF-CIMS): application to study SOA composition and processing, *Atmospheric Measurement Techniques*, 6, 3211-3224, 10.5194/amt-6-3211-2013, 2013.

Lee, B. H., Lopez-Hilfiker, F. D., Mohr, C., Kurten, T., Worsnop, D. R., and Thornton, J. A.: An Iodide-Adduct High-Resolution Time-of-Flight Chemical-Ionization Mass Spectrometer: Application to Atmospheric Inorganic and Organic Compounds, *Environmental Science & Technology*, 48, 6309-6317, 10.1021/es500362a, 2014.

Table 1: Summary of organic acids of interest, their detection limits and sensitivities of their X⁻ and X⁻•HF ions^a

Organic Acid	Detection limit (ppt) ^b	Sensitivity (Hz ppt ⁻¹)	
		X ⁻	X ⁻ •HF
Formic acid	30	1.29 ± 0.22	0.29 ± 0.05
Acetic acid	60	1.46 ± 0.29	0.30 ± 0.06
Oxalic acid	1	6.38 ± 0.32	0.97 ± 0.05
Butyric acid	30	0.41 ± 0.01	0.12 ± 0.004
Glycolic acid	2	5.53 ± 0.11	1.64 ± 0.03
Propionic acid	6	2.05 ± 0.02	1.26 ± 0.01
Valeric acid	10	0.76 ± 0.008	0.35 ± 0.004

^aOnly organic acids with calibration measurements are shown.

^bDetection limits are approximated from 3 times the standard deviation values (3σ) of the ion signals measured during background mode. Shown here are the average detection limits of the organic acids for 2.5 min averaging periods which corresponds to the length of a background measurement at a 4 % duty cycle for each mass.

7. Referee comment: “Please discuss the many possible interferences to the organic acids listed.

The discussion of calibrations for many compounds was valuable, but then compounds for which calibrations weren't successful (pyruvic, for example) were dismissed. It appears arbitrary to ignore compounds if the calibration didn't work. Those other compounds almost certainly contribute to the signals and make the calculations of WSOC fraction extremely unreliable. For example, the signals at oxalic likely are dominated by or include contributions from lactic acid (both mass 90), butyric includes contributions from pyruvic (both mass 88), propionic includes contributions from glyoxylic acid (both mass 74). The authors correctly note that the mass assignments are speculative. It is OK to speculate, but from then on it would be appropriate to report mixing ratios only as upper limits for that compound and then forego calculations that rely on quantifying abundance. The sensitivities of the reported compounds span a wide range (over an order of magnitude). Thus, if the signal at one of the reported masses comes instead from an isomer with a much higher or lower sensitivity, the organic acid abundance would be drastically over or under estimated. There needs to be considerably more work to justify the WSOC contributions."

Author response: The comparison of the total carbon contributed by the organic acids to the WSOC_g serves as a zeroth order check that the assignment of ion peaks to the different organic acids are plausible. We agree that the assignment of some ion peaks are speculative, hence we are more circumspect in our discussion of the carbon mass fraction of WSOC_g comprised of organic acids in the revised manuscript:

Page 19 line 573: "To estimate the fraction of WSOC_g that is comprised of organic acids, the total organic carbon contributed by formic, acetic, oxalic, butyric, glycolic, propionic and valeric acids is compared to the WSOC_g measurements. We emphasize that the ion peak assignment of some of these organic acids are speculative. Hence, this comparison primarily serves as a zeroth order check to determine if the peak assignments are plausible. Figures 6a and 6b show the time series and diurnal profiles of WSOC_g and the organic carbon contributed by the measured organic acids. Formic and acetic acids comprised majority of the total organic carbon contributed by the measured organic acids (study averages of 31 and 38 %, respectively). Assuming that the ion peak assignments are correct and the measured organic acids are completely water-soluble, the carbon mass fraction of WSOC_g comprised of these organic acids ranged from 7 to 100 %."

Figure 6: (a) Time series of WSOC_g and the total organic carbon contributed by the measured organic acids. All the data are displayed as 1-hour averages. (b) Diurnal profiles of WSOC_g and the total organic carbon contributed by the measured organic acids. Also shown are the diurnal profiles of the organic carbon contributed by the individual measured organic acids. All the concentrations represent the mean hourly averages and the standard errors are plotted as error bars. (c) Scatter plot of total organic carbon contributed by the measured organic acids with WSOC_g. Note that the ion peak assignment to some of these organic acids are speculative.

8. Referee comment: "I don't understand the count rates and normalization shown in figures 6-8. How do the count rates get to be small fractions of 1 Hz? Please use a unit that is more accurate and describe how the values are determined."

Author response: The data for malonic, succinic and glutaric acids are presented as the ratio of their ion signals (Hz) to the instrument's sensitivity to F₂³⁴SO₂ (Hz ppb⁻¹) since these organic acids

were not calibrated. The ion signals of these organic acids are 1 to 2 orders of magnitude smaller than the sensitivity of the $F_2^{34}SO_2^-$ ion (study-averaged sensitivity = 2928 ± 669 Hz ppb⁻¹), resulting in these ratios to be less than 1. We have changed the units in the figures and stated more explicitly how these values were obtained in the revised manuscript:

Page 18 line 551: “The time series of ion signals (Hz) of malonic, succinic and glutaric acids normalized to the instrument’s sensitivity to $F_2^{34}SO_2$ (Hz ppb⁻¹) are shown in Fig. S3. The ion signals of these organic acids are 1 to 2 orders of magnitude smaller than the sensitivity of the $F_2^{34}SO_2^-$ ion (study-averaged sensitivity = 2928 ± 669 Hz ppb⁻¹), resulting in these ratios to be less than 1.”

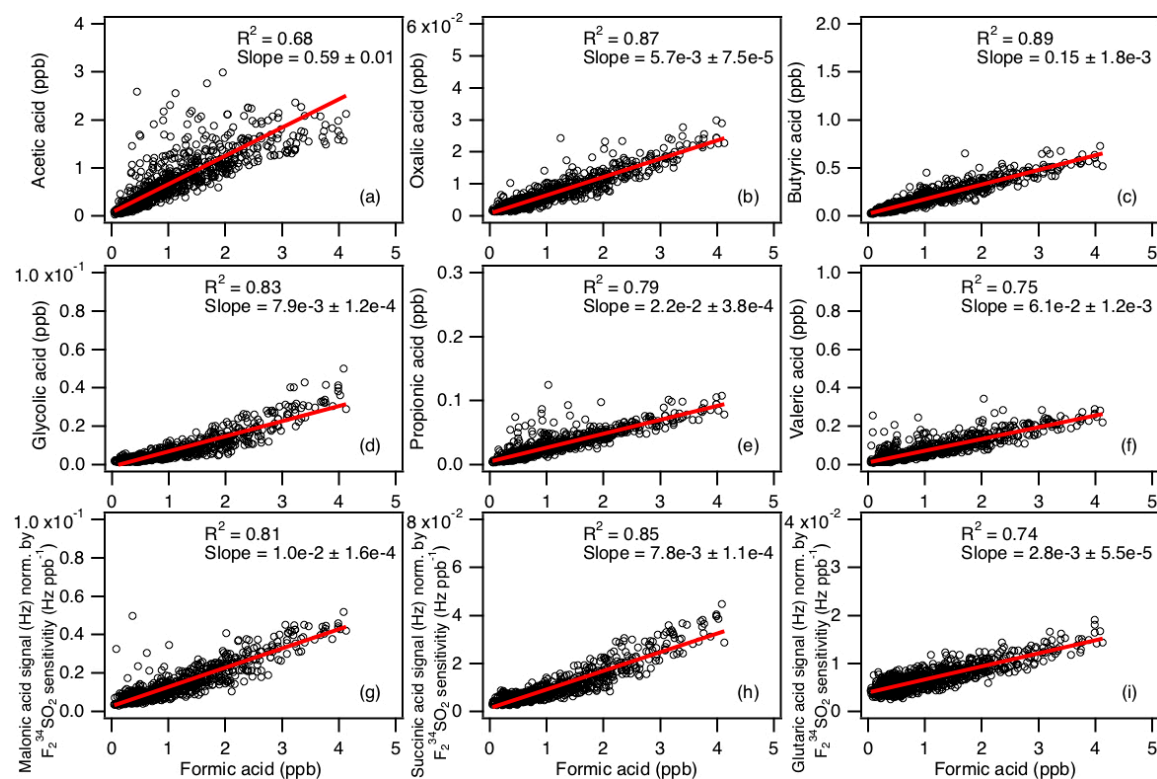


Figure 7: Scatter plots of concentrations (or signals) of (a) acetic, (b) oxalic, (c) butyric, (d) glycolic, (e) propionic, (f) valeric, (g) malonic, (h) succinic, and (i) glutaric acids with formic acid concentration. All the data are displayed as 1-hour averages. The data for malonic, succinic and glutaric acids are presented as the ratio of their ion signals (Hz) to the instrument’s sensitivity to $F_2^{34}SO_2$ (Hz ppb⁻¹) since these organic acids were not calibrated. Red lines shown are linear fits to the data.

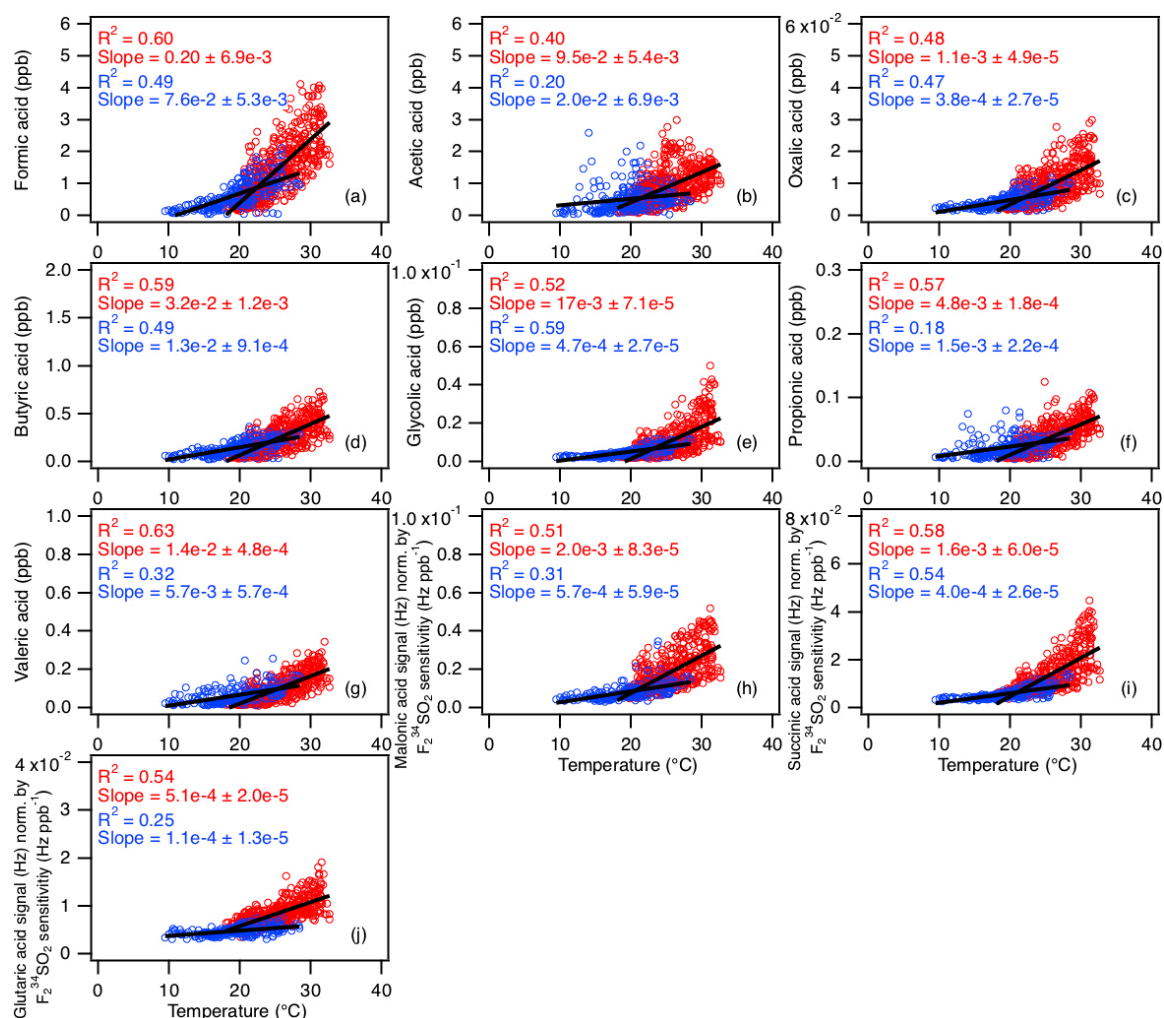


Figure 8: Scatter plots of concentrations (or signals) of (a) formic, (b) acetic, (c) oxalic, (d) butyric, (e) glycolic, (f) propionic, (g) valeric, (h) malonic, (i) succinic, and (j) glutaric acids with ambient temperature. The red symbols are data collected from 3 to 27 Sept, while the blue symbols are data collected from 28 Sept onwards. All the data are displayed as 1-hour averages. The data for malonic, succinic and glutaric acids are presented as the ratio of their ion signals (Hz) to the instrument's sensitivity to $F_2^{34}SO_2$ (Hz ppb⁻¹) since these organic acids were not calibrated. Black lines shown are linear fits to the datasets.

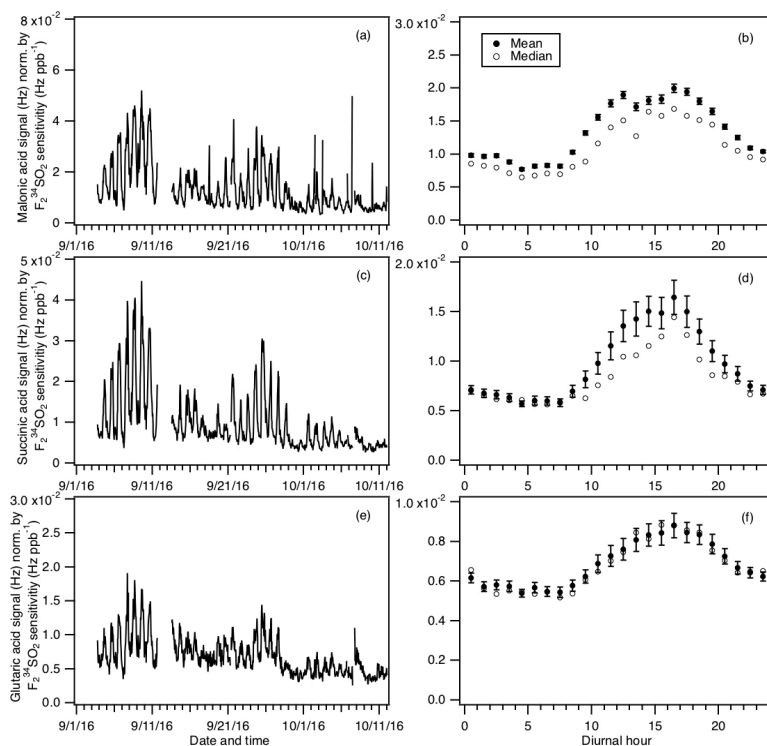


Figure S5: Time series of signals of (a) malonic, (c) succinic, and (e) glutaric acids measured during the field study. The data are displayed as 1-hour averages. Their corresponding diurnal profiles are shown in (b), (d) and (f), respectively. All the signals represent averages in 1-hour intervals and the standard errors are plotted as error bars. These organic acids were not calibrated so all the signals are presented here as Hz normalized by the instrument's sensitivity to $F_2^{34}SO_2$ (Hz ppb⁻¹) which was the primary calibrant used in the field study.

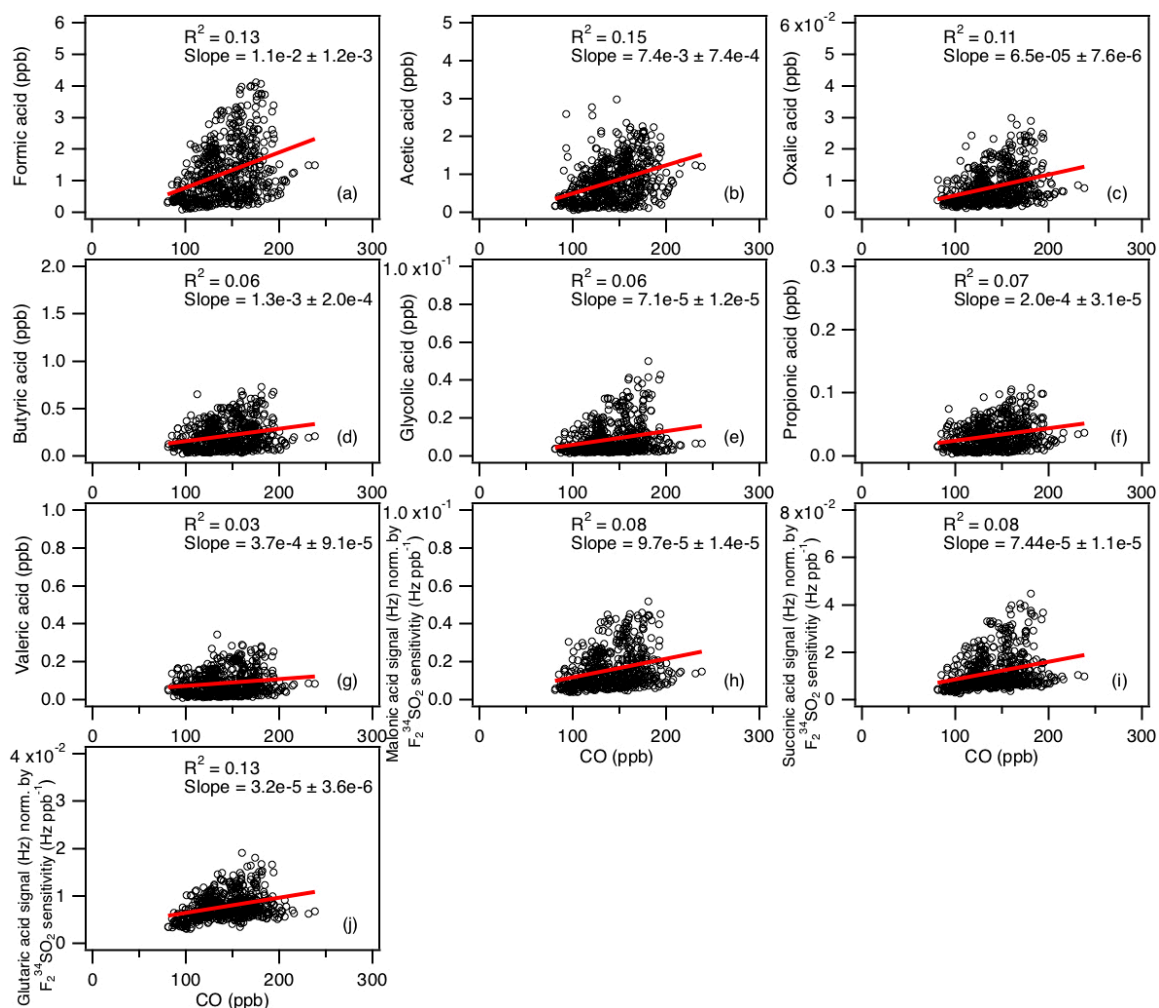


Figure S7: Scatter plots of concentrations (or signals) of (a) formic, (b) acetic, (c) oxalic, (d) butyric, (e) glycolic, (f) propionic, (g) valeric, (h) malonic, (i) succinic, and (j) glutaric acids with CO concentration. All the data are displayed as 1-hour averages. The data for malonic, succinic and glutaric acids are presented as the ratio of their ion signals (Hz) to the instrument's sensitivity to $F_2^{34}SO_2$ (Hz ppb $^{-1}$) since these organic acids were not calibrated. Red lines shown are linear fits to the data.

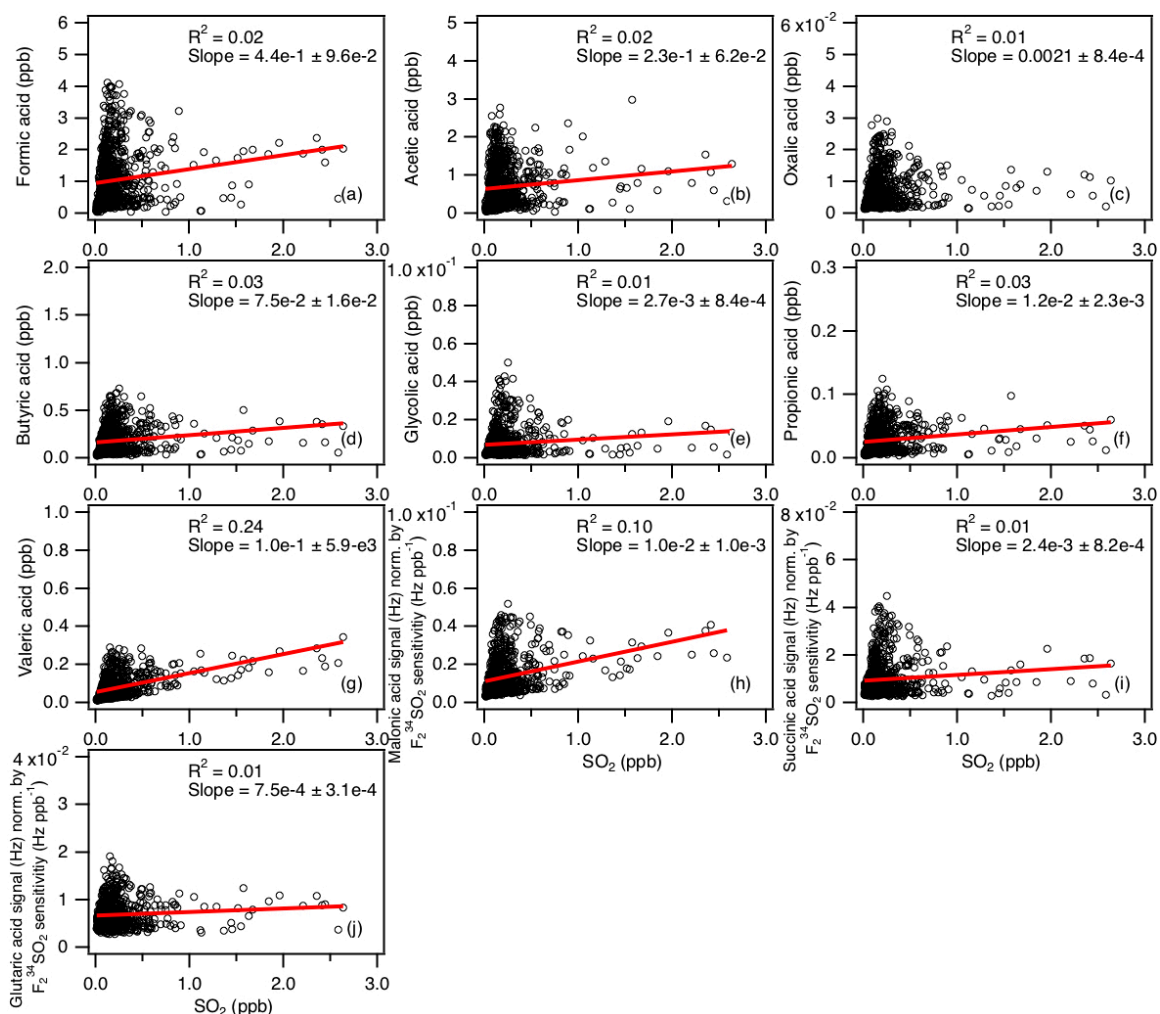


Figure S8: Scatter plots of concentrations (or signals) of (a) formic, (b) acetic, (c) oxalic, (d) butyric, (e) glycolic, (f) propionic, (g) valeric, (h) malonic, (i) succinic, and (j) glutaric acids with SO_2 concentration. All the data are displayed as 1-hour averages. The data for malonic, succinic and glutaric acids are presented as the ratio of their ion signals (Hz) to the instrument's sensitivity to $\text{F}_2^{34}\text{SO}_2$ (Hz ppb^{-1}) since these organic acids were not calibrated. Red lines shown are linear fits to the data.

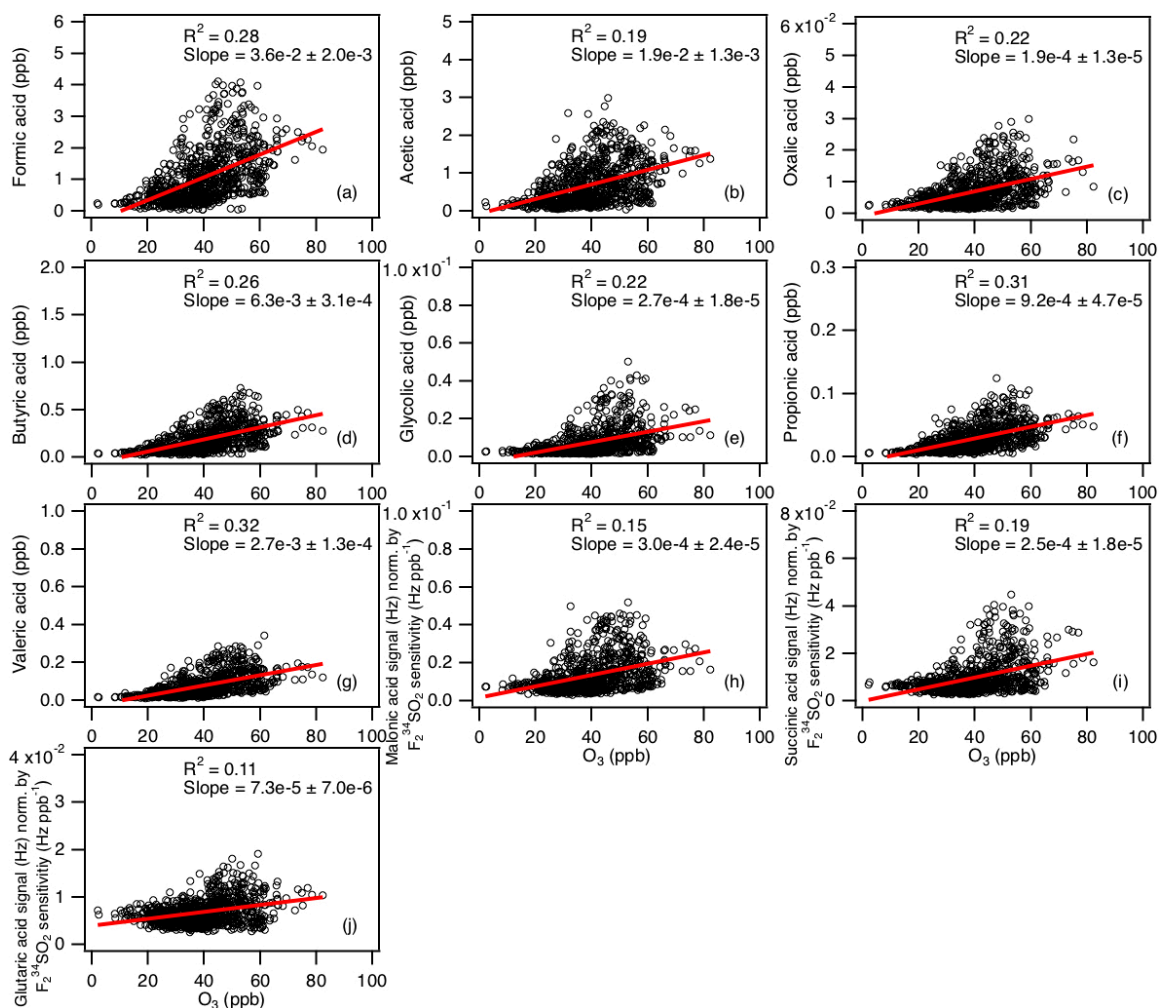


Figure S9: Scatter plots of concentrations (or signals) of (a) formic, (b) acetic, (c) oxalic, (d) butyric, (e) glycolic, (f) propionic, (g) valeric, (h) malonic, (i) succinic, and (j) glutaric acids with O_3 concentration. All the data are displayed as 1-hour averages. The data for malonic, succinic and glutaric acids are presented as the ratio of their ion signals (Hz) to the instrument's sensitivity to $F_2^{34}SO_2$ (Hz ppb $^{-1}$) since these organic acids were not calibrated. Red lines shown are linear fits to the data.

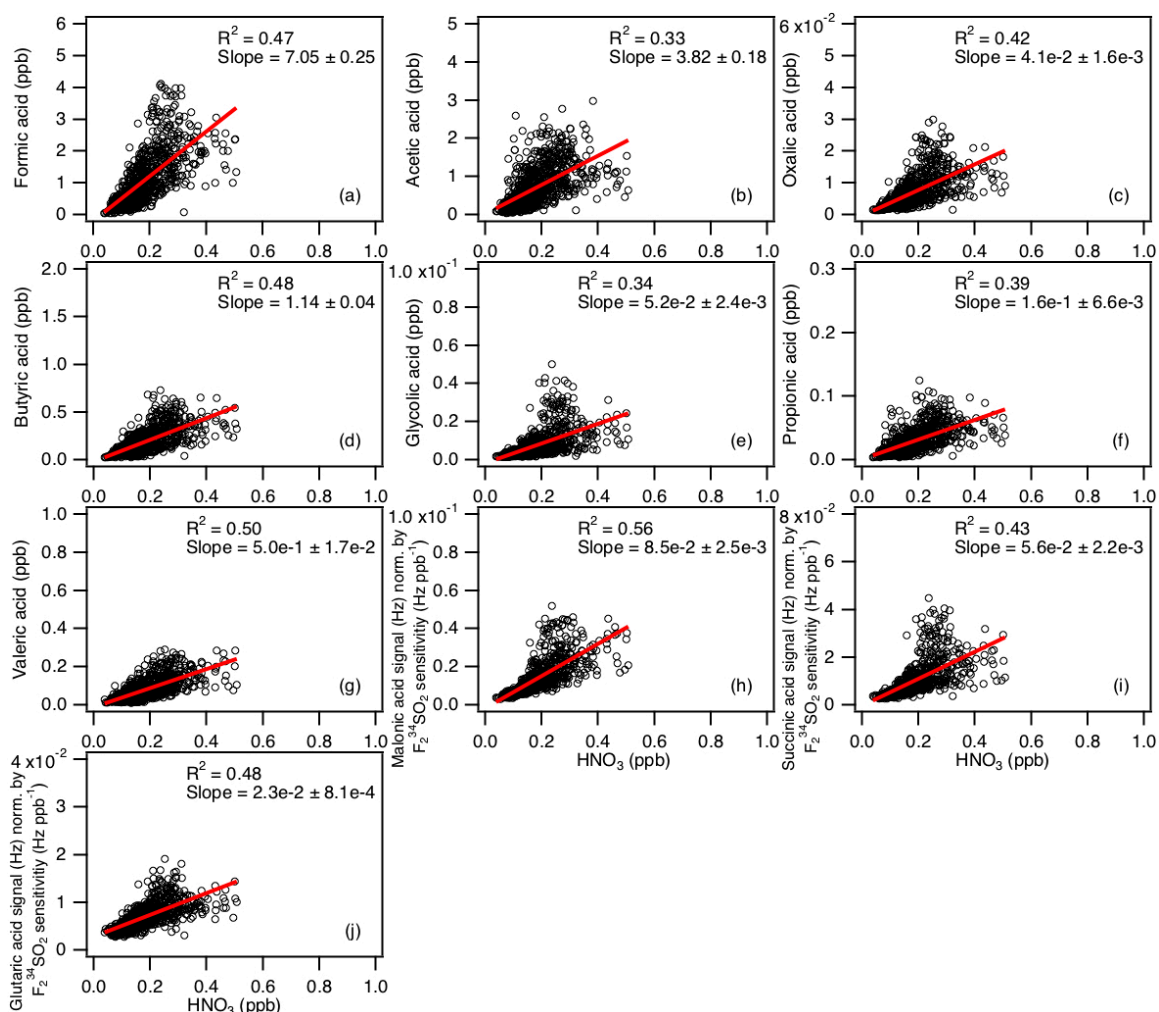


Figure S10: Scatter plots of concentrations (or signals) of (a) formic, (b) acetic, (c) oxalic, (d) butyric, (e) glycolic, (f) propionic, (g) valeric, (h) malonic, (i) succinic, and (j) glutaric acids with HNO_3 concentration. To exclude periods when the site was affected by urban or power plant emissions, data where $\text{HNO}_3 > 0.5$ ppb are excluded from these scatter plots. All the data are displayed as 1-hour averages. The data for malonic, succinic and glutaric acids are presented as the ratio of their ion signals (Hz) to the instrument's sensitivity to $\text{F}_2^{34}\text{SO}_2$ (Hz ppb^{-1}) since these organic acids were not calibrated. Red lines shown are linear fits to the data.

9. Referee comment: “I don’t understand the reagent ion signal and the use of sulfur isotopes. $^{34}\text{SF}_6^-$ is said to be the reagent ion (line 338). Is isotopically labeled SF_6 used? Why do the magnitudes of the peaks at mass 145 and 147 appear to be similar in Figure 2? Please clearly state the magnitude of the reagent ion signal. From figure 2, it appears that the reagent ion signal is approximately 400 kHz, and similar in magnitude to SF_5^- , CO_3^- . Wouldn’t ion chemistry from those other ions also contribute to the reactions? A more thorough description of the reagent ion is necessary to understand how the ion chemistry can be dominated by SF_6^- . Figure 2 makes it appear that other ions could be substantial contributors to the ion chemistry.”

Author response: Isotopically labeled SF_6^- was not used as the reagent ion. $^{32}\text{SF}_6^-$ (at m/z 146) is

the reagent ion. The signal of the reagent ion $^{32}\text{SF}_6^-$ was saturated for the entire field study, which led to the sharp drop in the ion signal at m/z 146 as shown in Fig. 2. Hence, we monitored the ion signal of its isotope $^{34}\text{SF}_6^-$ at m/z 148 (which was not saturated) to determine if the reaction of SF_6^- with ambient water vapor and O_3 depleted SF_6^- reagent ions. Despite fluctuations in ambient water vapor and O_3 concentrations, the $^{34}\text{SF}_6^-$ ion signal was relatively constant for the entire field study with a standard deviation of $< 3\%$. This indicates that the reaction of SF_6^- with ambient water vapor and O_3 do not deplete $^{32}\text{SF}_6^-$ reagent ions.

The ion signal of $^{34}\text{SF}_6^-$ (at m/z 148) and the isotopic abundances of ^{32}S vs. ^{34}S can be used to estimate the theoretical ion signal of the $^{32}\text{SF}_6^-$ reagent ion at m/z 146 (i.e., ion signal obtained if no signal saturation occurred). We find that the $^{32}\text{SF}_6^-$ reagent ion would have a theoretical ion signal of $\sim 9 \times 10^6$ Hz, which is 2 orders of magnitude larger than the CO_3^- signal. In addition, we expect the SF_6^- ion chemistry to dominate since SF_5^- is much more stable than SF_6^- and in any case will likely give similar product ions.

We have revised the manuscript and modified Fig. 2's caption to eliminate any confusion regarding the reagent ion used and contributions of other ions such as SF_5^- and CO_3^- to the ion chemistry:

Page 13 line 395: “Figure 2 shows a mass spectrum of ambient air. Interference peaks at m/z 39 ($\text{F}\cdot(\text{HF})$ and CO_3^- , respectively) can be attributed to the presence of water and O_3 , respectively. The reagent ion $^{32}\text{SF}_6^-$ is present at m/z 146. The $^{32}\text{SF}_6^-$ reagent ion signal was saturated, and this caused the sharp drop in the m/z 146 signal as shown in Fig. 2. Since the $^{32}\text{SF}_6^-$ reagent ion signal was saturated for the entire field study, we monitored the ion signal of its isotope $^{34}\text{SF}_6^-$ to determine if the reaction of SF_6^- with ambient water vapor (5.92×10^{-6} to 2.19×10^{-5} g cm^{-3}) and O_3 (2.1 to 82.4 ppb) depleted SF_6^- reagent ions. Figure S2a shows the time series of the $^{34}\text{SF}_6^-$ ion signal and ambient water vapor concentration for the entire field study. Despite fluctuations in ambient water vapor and O_3 concentrations, the $^{34}\text{SF}_6^-$ ion signal was relatively constant for the entire field study with a standard deviation of $< 3\%$. This indicates that the reaction of SF_6^- with ambient water vapor and O_3 did not significantly deplete the $^{32}\text{SF}_6^-$ reagent ions during the field study.”

Figure 2: Mass spectrum of ambient air and background measured in Yorkville, Georgia on 8 Sept 2016 using SF_6^- . Note that the $^{32}\text{SF}_6^-$ reagent ion signal (at m/z 146) is saturated, causing the sharp drop in its signal. As a result, the ion signal of its isotope $^{34}\text{SF}_6^-$ (at m/z 150) was monitored to determine if the reaction of SF_6^- with ambient water vapor and O_3 depleted SF_6^- reagent ions.

10. Referee comment: “*Since the major measurement technique advance here is using SF_6 in high water and ozone environments, there should be greater discussion of water and ozone mixing ratios in the main text, and the necessary modifications to make the ion chemistry work in this environment. Although the supplement shows some ozone and water data, simpler discussion of the range of ozone and water mixing ratios and the effect on the ion chemistry should be included in the manuscript. Please show how formic or acetic sensitivity varies with ozone and water.*”

Author response: Ambient water vapor concentrations ranged from 5.92×10^{-6} to 2.19×10^{-5} g cm^{-3} , while ambient O_3 concentrations ranged from 2.1 to 82.4 ppb during the study. The sampled air was diluted in the CIMS flow tube and the flow tube was operated at a low pressure to minimize interferences by water vapor and O_3 . Our results indicate that the reaction of SF_6^- with ambient

water vapor and O₃ did not deplete the ³²SF₆⁻ reagent ions. The SO₂ sensitivity showed a clear linear relationship to water vapor and varied within a factor of two for the entire field study, while the SO₂ sensitivity did not show any obvious dependence on ambient O₃ concentrations. The formic and acetic acid sensitivities did not show any obvious dependence on ambient water vapor and O₃ concentrations. Therefore, we do not expect the sensitivities of the other organic acids to depend on ambient water vapor and O₃ concentrations.

As requested, we have added more discussion about the ambient water vapor and O₃ concentrations and their effects on SF₆⁻ ion chemistry, the necessary sampling configurations needed to make SF₆⁻ ion chemistry to work in the field study, and how the formic and acetic acid sensitivity varies with water vapor and O₃:

Page 13 line 398: “Since the ³²SF₆⁻ reagent ion signal was saturated for the entire field study, we monitored the ion signal of its isotope ³⁴SF₆⁻ to determine if the reaction of SF₆⁻ with ambient water vapor (5.92 x 10⁻⁶ to 2.19 x 10⁻⁵ g cm⁻³) and O₃ (2.1 to 82.4 ppb) depleted SF₆⁻ reagent ions. Figure S2a shows the time series of the ³⁴SF₆⁻ ion signal and ambient water vapor concentration for the entire field study. Despite fluctuations in ambient water vapor and O₃ concentrations, the ³⁴SF₆⁻ ion signal was relatively constant for the entire field study with a standard deviation of < 3%. This indicates that the reaction of SF₆⁻ with ambient water vapor and O₃ did not significantly deplete the ³²SF₆⁻ reagent ions during the field study.

The F₂³⁴SO₂⁻ ion signal was used to monitor the CIMS SO₂ sensitivity during the field study. Figure S2b shows the time series of the F₂³⁴SO₂⁻/³⁴SF₆⁻ ion signal ratio obtained in calibration measurements. There is a noticeable increase in the F₂³⁴SO₂⁻/³⁴SF₆⁻ ion signal ratio on 28 Sept 2016, indicating an increase in the CIMS instrument sensitivity. The increase in CIMS instrument sensitivity is due to the decrease in ambient water vapor concentrations on 28 Sept 2016 (Fig. S2a). Previous laboratory and field studies showed that this was due to the hydrolysis of F₂³⁴SO₂⁻, which led to the loss of this ion and diminished sensitivity at higher levels of ambient water vapor (Arnold and Viggiano, 2001; Slusher et al., 2001). However, the SO₂ sensitivity at F₂³⁴SO₂⁻ only varied within a factor of two for the entire field study with a clear relationship to water vapor (Fig. S2c). The SO₂ sensitivity did not show any obvious dependence on ambient O₃ concentrations (Fig. S2d).

The formic (HCOO⁻ at m/z 45 and HCOO•HF at m/z 65) and acetic (CH₃COO•HF at m/z 79) acid ions did not show any obvious dependence on ambient water vapor and O₃ concentrations during calibration measurements (Fig. S3). Therefore, we do not expect the sensitivities of the X⁻ and X•HF ions of the studied organic acids to depend on ambient water vapor and O₃ concentrations. We accounted for water vapor dependence of the F₂³⁴SO₂⁻ ion signal in our post-field calibrations where the response of the CIMS acid signals were measured relative to the of the ³⁴SO₂ sensitivity.”

References:

Arnold, S. T., and Viggiano, A. A.: Turbulent ion flow tube study of the cluster-mediated reactions of SF₆⁻ with H₂O, CH₃OH, and C₂H₅OH from 50 to 500 torr, *J. Phys. Chem. A*, 105, 3527-3531, 10.1021/jp003967y, 2001.

Slusher, D. L., Pitteri, S. J., Haman, B. J., Tanner, D. J., and Huey, L. G.: A chemical ionization technique for measurement of pernitric acid in the upper troposphere and the polar boundary layer, *Geophys. Res. Lett.*, **28**, 3875-3878, 10.1029/2001gl013443, 2001.

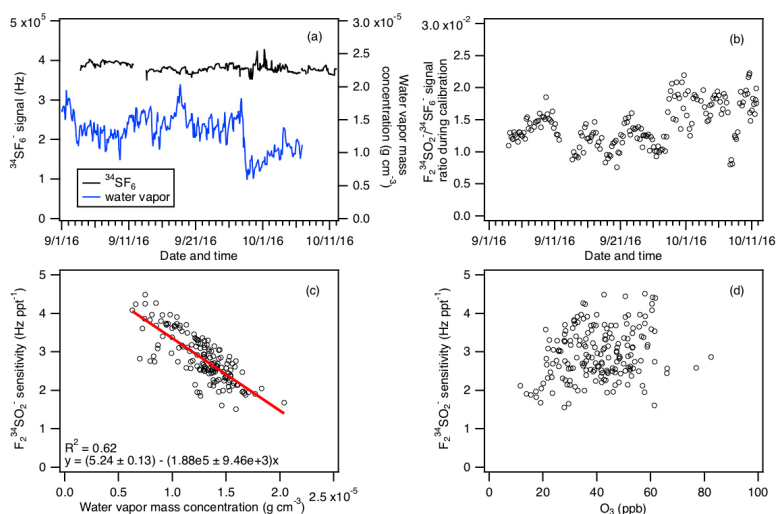


Figure S2: (a) Time series of $^{34}\text{SF}_6^-$ reagent ion signal and ambient water vapor concentration for the entire field study. The ambient water vapor mass concentrations are determined from ambient relative humidities and temperatures. (b) Time series of $\text{F}_2^{34}\text{SO}_2^-/^{34}\text{SF}_6^-$ ion signal ratio obtained during calibration measurements. Panels (c) and (d) show the $\text{F}_2^{34}\text{SO}_2^-$ ion sensitivity obtained from calibration measurements as a function of ambient water vapor and O_3 concentrations. Data in panels (a) to (d) are displayed as 1-hour averages.

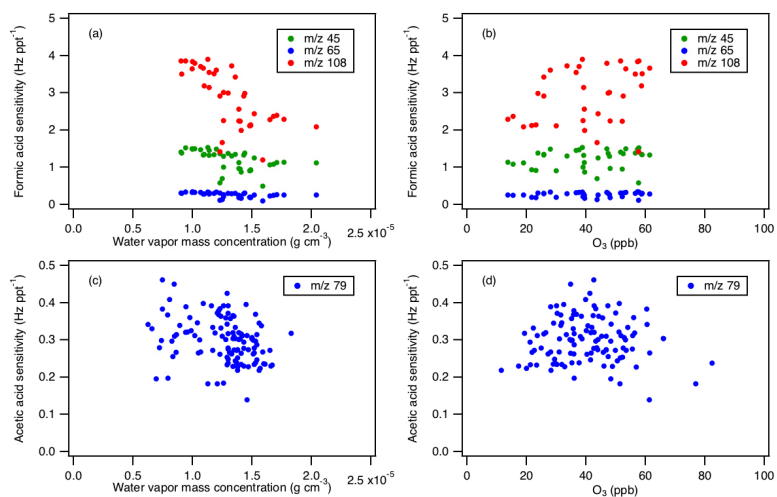


Figure S3: Panels (a) and (b) show the sensitivities of formic acid ions (HCOO^- at m/z 45, $\text{HCOO}\cdot\text{HF}$ at m/z 65, and SF_4^- at m/z 108) obtained from calibration measurements as a function of ambient water vapor and O_3 concentrations. Panels (c) and (d) show the acetic acid sensitivity ($\text{CH}_3\text{COO}\cdot\text{HF}$ at m/z 79) obtained from calibration measurements as a function of ambient water vapor and O_3 concentrations.

11. Referee comment: “One overlooked feature in the results is the differing diurnal variations of

acetic and formic acids in figures 3-4. Rather than focus on organic acid budgets that rely on speculative assignments and suffer from unexamined interferences, a study of the diurnal variability of acetic and formic acids could prove interesting.”

Author response: We do not know what caused the observed differing diurnal variations of formic and acetic acids. We are currently employing laboratory and modeling studies to explain these field observations. Results of these studies will be the subject of future papers.

Response to Referee 2 (Referees' comments are italicized)

1. Referee comment: *“The authors make a strong statement (line 95) that new techniques for the real-time measurement of gas-phase organic acids are needed due to deficiencies in existing CIMS based ion chemistry (acetate and iodide CIMS). The authors cite issues with acetate CIMS in the detection of acetic acid and the wide range of sensitivities to different organic acids in iodide CIMS. After reading this paper it was not clear to me that SF₆⁻ has an advantage over these techniques. It was shown that interferences due to O₃ hinder detection of acetic acid and there is an order of magnitude spread in sensitivity to various organic acids in Table 1. I think the authors need to better articulate how this technique is an advance over existing ion chemistry or acknowledge that it is a parallel approach to existing ion chemistry.”*

Author response: The SF₆⁻-CIMS technique serves as an alternative approach to existing CIMS techniques in the detection of organic acids. The major advantage that SF₆⁻ has over I⁻ and CH₃CO₂⁻ is that it allows for the detection of acetic acid and SO₂. CF₃O⁻ has a similar chemistry to SF₆⁻ but it also has issues due to hydrolysis and the ion precursor is not commercially available. This information has been added in the revised manuscript:

Page 4 line 107: “The sulfur hexafluoride (SF₆⁻) anion has been used as a CIMS reagent ion to measure atmospheric inorganic species such as sulfur dioxide (SO₂), nitric acid (HNO₃) and peroxyxynitric acid (HO₂NO₂) (Slusher et al., 2001; Slusher et al., 2002; Huey et al., 2004; Kim et al., 2007). SF₆⁻ commonly reacts with most acidic gases at the collision rate by either proton or fluoride transfer reactions (Huey et al., 1995). The SF₆⁻ ion chemistry is selective to acidic species, which can simplify the mass spectral analysis of organic acids. However, SF₆⁻ is reactive to both ozone (O₃) and water vapor, which can lead to interfering reactions that limit its applicability to many species in certain environments (Huey et al., 2004). For these reasons, this work is focused on assessing the ability of SF₆⁻ to measure a series of organic acids in ambient air. The major advantage that SF₆⁻ has over I⁻ and CH₃CO₂⁻ is that it allows for the detection of acetic acid and SO₂. CF₃O⁻ has a similar chemistry to SF₆⁻ but it also has issues due to hydrolysis and the ion precursor is not commercially available.”

References:

Huey, L. G., Hanson, D. R., and Howard, C. J.: Reactions of SF₆⁻ and I⁻ with Atmospheric Trace Gases, *Journal of Physical Chemistry*, 99, 5001-5008, 10.1021/j100014a021, 1995.

Huey, L. G., Tanner, D. J., Slusher, D. L., Dibb, J. E., Arimoto, R., Chen, G., Davis, D., Buhr, M. P., Nowak, J. B., Mauldin, R. L., Eisele, F. L., and Kosciuch, E.: CIMS measurements of

HNO₃ and SO₂ at the South Pole during ISCAT 2000, *Atmospheric Environment*, 38, 5411-5421, 10.1016/j.atmosenv.2004.04.037, 2004.

Kim, S., Huey, L. G., Stickel, R. E., Tanner, D. J., Crawford, J. H., Olson, J. R., Chen, G., Brune, W. H., Ren, X., Leshner, R., Wooldridge, P. J., Bertram, T. H., Perring, A., Cohen, R. C., Lefer, B. L., Shetter, R. E., Avery, M., Diskin, G., and Sokolik, I.: Measurement of HO₂NO₂ in the free troposphere during the intercontinental chemical transport experiment - North America 2004, *Journal of Geophysical Research-Atmospheres*, 112, 10.1029/2006jd007676, 2007.

Slusher, D. L., Pitteri, S. J., Haman, B. J., Tanner, D. J., and Huey, L. G.: A chemical ionization technique for measurement of pernitric acid in the upper troposphere and the polar boundary layer, *Geophys. Res. Lett.*, 28, 3875-3878, 10.1029/2001gl013443, 2001.

Slusher, D. L., Huey, L. G., Tanner, D. J., Chen, G., Davis, D. D., Buhr, M., Nowak, J. B., Eisele, F. L., Kosciuch, E., Mauldin, R. L., Lefer, B. L., Shetter, R. E., and Dibb, J. E.: Measurements of pernitric acid at the South Pole during ISCAT 2000, *Geophys. Res. Lett.*, 29, 10.1029/2002gl015703, 2002.

2. Referee comment: “Given the focus of the journal, I think more emphasis on the experimental configuration of the CIMS should be given. Direct comparisons to existing measurements are always welcome, but the focus should remain on describing the details of the ion chemistry and or instrument operation.”

Author response: We have added more details on the ion chemistry and instrument operation and more discussions on interferences in the revised manuscript. Please refer to our responses to comments on experimental details and interferences from referee 1 and 2.

3. Referee comment: “Line 46: I would cite Molina et al. (2004), or Vlasenko et al. (2008) for the heterogeneous source of organic acids from the chemical aging of organic aerosol.”

Author response: These references have been added.

4. Referee comment: “Line 166: Please elaborate on how the lower pressure (13 mbar) minimizes interferences in reactions of SF₆⁻ with water vapor.”

Author response: SF₆⁻ reacts with water vapor to form F⁻•(HF)_n cluster ions. Arnold and Viggiano (2001) showed previously that the formation of these F⁻•(HF)_n cluster ions are enhanced at high flow tube pressures due to increased reactive collisions between SF₆⁻ and water vapor. We maintained the flow tube at a low pressure to reduce reactive SF₆⁻/water vapor collisions in the flow tube, thus minimizing interferences from SF₆⁻ reaction with water vapor.

We made the following changes in the revised manuscript:

Page 6 line 174: “Arnold and Viggiano (2001) showed that the formation of F⁻•(HF)_n cluster ions from the reaction of SF₆⁻ and water vapor is enhanced at high flow tube pressures. Since these F⁻•(HF)_n cluster ions could interfere with mass spectral analysis, the flow tube was maintained at a low pressure (~13 mbar, 0.5 % uncertainty) in this study to reduce both the water vapor concentration and reaction time in the flow tube, thus minimizing interferences

from SF₆⁻ reaction with water vapor.”

5. Referee comment: *“Line 171: Rather than reporting voltages, it would be better to report electric fields or relative electric fields (E/N).”*

Author response: The electric field of the CDC is reported in the revised manuscript:

Page 6 line 184: “For this study, the CDC was operated at a relatively high electric field (~113 V cm⁻¹) to efficiently dissociate cluster ions.”

6. Referee comment: *“Line 182: Why was the background measurement period so long (~4 minutes). It would be helpful to show one of these in time. I would have expected that the background measurement period could be significantly shorter and still capture the baseline, unless there are inlet equilibration issues.”*

Author response: We chose a 4 min background measurement time to give the scrubber (during background measurements) and flow tube ample time to equilibrate when the three-way PFA Teflon valve was switched between ambient and background modes, and to obtain good averaging statistics. This is stated explicitly in the revised manuscript:

Page 7 line 204: “Each background and calibration measurement period lasted ~4 and ~3.5 min, respectively, which not only gave the scrubber (during background measurements) and flow tube ample time to equilibrate when the three-way PFA Teflon valve was switched between ambient and background modes, but also allowed us to obtain good averaging statistics during background and calibration measurements.”

We also added a section (3.1.3) and a figure (Fig. S4) discussing instrument time response during background and calibration measurements in the revised manuscript. Please refer to our response to comment 4 from referee 1.

7. Referee comment: *“Line 183: What was the 1.12 ppm SO₂ standard diluted to? Presumably calibrations were not done at this mixing ratio.”*

Author response: 1.85 ppb of ³⁴SO₂ was used in calibration measurements. This information has been added to the revised manuscript:

Page 7 line 209: “1.85 ppb of ³⁴SO₂ was added to sampled air flow during calibration measurements.”

8. Referee comment: *“Line 184: Again, it would be more helpful to present as the concentration of FA or AA that is delivered instead of the permeation tube emission rates.”*

Author response: As requested, this information has been added to the revised manuscript:

Page 7 line 216: “6.75 ppb of formic acid and 5.87 ppb of acetic acid was added to sampled air flow during calibration measurements.”

9. Referee comment: *“Line 308: For reactions 1a-c, should one think of these as separate reaction channels governed by ion-molecule kinetics or does every reaction proceed through 1a and the electric field strength of the CDC sets the ratio of the observed products. This may lead to strong*

deviations in the observed products based on instrument configuration.”

Author response: Every reaction of SF₆⁻ with organic acids (HX) proceeds through reactions 1a to 1c, where the ratio of the observed product ions can be controlled by the field strength of the CDC. This is stated explicitly in the revised manuscript:

Page 11 line 331: “CIMS measurements of atmospheric constituents use ion-molecule reactions to selectively ionize compounds of interest in the complex matrix of ambient air and produce characteristic ions. The reactions of SF₆⁻ with the organic acids (HX) proceed through reactions 1a to 1c, and gave similar products to those reported previously for SF₆⁻ reactions with inorganic acids (Huey et al., 1995): SF₅⁻, X⁻ and X•HF where X⁻ is the conjugate base of the organic acid (reactions 1a-c).



The effective branching ratios of the SF₅⁻, X⁻ and X•HF product ions can be impacted by the field strength of the CDC.”

References:

Huey, L. G., Hanson, D. R., and Howard, C. J.: Reactions of SF₆⁻ and I⁻ with Atmospheric Trace Gases, *Journal of Physical Chemistry*, 99, 5001-5008, 10.1021/j100014a021, 1995.

10. Referee comment: “Line 334: Can the mass (or molar) dilution constant be reported here instead of the inlet flow? This would help the reader understand how much ambient O₃ and H₂O are reduced by the sampling geometry. Also, perhaps it would be helpful to more explicitly state how a reduction in ion-molecule reaction time is helpful. This would not help in sensitivity (assuming all reactions are at the collision limit), but presumably would help minimize secondary ion chemistry, correct?”

Author response: The ratio of the sampled air to the N₂/SF₆ mixture introduced into the CIMS flow tube is approximately 1:13. The referee is correct in pointing out that the reduction in ion-molecule reaction time helps minimize interfering secondary ion chemistry. We reduced the ion-molecule reaction time by sampling only 0.3 L min⁻¹ of air through the variable orifice into the flow tube and maintaining the flow tube at a low pressure (~13 mbar). This information is stated explicitly in the revised manuscript.

Page 13 line 384: “These reactions can deplete SF₆⁻ as well as form a variety of potentially interfering ions from secondary reactions (e.g., F⁻•(HF)_n and CO₃⁻ ions) that depend on more abundant atmospheric species. For these reasons, efforts were made to minimize interferences by limiting reaction times and the flow sampled into the CIMS. This was accomplished by sampling only 0.3 L min⁻¹ of air through the variable orifice into the flow tube and maintaining the flow tube at a low pressure (~13 mbar). The 0.3 L min⁻¹ sampled air flow is diluted by 3.7 slpm of N₂/SF₆ flow in the flow tube. The ratio of the sampled air flow to the N₂/SF₆ flow introduced into the flow tube is approximately 1:13. While the high

N₂/SF₆ flow (3.7 slpm) passed through the radioactive source into the flow tube increased the SF₆⁻ reagent ion signal, the high dilution of the sampled air flow in the flow tube reduced the CIMS instrument sensitivity by decreasing the number density of the analytes.”

11. Referee comment: *“Line 335: What is the uncertainty in the IMR and CDC pressure? Are these pressures also controlled?”*

Author response: The uncertainty in the flow tube pressure (the so-called IMR) is 0.5 %, while the uncertainty in the CDC pressure is 10 %. These pressures are controlled by a variable orifice. This information has been added to the revised manuscript:

Page 6 line 176: “Since these F⁻(HF)_n cluster ions could interfere with mass spectral analysis, the flow tube was maintained at a low pressure (~13 mbar, 0.5 % uncertainty) in this study to minimize interferences from SF₆⁻ reaction with water vapor. The analyte ions exited the flow tube and were accelerated through the collisional dissociation chamber (CDC), which was maintained at ~0.8 mbar (10 % uncertainty). The molecular collisions in the CDC served to dissociate weakly bound cluster ions into their core ions to simplify mass spectral analysis. Flow tube and CDC pressures were controlled by the automatic variable orifice.”

The following are additional minor changes the authors have made to the manuscript:

1. We corrected the model series of the CIMS turbo pumps:

Page 6 line 168: “These sections were evacuated by a scroll pump (Edward nXDS 20i), a drag pump (Adixen MDP 5011) and two turbo pumps (Varian Turbo-V301), respectively.”

2. We corrected the uncertainty in nitric acid ambient concentrations:

Page 10 line 283: “For nitric acid which was calibrated in post-field laboratory work using a permeation tube and UV optical absorption, the uncertainty in its ambient concentrations was estimated to be 13 % based on uncertainties in UV absorption measurements (10 %) and one standard deviation of the acid’s UV absorption signals (3 %), ³⁴SO₂ sensitivity (3 %) and acid’s calibrant ion signals (8 %).”

1 **Real-time measurements of gas-phase organic acids using SF₆⁻ chemical ionization**
2 **mass spectrometry**

3
4 Theodora Nah,¹ Yi Ji,^{1,2} David J. Tanner,¹ Hongyu Guo,¹ Amy P. Sullivan,³ Nga Lee Ng,^{1,2}
5 Rodney J. Weber¹ and L. Gregory Huey^{1*}

6
7 ¹*School of Earth and Atmospheric Sciences, Georgia Institute of Technology, Atlanta, GA, USA*

8 ²*School of Chemical and Biomolecular Engineering, Georgia Institute of Technology, Atlanta, GA, USA*

9 ³*Department of Atmospheric Science, Colorado State University, Fort Collins, CO, USA*

10
11 * *To whom correspondence should be addressed: greg.huey@eas.gatech.edu*
12

13 **Abstract**

14 The sources and atmospheric chemistry of gas-phase organic acids are currently poorly
15 understood due in part to the limited range of measurement techniques available. In this
16 work, we evaluated the use of SF₆⁻ as a sensitive and selective chemical ionization reagent
17 ion for real-time measurements of gas-phase organic acids. Field measurements are made
18 using a chemical ionization mass spectrometer (CIMS) at a rural site in Yorkville, Georgia
19 from September to October 2016 to investigate the capability of this measurement
20 technique. Our measurements demonstrate that SF₆⁻ can be used to measure a range of
21 organic acids in the atmosphere. **1-hour averaged ambient** concentrations of organic acids
22 ranged from a few parts per trillion by volume (ppt) to several parts per billion by volume
23 (ppb). ~~All the organic acids displayed similar strong diurnal behaviors, reaching maximum~~
24 ~~concentrations between 5 and 7 pm local time. The organic acid concentrations are~~
25 ~~dependent on ambient temperature, with higher organic acid concentrations being~~
26 ~~measured during warmer periods.~~

Deleted: Assuming that these organic acids are completely water-soluble, the carbon mass fraction of gas-phase water-soluble organic carbon (WSOC_g) comprised of these organic acids ranged from 7 to 100 % with a study average of 30 %.

27 **Introduction**

28 Organic acids are ubiquitous and important species in the troposphere. They are
29 major contributors of free acidity in precipitation (Galloway et al., 1982; Keene et al., 1983;
30 Keene and Galloway, 1984), and can also affect the formation of secondary organic
31 aerosols (SOA) (Zhang et al., 2004; Carlton et al., 2006; Sorooshian et al., 2010; Yatavelli
32 et al., 2015). As end products of oxidation, organic acids can also serve as useful tracers of
33 air mass history (Sorooshian et al., 2007; Sorooshian et al., 2010). Organic acids are found

38 in urban, rural and remote marine environments in the gas, aqueous and particle phases.
39 While organic acids are emitted directly from biogenic sources (e.g., microbial activity,
40 vegetation and soil) and anthropogenic activities (e.g., fossil fuel combustion, vehicular
41 emissions and biomass burning) (Kawamura et al., 1985; Talbot et al., 1988; Chebbi and
42 Carlier, 1996; Talbot et al., 1999; Seco et al., 2007; Veres et al., 2010; Paulot et al., 2011;
43 Veres et al., 2011; Millet et al., 2015), they can also be formed from photooxidation of
44 non-methane volatile organic compounds and aqueous-phase photochemistry of semi-
45 volatile organic compounds (Chebbi and Carlier, 1996; Hansen et al., 2003; Orzechowska
46 and Paulson, 2005; Carlton et al., 2006; Sorooshian et al., 2007; Ervens et al., 2008; Paulot
47 et al., 2011; Millet et al., 2015). The chemical aging of organic aerosols has also been
48 proposed as a major source of organic acids (Molina et al., 2004; Vlasenko et al., 2008;
49 Paulot et al., 2011). The relative importance of primary and secondary sources of organic
50 acids are currently poorly constrained though their emissions likely depend on the
51 magnitude of biogenic and anthropogenic activities and the meteorological conditions. Wet
52 and dry deposition are the primary sinks of organic acids in the atmosphere (Chebbi and
53 Carlier, 1996).

54 Formic and acetic acids are the dominant gas-phase monocarboxylic acids in the
55 troposphere (Chebbi and Carlier, 1996). Due to their high vapor pressures, the gas-phase
56 concentrations of formic and acetic acids are usually 1 to 2 orders of magnitudes higher
57 than their particle-phase concentrations. Some field studies report strong correlations
58 between formic and acetic acids, suggesting that these two organic acids have similar
59 sources (Nolte et al., 1997; Souza and Carvalho, 2001; Paulot et al., 2011). A recent
60 modeling study suggested that the dominant sources of formic acid in the southeastern U.S.
61 are primarily biogenic in nature (Millet et al., 2015). These sources include direct emissions
62 from vegetation and soil and photochemical production from biogenic volatile organic
63 compounds (BVOCs). Currently, atmospheric formic and acetic acid concentrations are
64 higher than those predicted by models, indicating that present model estimates of source
65 and sink magnitudes are incorrect (Paulot et al., 2011; Millet et al., 2015). In the case of
66 formic acid, deposition and secondary photochemical production via mechanisms such as
67 photooxidation of isoprene and reaction of stabilized criegee intermediates need to be
68 better constrained in models. Given that formic and acetic acids are major trace gases in

69 the atmosphere, there is a need to resolve the discrepancy between measurements and
70 model predictions to close the atmospheric reactive carbon budget and improve our overall
71 understanding of VOC chemistry in the atmosphere.

72 Currently, research on gas-phase organic acids has focused primarily on formic and
73 acetic acids (Andreae et al., 1988; Talbot et al., 1988; Grosjean, 1991; Hartmann et al.,
74 1991; Talbot et al., 1995; Talbot et al., 1999). This is due, in part, to the analytical
75 difficulties in measuring gas-phase $> C_2$ organic acids and oxidized organic acids (i.e.,
76 containing more than 2 oxygen atoms) in real time. These organic acids have low vapor
77 pressures and are generally present in low concentrations in the gas phase. For example,
78 dicarboxylic acids typically have vapor pressures that are 2 to 4 orders of magnitude lower
79 than their analogous monocarboxylic acids (Chebbi and Carlier, 1996), and are present
80 mainly in the particle and aqueous phases. Rapid and accurate measurements of gas-phase
81 $> C_2$ organic acids and oxidized organic acids are necessary for constraining the regional
82 and global SOA budget since these acids can partition readily between the gas and particle
83 and aqueous phases and subsequently affect SOA formation (Zhang et al., 2004; Carlton
84 et al., 2006; Ervens et al., 2008; Sorooshian et al., 2010; Yatavelli et al., 2015).

85 Chemical ionization mass spectrometry (CIMS) is commonly used to selectively
86 measure atmospheric trace gases in real-time with high sensitivity. CIMS measurements
87 rely on reactions between reagent ions and compounds of interest present in the sampled
88 air to produce analyte ions that are detected by a mass spectrometer. The subset of
89 molecular species detected is determined by the reagent ion employed since the specificity
90 of the ionization process is governed by the ion-molecule reaction mechanism. CIMS is a
91 popular tool for atmospheric measurements since it ~~is versatile and has~~ high time resolution
92 ~~and sensitivity~~. It is also ~~often~~ a soft ionization technique with minimal ion fragmentation,
93 thus preserving the parent molecule's elemental composition and allowing for molecular
94 speciation. Recent developments in chemical ionization methods and sources have greatly
95 improved our ability to measure atmospheric acidic species. Some of the CIMS reagent
96 ions that have been used to measure atmospheric organic acids include acetate ($CH_3CO_2^-$),
97 iodide (I^-) and CF_3O^- anions (Crouse et al., 2006; Veres et al., 2008; Lee et al., 2014;
98 Brophy and Farmer, 2015; Nguyen et al., 2015). However, each of these CIMS reagent

Deleted: provides

Deleted: , linear and reproducible measurements

101 ions has its drawbacks, which are generally related to their selectivity and sensitivity
102 towards different atmospheric species. For example, acetic acid is difficult to measure with
103 CH_3CO_2^- as the CIMS reagent ion due to interferences from the reagent ion chemistry that
104 complicates the desired ion-molecule reactions. In addition, while many organic acids can
105 be detected using I^- as a reagent ion, its sensitivity to different acids can vary by orders of
106 magnitude (Lee et al., 2014).

107 The sulfur hexafluoride (SF_6^-) anion has been used as a CIMS reagent ion to
108 measure atmospheric inorganic species such as sulfur dioxide (SO_2), nitric acid (HNO_3)
109 and peroxyxynitric acid (HO_2NO_2) (Slusher et al., 2001; Slusher et al., 2002; Huey et al.,
110 2004; Kim et al., 2007). SF_6^- commonly reacts with most acidic gases at the collision rate
111 by either proton or fluoride transfer reactions (Huey et al., 1995). The SF_6^- ion chemistry
112 is selective to acidic species, which can simplify the mass spectral analysis of organic acids.
113 However, SF_6^- is reactive to both ozone (O_3) and water vapor, which can lead to interfering
114 reactions that limit its applicability to many species in certain environments (Huey et al.,
115 2004). For these reasons, this work is focused on assessing the ability of SF_6^- to measure a
116 series of organic acids in ambient air. The major advantage that SF_6^- has over I^- and
117 CH_3CO_2^- is that it allows for the detection of acetic acid and SO_2 . CF_3O^- has a similar
118 chemistry to SF_6^- but it also has issues due to hydrolysis and the ion precursor is not
119 commercially available. We present ambient measurements of gas-phase organic acids
120 conducted in a mixed forest-agricultural area in Georgia in early fall of 2016 to evaluate
121 the performance of a SF_6^- CIMS technique. Gas-phase organic acid measurements are
122 compared to gas-phase water-soluble organic carbon (WSOC_g) measurements performed
123 during the field study to estimate the fraction of WSOC_g that is comprised of organic acids
124 at this rural site. Laboratory experiments are conducted to measure the sensitivity of SF_6^-
125 with a series of organic acids of atmospheric relevance.

126 2. Methods

127 2.1. Field site

128 Real-time ambient measurements of gas-phase organic acids were obtained using a
129 chemical ionization mass spectrometer from 3 Sept to 12 Oct 2016 at the SouthEastern

130 Aerosol Research and Characterization (SEARCH) site located in Yorkville, Georgia. A
131 detailed description of the field site has been provided by Hansen et al. (2003). Briefly, the
132 Yorkville field site (33.931 N, 85.046 W) was located ~55 km northwest of Atlanta, and
133 was on a broad ridge in a large pasture where there were occasionally grazing cattle. The
134 field site was surrounded by forest and agricultural land. There were no major roads near
135 the field site and nearby traffic emissions were negligible. The sampling period was
136 characterized by moderate temperatures (24.0 °C average, 32.6 °C max, 9.5 °C min) and
137 high relative humidities (68.9% RH average, 100% RH max, 21.6% RH min). The study-
138 averaged diurnal trends of relative humidity, temperature and solar radiance are shown in
139 Fig. S1. Data reported are displayed in EDT. Volumetric gas concentrations reported are
140 at ambient temperature and relative humidity.

141 2.2. SF₆ CIMS

142 2.2.1. CIMS instrument and air sampling inlet

143 The CIMS instrument was housed in a temperature controlled trailer during the
144 field study. The inlet configuration and CIMS instrument used in this study is shown in
145 Fig. 1. Since HNO₃ and organic acids may condense on surfaces, an inlet configuration
146 with a minimal wall interaction was used. This inlet configuration was previously described
147 by Huey et al. (2004) and Nowak et al. (2006); hence, only a brief description will be
148 provided here. The inlet was a 7.6 cm ID aluminum pipe that extended ~40 cm into the
149 ambient air through a hole in the trailer's wall. This positioned the inlet ~2 m above the
150 ground. A donut-shaped ring was attached to the ambient sampling port of the pipe to
151 reduce the influence of crosswinds on the pipe's flow dynamics. This ring was wrapped
152 with a fine wire mesh to prevent insects from being drawn through the pipe. A flow of
153 ~2800 L min⁻¹ was maintained in the pipe using a regenerative blower (AMETEK
154 Windjammer 116637-03). Part of this flow (7 L min⁻¹) was sampled through a custom-
155 made three-way PFA Teflon valve, which connected the pipe's center to the CIMS
156 sampling orifice. The valve was maintained at a temperature of 40 °C in an insulated
157 aluminum oven and could be switched automatically between ambient and background
158 modes. In ambient mode, ambient air was passed through a 25 cm long, 0.65 cm ID Teflon
159 tube into the CIMS. In background mode, ambient air was first drawn through an activated

160 charcoal scrubber before being delivered into the CIMS. A small flow of ambient air (~0.05
161 L min⁻¹) was continuously passed through the scrubber to keep it at equilibrium with
162 ambient humidity levels. Most of the sampled air flow (6.7 L min⁻¹) was exhausted using
163 a small diaphragm pump. The rest of the sampled air flow (0.3 L min⁻¹) was introduced
164 into the CIMS instrument through an automatic variable orifice, which was used to
165 maintain a constant sample air mass flow.

166 The CIMS instrument was comprised of a series of differentially pumped regions:
167 a flow tube, a collisional dissociation chamber, an octopole ion guide, a quadrupole mass
168 filter and an ion detector. These sections were evacuated by a scroll pump (Edward nXDS
169 20i), a drag pump (Adixen MDP 5011) and two turbo pumps (Varian Turbo-V301),
170 respectively. Ambient air was drawn continuously into the flow tube. A flow of 3.7 slpm
171 of N₂ containing a few ppm of SF₆ (Scott-Marrin Inc.) was passed through a ²¹⁰Po ion
172 source into the flow tube. SF₆⁻ anions, which were produced via associative electron
173 attachment in the ²¹⁰Po ion source, reacted with the sampled ambient air in the flow tube
174 to generate analyte ions. Arnold and Viggiano (2001) showed that the formation of F⁻
175 •(HF)_n cluster ions from the reaction of SF₆⁻ and water vapor is enhanced at high flow tube
176 pressures. Since these F⁻•(HF)_n cluster ions could interfere with mass spectral analysis, the
177 flow tube was maintained at a low pressure (~13 mbar, 0.5 % uncertainty) in this study to
178 reduce both the water vapor concentration and reaction time in the flow tube, thus
179 minimizing interferences from SF₆⁻ reaction with water vapor. The analyte ions exited the
180 flow tube and were accelerated through the collisional dissociation chamber (CDC), which
181 was maintained at ~0.8 mbar (10 % uncertainty). The molecular collisions in the CDC
182 served to dissociate weakly bound cluster ions into their core ions to simplify mass spectral
183 analysis. Flow tube and CDC pressures were controlled by the automatic variable orifice.
184 For this study, the CDC was operated at a relatively high electric field (~113 V cm⁻¹) to
185 efficiently dissociate cluster ions. The resulting ions were then passed into the octopole ion
186 guide (maintained at ~6 x 10⁻³ mbar), which collimated the ions and transferred them into
187 the quadrupole mass spectrometer (maintained at ~10⁻⁵ mbar) for mass selection and
188 detection.

Deleted: then

Deleted: voltage

Deleted: -50 V

192 Ions monitored during the field study included m/z 45, 59, 65, 73, 75, 79, 82, 87,
193 89, 101, 102, 103, 108, 117, 131 and 148. The assignment of these ions will be discussed
194 in section 3. The dwell time for each m/z ion was set to 0.5 s and measurements of these
195 ions were obtained every ~13 s, which resulted in a ~4 % (= 0.5/13 x 100 %) duty cycle
196 for each ion monitored. The data presented in this paper was averaged to 1-hour intervals
197 unless stated otherwise.

198 **2.2.2. Background and calibration measurements during field study**

199 Background measurements were performed every 25 min during the field study.
200 During each background measurement, the sampled air flow was passed through an
201 activated charcoal scrubber prior to delivery into the CIMS. The scrubber removed > 99 %
202 of the targeted species in ambient air. Calibration measurements were performed every 5 h
203 during the field study through standard additions of $^{34}\text{SO}_2$ and either formic or acetic acid
204 to the sampled air flow. Each background and calibration measurement period lasted ~4
205 and ~3.5 min, respectively, which not only gave the scrubber (during background
206 measurements) and flow tube ample time to equilibrate when the three-way PFA Teflon
207 valve was switched between ambient and background modes, but also allowed us to obtain
208 good averaging statistics during background and calibration measurements. A 1.12 ppm
209 $^{34}\text{SO}_2$ gas standard was used as the source of the sulfur standard addition. 1.85 ppb of $^{34}\text{SO}_2$
210 was added to sampled air flow during calibration measurements. The formic and acetic
211 acid calibration sources were permeation tubes (VICI Metronics) with emission rates of 91
212 and 110 ng min^{-1} , respectively. The emission rates were measured by scrubbing the output
213 of the permeation tube in deionized water via a gas impinge immersed in water, which was
214 then analyzed for formate and acetate using ion chromatography (Thermo Fisher
215 Scientific). Eight samples of each acid were analyzed over the course of the field study and
216 the standard deviations of the permeation rates were $\leq 6\%$. 6.75 ppb of formic acid and
217 5.87 ppb of acetic acid was added to sampled air flow during calibration measurements.
218 The CIMS instrument sensitivity measured by the $\text{F}_2^{34}\text{SO}_2^-$ ion signal (m/z 104) was
219 similarly applied to all the other measured species (except for formic and acetic acids)
220 using relative sensitivities determined in laboratory studies. The $\text{F}_2^{34}\text{SO}_2^-$ calibrant ion

221 signals were also used to calibrate ambient $F_2^{32}SO_2^-$ ion signals and determine ambient SO_2
222 concentrations as discussed in section 3.2.5.

223 **2.2.3. Laboratory calibration**

224 HNO_3 , oxalic, butyric, glycolic, propionic and valeric acid standard addition
225 calibrations were performed in post-field laboratory work. The response of the CIMS acid
226 signals were measured relative to the sensitivity of $^{34}SO_2$ in these calibration
227 measurements. The HNO_3 calibration source was a permeation tube (KIN-TEK) with a
228 permeation rate of 39 ng min^{-1} , which was measured using UV optical absorption (Neuman
229 et al., 2003). Solid or liquid samples of oxalic (Sigma Aldrich, $\geq 99 \%$), butyric (Sigma
230 Aldrich, $\geq 99 \%$), glycolic (Sigma Aldrich, 99 %), propionic (Sigma Aldrich, $\geq 99.5 \%$)
231 and valeric (Sigma Aldrich, $\geq 99 \%$) acids were used in calibration measurements. The acid
232 sample was placed in a glass impinger, which was immersed in an ice bath to provide a
233 constant vapor pressure. A flow of 6 to 10 mL min^{-1} of N_2 was passed over the organic acid
234 in the glass impinger. This organic acid air stream was then diluted with varying flows of
235 N_2 (1 to 5 L min^{-1}) to achieve different mixing ratios of the organic acid. Mixing ratios
236 were calculated from either the acid's emission rate from the impinger or the acid's vapor
237 pressure. The emission rate of gas-phase oxalic acid from the impinger was measured by
238 scrubbing the output in deionized water using the same method for calibrating the formic
239 and acetic acid permeation tubes, followed by ion chromatography analysis for oxalate.
240 Three samples were analyzed and the emission rate was determined to be 14 ng min^{-1} with
241 a standard deviation of $< 5 \%$. The vapor pressures of butyric and propionic acids at $0 \text{ }^\circ\text{C}$
242 were measured using a capacitance manometer (MKS Instruments). The vapor pressures
243 of glycolic and valeric acids at $0 \text{ }^\circ\text{C}$ were estimated using their literature vapor pressures
244 at $25 \text{ }^\circ\text{C}$ and enthalpies of vaporization (Daubert and Danner, 1989; Lide, 1995; Acree and
245 Chickos, 2010).

246 Attempts to generate a calibration plot for pyruvic acid using its liquid sample
247 (Sigma Aldrich, 98 %) and the setup described above were unsuccessful as this acid was
248 found to interact very strongly with surfaces. Glyoxylic acid calibrations were not
249 performed due to the presence of impurities in the glyoxylic acid monohydrate solution
250 used (Sigma Aldrich, 98 %), which resulted in the appearance of ions not attributed to

251 glyoxylic acid. We attempted to generate calibration plots for malonic (Sigma Aldrich, \geq
252 99.5 %), succinic (Sigma Aldrich, 99 %) and glutaric (Sigma Aldrich, 99 %) acids by
253 passing N₂ over their solid samples at room temperature. However, it was not possible to
254 generate large enough gas phase concentrations for calibration since these organic acids
255 have very low vapor pressures.

256 2.2.4. Detection limits and measurement uncertainties

257 The detection limits of the organic acids were estimated as 3 times the standard
258 deviation values (3σ) of the ion signals measured during background mode. Although each
259 background measurement period lasted ~4 min, ion signals of the different organic acids
260 took up to 1.5 min to stabilize during the switch between ambient, calibration and
261 background measurements during the field study. Thus, ion signals measured during the
262 first 1.5 min were not included in the calculation of the average and standard deviation of
263 ion signals measured during background mode. Table 1 summarizes the average detection
264 limits of the organic acids for 2.5 min averaging periods which corresponds to the length
265 of a background measurement with a 4 % duty cycle for each m/z. The mean difference
266 between successive background measurements ranged from 1 to 40 ppt for the different
267 organic acids. Future work will focus on reducing the instrument background, and therefore
268 improving the detection limits of these organic acids.

Deleted: approximated from

Deleted: integration

Deleted: 0.04 s

269 The uncertainties (1σ) in our ambient measurements of formic, acetic and oxalic
270 acid concentrations originated from CIMS and IC calibration measurements. The IC
271 measurement uncertainty was estimated to be 10 %. For formic and acetic acids, which
272 were calibrated during the field study using permeation tubes, their CIMS measurement
273 uncertainties were estimated to be 6 and 7 %, respectively, based on one standard deviation
274 of the acids' calibrant ion signals. For oxalic acid which was calibrated in post-field
275 laboratory work, the CIMS measurement uncertainty was estimated to be 9 % based on one
276 standard deviation of the ³⁴SO₂ sensitivity (3 %), the acid's calibrant ion signals (7 %) and
277 linear fit of the calibration curve (5 %). Hence, the uncertainties in our ambient
278 measurements of formic, acetic and oxalic acid concentrations were estimated to be 12, 12
279 and 14 %, respectively.

283 For nitric acid which was calibrated in post-field laboratory work using a
284 permeation tube and UV optical absorption, the uncertainty in its ambient concentrations
285 was estimated to be 13 % based on uncertainties in UV absorption measurements (10 %)
286 and one standard deviation of the acid's UV absorption signals (3 %), ³⁴SO₂ sensitivity (3
287 %) and acid's calibrant ion signals (8 %). For butyric and propionic acids which were
288 calibrated in post-field laboratory work using vapor pressures measured by a capacitance
289 manometer, the uncertainties in their ambient concentrations were estimated to be 14 %
290 based on the vapor pressure measurement uncertainty (10 %) and one standard deviation
291 of the ³⁴SO₂ sensitivity (3 %), the acids' calibrant ion signals (8 %) and linear fits of the
292 acids' calibration curves (3 %). For glycolic and valeric acids which were calibrated in
293 post-field laboratory work using vapor pressures estimated from literature vapor pressures
294 at 25 °C and enthalpies of vaporization, the uncertainties in their ambient concentrations
295 were likely significantly larger compared to the other measured organic acids due to
296 uncertainties in their estimated vapor pressures. We estimate the uncertainties in ambient
297 concentrations of glycolic and valeric acids to be 22 % based on an assumed vapor pressure
298 uncertainty of 20 % and one standard deviation of the ³⁴SO₂ sensitivity (3 %), the acids'
299 calibrant ion signals (8 %) and linear fits of the acids' calibration curves (2 %).

300 2.3. WSOC_g measurements

301 WSOC_g was measured with a MIST chamber coupled to a total organic carbon
302 (TOC) analyzer (Sievers 900 series, GE Analytical Instruments). Ambient air first passed
303 through a Teflon filter (45 mm diameter, 2.0 μm pore size, Pall Life Sciences) to remove
304 particles in the air stream. This filter was changed every 3 to 4 days. The particle-free air
305 was then pulled into a glass Mist Chamber filled with ultrapure deionized water at a flow
306 rate of 20 L min⁻¹. The MIST chamber scrubbed soluble gases with Henry's law constants
307 greater than 10³ M atm⁻¹ into deionized water (Spaulding et al., 2002). The resulting liquid
308 samples from the MIST chamber were analyzed by the TOC analyzer. The TOC analyzer
309 converted the organic carbon in the liquid samples to carbon dioxide using UV light and
310 chemical oxidation. The carbon dioxide formed was then measured by conductivity. The
311 amount of organic carbon in the liquid samples is proportional to the measured increase in
312 conductivity of the dissolved carbon dioxide. Each WSOC_g measurement lasted 4 min.

313 Background WSOC_g measurements were performed for 45 min every 12 h by stopping the
314 sample air flow and rinsing the sampling lines with deionized water. The TOC analyzer
315 was calibrated using different concentrations of sucrose (as specified by the instrument
316 manual) before and after the field study. The limit of detection was 0.4 µgC m⁻³. The
317 measurement uncertainty was estimated to be 10 % based on uncertainties in the sample
318 air flow, liquid flow and TOC analyzer uncertainty. The MIST chamber and upstream
319 particle filter were located in an air-conditioned building so were generally below ambient
320 temperature. Hence, evaporation of collected particles (which will lead to positive artifacts
321 in WSOC_g measurements) are not expected to be significant.

322 2.4. Supporting gas measurements

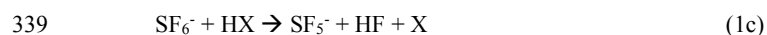
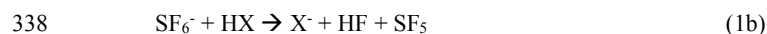
323 Supporting gas measurements were provided by a suite of instruments operated by
324 the SEARCH network. A non-dispersive infrared spectrometer (Thermo Fisher Scientific)
325 provided hourly CO measurements. A UV absorption analyzer (Thermo Fisher Scientific)
326 provided hourly O₃ measurements. A gas chromatography-flame ionization detector (GC-
327 FID, Agilent Technologies) provided hourly VOC measurements.

328 3. Results and discussion

329 3.1. General SF₆⁻ CIMS field performance

330 3.1.1. SF₆⁻ ion chemistry with organic acids

331 CIMS measurements of atmospheric constituents use ion-molecule reactions to
332 selectively ionize compounds of interest in the complex matrix of ambient air and produce
333 characteristic ions. The reactions of SF₆⁻ with the organic acids (HX) proceed through
334 reactions 1a to 1c, and gave similar products to those reported previously for SF₆⁻ reactions
335 with inorganic acids (Huey et al., 1995): SF₅⁻, X⁻ and X⁻•HF where X⁻ is the conjugate base
336 of the organic acid (reactions 1a-c).



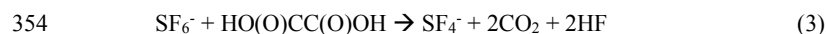
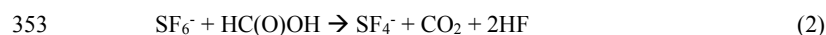
Deleted: The underlying aspect of

Deleted: is the

Deleted: of

343 The effective branching ratios of the SF₅⁻, X⁻ and X⁻•HF product ions can be impacted by
344 the field strength of the CDC. The SF₅⁻ ion (m/z 127, reaction 1c) is a common reaction
345 product of the reactions of SF₆⁻ with many species and is probably thermodynamically
346 driven by the formation of HF (Huey et al., 1995). Unfortunately, the production of SF₅⁻
347 does not allow for the selective detection of any atmospheric species. In addition, the larger
348 the branching ratio of the SF₅⁻ channel, the lower the CIMS sensitivity to an individual acid
349 since the effective rate constants for the X⁻ and X⁻•HF channels are lower.

350 The reaction of SF₆⁻ with formic acid and oxalic acid also produced SF₄⁻ ions (m/z
351 108). These reactions are probably thermodynamically driven by the formation of CO₂ and
352 HF:



355 We used the X⁻ and/or X⁻•HF ions to determine ambient organic acid concentrations
356 since these ions are characteristic of the individual acids. For all the organic acids, the X⁻
357 •HF ion signal is substantially lower than that of the X⁻ ion for the conditions in this study.
358 However, this is probably largely due to the relatively high collision energy used in the
359 CDC which led to efficient dissociation of the fluoride adducts to form X⁻ ions.
360 Consequently, only the proton transfer channel (1b) is used to quantify most of the organic
361 acids in the field study. The exceptions are formic and acetic acid as discussed in section
362 3.2.1 and 3.2.2

363 _____ Table 1 shows a summary of the sensitivities of X⁻ and X⁻•HF ions of organic acids.
364 The average sensitivities of the HCOO⁻ (m/z 45) and HCOO⁻•HF (m/z 65) ions of formic
365 acid were 1.29 ± 0.22 and 0.29 ± 0.05 Hz ppt⁻¹, respectively, while the average sensitivities
366 of the CH₃COO⁻ (m/z 59) and CH₃COO⁻•HF (m/z 79) ions of acetic acid were 1.46 ± 0.29
367 and 0.30 ± 0.06 Hz ppt⁻¹, respectively. A weak ²¹⁰Po ion source (< 1 mCi) was used by SF₆⁻
368 -CIMS instrument during the field study, hence these sensitivities will be substantially
369 higher if a stronger radioactive source is used. Nevertheless, these sensitivities are
370 compared to formic and acetic acid sensitivities measured by a high-resolution time-of-
371 flight chemical ionization mass spectrometer (Aerodyne Research Inc.) that utilized I-

Deleted: relative to that of the F₂³⁴SO₂⁻ ion

373 reagent ions during the field study. Although the formic acid sensitivity measured by I-
374 CIMS (1.33 ± 0.28 Hz ppt⁻¹) was comparable to that measured by SF₆⁻-CIMS, the acetic
375 acid sensitivity measured by I-CIMS (< 0.1 Hz ppt⁻¹) was substantially lower than that
376 measured by SF₆⁻-CIMS. Previous studies have similarly reported low acetic acid
377 sensitivity measured by I-CIMS (Aljawhary et al., 2013; Lee et al., 2014).

378 3.1.2. Characterization of interferences

379 SF₆⁻ is very sensitive to many trace atmospheric species but its reactions with water
380 vapor and O₃ when sampling ambient air can lead to issues both with selectivity and
381 stability. For example, SF₆⁻ reacts nonlinearly with water vapor to form a series of F•(HF)_n
382 cluster ions (Huey et al., 1995; Arnold and Viggiano, 2001). SF₆⁻ also reacts efficiently
383 with O₃ to form O₃⁻, which is rapidly converted to CO₃⁻ in ambient air (Slusher et al., 2001).
384 These reactions can deplete SF₆⁻ as well as form a variety of potentially interfering ions
385 from secondary reactions (e.g., F•(HF)_n and CO₃⁻ ions) that depend on more abundant
386 atmospheric species. For these reasons, efforts were made to minimize interferences by
387 limiting reaction times and the flow sampled into the CIMS. This was accomplished by
388 sampling only 0.3 L min⁻¹ of air through the variable orifice into the flow tube and
389 maintaining the flow tube at a low pressure (~13 mbar). The 0.3 L min⁻¹ sampled air flow
390 is diluted by 3.7 slpm of N₂/SF₆ flow in the flow tube. The ratio of the sampled air flow to
391 the N₂/SF₆ flow introduced into the flow tube is approximately 1:13. While the high N₂/SF₆
392 flow (3.7 slpm) passed through the radioactive source into the flow tube increased the SF₆⁻
393 reagent ion signal, the high dilution of the sampled air flow in the flow tube reduced the
394 CIMS instrument sensitivity by decreasing the number density of the analytes.

395 _____ Figure 2 shows a mass spectrum of ambient air. Interference peaks at m/z 39 (F•
396 •(HF) and CO₃⁻, respectively) can be attributed to the presence of water and O₃,
397 respectively. The reagent ion ³²SF₆⁻ is present at m/z 146. The ³²SF₆⁻ reagent ion signal was
398 saturated, and this caused the sharp drop in the m/z 146 signal as shown in Fig. 2. Since
399 the ³²SF₆⁻ reagent ion signal was saturated for the entire field study, we monitored the ion
400 signal of its isotope ³⁴SF₆⁻ to determine if the reaction of SF₆⁻ with ambient water vapor
401 (5.92×10^{-6} to 2.19×10^{-5} g cm⁻³) and O₃ (2.1 to 82.4 ppb) depleted SF₆⁻ reagent ions.
402 Figure S2a shows the time series of the ³⁴SF₆⁻ ion signal and ambient water vapor

Deleted: reagent

404 concentration for the entire field study. Despite fluctuations in ambient water vapor and O₃
405 concentrations, the ³⁴SF₆⁻ ion signal was relatively constant for the entire field study with
406 a standard deviation of < 3%. This indicates that the reaction of SF₆⁻ with ambient water
407 vapor and O₃ did not significantly deplete the ³²SF₆⁻ reagent ions during the field study.

Deleted: reagent

Deleted: (

Deleted:)

408 The F₂³⁴SO₂⁻ ion signal was used to monitor the CIMS SO₂ sensitivity during the
409 field study. Figure S2b shows the time series of the F₂³⁴SO₂⁻/³⁴SF₆⁻ ion signal ratio obtained
410 in calibration measurements. There is a noticeable increase in the F₂³⁴SO₂⁻/³⁴SF₆⁻ ion signal
411 ratio on 28 Sept 2016, indicating an increase in the CIMS instrument sensitivity. The
412 increase in CIMS instrument sensitivity is due to the decrease in ambient water vapor
413 concentrations on 28 Sept 2016 (Fig. S2a). Previous laboratory and field studies showed
414 that this was due to the hydrolysis of F₂³⁴SO₂⁻, which led to the loss of this ion and
415 diminished sensitivity at higher levels of ambient water vapor (Arnold and Viggiano, 2001;
416 Slusher et al., 2001). However, the SO₂ sensitivity at F₂³⁴SO₂⁻ only varied within a factor
417 of two for the entire field study with a clear relationship to water vapor (Fig. S2c). The SO₂
418 sensitivity did not show any obvious dependence on ambient O₃ concentrations (Fig. S2d).

419 The formic (HCOO⁻ at m/z 45 and HCOO⁻•HF at m/z 65) and acetic (CH₃COO⁻
420 •HF at m/z 79) acid ions did not show any obvious dependence on ambient water vapor
421 and O₃ concentrations during calibration measurements (Fig. S3). Therefore, we do not
422 expect the sensitivities of the X⁻ and X⁻•HF ions of the studied organic acids to depend on
423 ambient water vapor and O₃ concentrations. We accounted for water vapor dependence of
424 the F₂³⁴SO₂⁻ ion signal in our post-field calibrations where the response of the CIMS acid
425 signals were measured relative to the of the ³⁴SO₂ sensitivity.

426 **3.1.3. Background and calibration measurements**

427 Figure S4 shows an example of the CIMS instrument response during the switch
428 between background, calibration and ambient measurements of formic and acetic acids
429 during the field study. The 13 s time resolution data was used to determine the CIMS
430 instrument time response. Formic (m/z 45, 65 and 108) and acetic (m/z 79) acid ion signals
431 took ~1.5 min to reach a steady state after switches between ambient, calibration and
432 background measurements (Figs. S4a and S4c).

436 The decays in the formic and acetic acid ion signals and times required for them to
437 reach steady state after the removal of calibration gases during the switch from standard
438 addition calibration to ambient sampling were used to determine the CIMS response time.
439 The signal decays were fitted using double exponential functions. For formic acid, the m/z
440 45, 65 and 108 ion signals decayed to $1/e^2$ in 37 ± 2 , 33 ± 2 and 32 ± 2 s, respectively (Fig.
441 S4b). For acetic acid, the m/z 79 ion signal decayed to $1/e^2$ in 42 ± 2 s (Fig. S4d).

442 3.2. Ambient measurements

443 3.2.1. Formic acid

444 Figure 2 shows typical mass spectra obtained under background and measurement
445 modes during the field study. The SF_6^- reagent ion is present at m/z 146. One of the
446 prominent species in the mass spectrum is formic acid, which is detected as HCOO^- and
447 $\text{HCOO}\cdot\text{HF}$ at m/z 45 and 65, respectively. Our laboratory studies demonstrated that the
448 reaction of formic acid with SF_6^- also produced a large fraction of SF_4^- ions at m/z 108.
449 The reaction of SF_6^- with oxalic acid also produced SF_4^- ions, but its SF_4^- product ion yield
450 is low and gas phase oxalic acid is not present in large concentrations. In addition, SF_4^- is
451 present in the mass spectrum obtained under background mode but the SF_4^- background
452 ion signals are lower than those typically observed in measurement mode at the Yorkville
453 site. As a result, we determined the ambient formic acid concentrations using the HCOO^- ,
454 $\text{HCOO}\cdot\text{HF}$ and SF_4^- ions. Figure 3a shows a scatter plot comparing the ambient formic
455 acid concentrations measured at Yorkville using the HCOO^- , $\text{HCOO}\cdot\text{HF}$ and SF_4^- ions.
456 Linear regression analysis reveals that the formic acid concentrations determined by the
457 three ions are highly correlated ($R^2 = 0.99$) with slopes exhibiting a near 1:1 correlation.
458 The excellent correlation between these three ions and the agreement with laboratory data
459 indicates that formic acid is selectively measured by this method.

460 The time series of formic acid, temperature and solar radiation measured at
461 Yorkville are shown in Fig. 3b. Formic acid concentrations ranged from 40 ppt to 4 ppb
462 during the field study, with strong and consistent diurnal trends. The day-to-day variability
463 in formic acid concentrations are associated with changes in solar radiation and
464 temperature. Higher formic acid concentrations are measured during warm and sunny days,

465 similar to formic acid measurements performed in Centreville, rural Alabama during the
466 2013 Southern Oxidant Aerosol Study (SOAS) (Brophy and Farmer, 2015; Millet et al.,
467 2015). Figure 3c shows the study-averaged diurnal profiles of formic acid and solar
468 irradiance. Formic acid started to increase at 7:30, which coincided with a sharp increase
469 in solar irradiance. Concentrations continued to increase throughout the day and peaked at
470 18:30, which coincided with the approximate time just before solar irradiance reached zero.
471 Formic acid then decreased continuously throughout the night.

472 The immediate early-morning increase in formic acid observed in this field study
473 is similar to that seen during the SOAS study (Millet et al., 2015). However, there are some
474 differences in the formic acid diurnal cycles measured in this field study and the SOAS
475 study. Formic acid peaked at 15:30 during SOAS, approximately 3 hours before solar
476 irradiance decreased to zero. In contrast, formic acid concentrations only started to
477 decrease at sunset (at 19:30) in this study. This suggests that there may be differences in
478 the types and/or magnitudes of formic acid sources and sinks in this two field studies. Land
479 cover and/or land use differences may have contributed to differences in formic acid
480 sources and sinks at the Centreville and Yorkville field sites. The area surrounding the
481 Yorkville field site is covered primarily by hardwood mixed with farmland and open
482 pastures. In contrast, the Centreville field site is surrounded by forests comprised of mixed
483 oak-hickory and loblolly trees (Hansen et al., 2003). It is also possible that seasonal
484 differences contributed to differences in formic acid sources and sinks in the two field
485 studies. The SOAS campaign took place in the middle of summer (1 June to 15 July 2013)
486 when biogenic emissions are typically higher while this field study took place in early fall
487 when biogenic emissions are lower due to cooler temperatures. For example, the average
488 concentration of isoprene (a formic acid source) in this study (1.21 ppb) is lower than that
489 in SOAS (1.92 ppb (Millet et al., 2015)). Despite these differences, our overall results are
490 similar to the formic acid measurements performed in SOAS in both magnitude and diurnal
491 variability.

492 3.2.2. Acetic acid

493 Acetic acid is detected with SF_6^- as CH_3COO^- and $\text{CH}_3\text{COO}\cdot\text{HF}$ at m/z 59 and 79,
494 respectively. However, these ions are subject to interferences from the reaction of SF_6^- with

495 water vapor present in the sampled ambient air. Two of these interfering ions $F\cdot(HF)_2$ and
496 $F\cdot(HF)_3$ occur at m/z 59 and 79, respectively. As discussed earlier, we minimized the
497 impact of these interferences by diluting the sample flow into the CIMS and running the
498 CDC at a high collision energy to dissociate the HF cluster ions. As expected from cluster
499 bond strengths, we found that larger HF cluster ions dissociated more easily than smaller
500 ones. For example, at a CDC electric field of $\sim 113 \text{ V cm}^{-1}$ (the configuration used in this
501 field study), virtually all of the $F\cdot(HF)_3$ cluster ions dissociated while very few of the $F\cdot$
502 (HF) cluster ions dissociated. This indicates that the m/z 79 channel for acetic acid is more
503 immune to interference from water vapor than the m/z 59 channel. This is supported by the
504 observation that the background ion signal at m/z 59 ($R^2 = 0.50$) is more highly correlated
505 with ambient water vapor concentrations than the background ion signal of m/z 79 ($R^2 =$
506 0.30). In addition, the m/z 59 ion is subjected to interference from the reaction of SF_6^- with
507 O_3 present in the sampled ambient air. SF_6^- reacts with O_3 in the presence of CO_2 to form
508 CO_3^- at m/z 60 (Slusher et al., 2001). As shown in Fig. 2, the large CO_3^- peak at m/z 60 is
509 a potential interference to the m/z 59 signal. As the background scrubber also removed O_3
510 from the ambient air, there is a large difference in the m/z 60 ion signal between the
511 measurement and background modes ($\sim 100,000 \text{ Hz}$). Thus, even a few percent bleed over
512 of m/z 60 to m/z 59 can lead to an over-estimation of ambient acetic acid concentrations.
513 For these reasons, we used m/z 79 ($X\cdot HF$) to determine ambient acetic acid concentrations
514 even though this channel has a lower sensitivity than the m/z 59 channel (X).

515 The time series of acetic acid, temperature and solar radiation measured at
516 Yorkville are shown in Fig. 4a. Acetic acid concentrations ranged from 30 ppt to 3 ppb
517 during the field study. The day-to-day variability in acetic acid concentrations resembled
518 the behavior of formic acid concentrations, with higher concentrations being measured
519 during warm and sunny days. Figure 4b shows the study-averaged diurnal profiles of acetic
520 acid and solar irradiance. The diurnal profile of acetic acid is similar to that of formic acid
521 with a more pronounced evening maximum. Acetic acid started to increase at 7:30 and
522 built up through the day, peaking at 19:30 and decreased continuously overnight. In
523 general, acetic acid concentrations are well correlated with ($R^2 = 0.67$) and comparable in
524 magnitude ($\sim 60\%$ on average) to formic acid. The study-averaged formic acid/acetic acid
525 concentration ratio (1.65) is comparable to ratios from previous field studies in rural and

526 urban environments (Talbot et al., 1988; Talbot et al., 1995; Granby et al., 1997; Khare et
527 al., 1999; Talbot et al., 1999; Baboukas et al., 2000; Singh et al., 2000; Kuhn et al., 2002;
528 Baasandorj et al., 2015; Millet et al., 2015).

529 3.2.3. Larger organic acids

530 In addition to formic acid and acetic acid, eight other ions were monitored during
531 the field study: m/z 73, 75, 87, 89, 101, 103, 117 and 131. These ions were chosen as they
532 had significant signals when ambient air was sampled and were not obviously formed from
533 SF_6^- reaction with water vapor or O_3 . Since the CIMS utilized in this study only had unit
534 mass resolution, these ions are the sum of all organic acid isomers and isobaric organic
535 acids of the same molecular weight as well as other product ions from species that might
536 react with SF_6^- . However, real-time ion chromatography measurements of aerosol
537 composition performed during the field study demonstrated the presence of particulate
538 oxalic, malonic, succinic and glutaric acids (Nah et al., 2018). For this reason, for m/z 89,
539 103, 117 and 131 ions, we assigned them as X^- ions of oxalic, malonic, succinic and glutaric
540 acids, respectively. As these organic acids have low vapor pressures, their gas-phase
541 concentrations are expected to be lower than their particle-phase concentrations, though
542 their gas-particle ratios will depend on thermodynamic conditions (Nah et al., 2018).
543 Particulate formic acid and acetic acid were also detected by ion chromatography during
544 the field study, but were at much lower concentrations relative to the gas phase (Nah et al.,
545 2018). For simplicity, we also denoted m/z 73, 75, 87 and 101 ions as X^- ions of propionic,
546 glycolic, butyric and valeric acids, respectively, for the remainder of this paper. These
547 organic acids have previously been measured in rural and urban environments (Kawamura
548 et al., 1985; Veres et al., 2011; Brophy and Farmer, 2015). However, we note that these
549 assignments are speculative. Post-field calibration measurements were used to estimate the
550 ambient concentrations of these organic acids.

551 Figure 5 shows the time series and diurnal profiles of oxalic, butyric, glycolic,
552 propionic and valeric acids measured during the field study. Daytime concentrations of
553 these organic acids ranged from a few tens of ppt to several hundred ppt. The time series
554 of ion signals (Hz) of malonic, succinic and glutaric acids normalized to the instrument's
555 sensitivity to $F_2^{34}SO_2$ (Hz ppb⁻¹) are shown in Fig. S3. The ion signals of these organic

556 acids are 1 to 2 orders of magnitude smaller than the sensitivity of the $F_2^{34}SO_2^-$ ion (study-
557 averaged sensitivity = 2928 ± 669 Hz ppb⁻¹), resulting in these ratios to be less than 1.

558 Concentrations of these organic acids are not available since calibrations were not
559 performed for these compounds. The eight organic acids displayed very similar day-to-day
560 variability as formic and acetic acids, with higher concentrations (or ion signals) being
561 measured on warm and sunny days. The diurnal profiles of all the measured organic acids
562 have similar diurnal trends, with their concentrations reaching a maximum between 17:30
563 and 19:30 and rapidly decreasing after sunset.

564 **3.2.4. Comparison with WSOC_g**

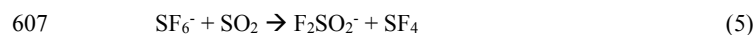
565 WSOC_g measurements were performed during the field study using a MIST
566 chamber coupled to a TOC analyzer. The study average WSOC_g was 3.6 ± 2.7 $\mu\text{gC m}^{-3}$,
567 slightly lower than that measured during the SOAS study (4.9 $\mu\text{gC m}^{-3}$) (Xu et al., 2017),
568 and approximately four times lower than that measured in urban Atlanta, Georgia (13.7
569 $\mu\text{gC m}^{-3}$) (Hennigan et al., 2009). Despite being comparable in magnitude, the diurnal
570 profiles of WSOC_g measured in this study and the SOAS study are different. WSOC_g
571 measured in the SOAS study decreased at sunset, while WSOC_g measured in this study
572 decreased 2 hours after sunset. Differences in WSOC_g concentrations and diurnal profiles
573 at the three different sites may be due to differences in emission sources as a result of
574 different measurement periods, land use and/or land cover.

575 To estimate the fraction of WSOC_g that is comprised of organic acids, the total
576 organic carbon contributed by formic, acetic, oxalic, butyric, glycolic, propionic and
577 valeric acids is compared to the WSOC_g measurements. We emphasize that the ion peak
578 assignment of some of these organic acids are speculative. Hence, this comparison
579 primarily serves as a zeroth order check to determine if the peak assignments are plausible.
580 Figures 6a and 6b show the time series and diurnal profiles of WSOC_g and the organic
581 carbon contributed by the measured organic acids. Formic and acetic acids comprised
582 majority of the total organic carbon contributed by the measured organic acids (study
583 averages of 31 and 38 %, respectively). Assuming that the ion peak assignments are correct
584 and the measured organic acids are completely water-soluble, the carbon mass fraction of
585 WSOC_g comprised of these organic acids ranged from 7 to 100 %. Based on the orthogonal

586 distance regression slope shown in Fig. 6c, the study-averaged carbon mass fraction of
587 WSOC_g comprised of the measured organic acids is 30 %. The total organic carbon
588 contributed by the measured organic acids are moderately correlated with WSOC_g (R² =
589 0.38). This is likely due to the presence of other water-soluble gas phase species (with
590 different day-to-day variability from the organic acids) that contribute to the WSOC_g. This
591 is supported by slight differences in the diurnal profiles of WSOC_g and the organic carbon
592 contributed by the organic acids (Fig. 6b). While the diurnal profiles of WSOC_g and the
593 organic carbon contributed by the organic acids have similar general shapes, WSOC_g
594 peaked at 21:30, approximately 2 hours after the solar irradiance have decreased to zero.
595 In contrast, the organic carbon contributed by the organic acids start to decrease at sunset
596 (at 19:30).

597 3.2.5. SO₂ and HNO₃ observations

598 In addition to evaluating the field performance of the SF₆⁻ CIMS technique in gas-
599 phase organic acid measurements, another focus of this study was to investigate the
600 possible sources of the measured organic acids. For this reason, HNO₃ and SO₂ (two
601 common anthropogenic tracers) were also measured by SF₆⁻ CIMS during the field study.
602 Correlations between the concentrations of organic acids and those of HNO₃ and SO₂ were
603 then examined to determine if the organic acids were anthropogenic in nature (section 3.3).
604 While their reactions with SF₆⁻ have multiple product channels (Huey et al., 1995), only
605 the NO₃⁻•HF (m/z 82) and F₂SO₂⁻ (m/z 102) ions were used for quantitative purposes:



608 Figure S4 shows the time series of SO₂ and HNO₃ measured during the field study.
609 As expected at a rural site, SO₂ and HNO₃ concentrations are low most of the time (study
610 averages of 230 and 180 ppt, respectively). However, there were occasional periods when
611 the site was impacted by anthropogenic pollution. In particular, there are spikes in both
612 SO₂ and HNO₃ concentrations throughout the study that corresponded to the site being
613 impacted by power plant or urban emissions. Outside of these anthropogenic spikes, HNO₃

614 showed a clear diurnal profile with a maximum at approximately 12:30, consistent with
615 local photochemical production.

616 **3.3. Potential sources of organic acids**

617 Correlation analysis on organic acid concentrations can provide insights on their
618 sources. Figure 7 shows that the concentration of formic acid is strongly correlated with
619 those of the other measured organic acids ($R^2 = 0.68$ to 0.89). This suggests that these
620 organic acids have the same or similar sources at Yorkville. The sources of organic acids
621 can be biogenic or anthropogenic in nature. To determine if the primary sources of organic
622 acids are of biogenic or anthropogenic origin, we first examined the correlations of organic
623 acid concentrations with those of anthropogenic pollutants CO, SO₂, O₃ and HNO₃. CO
624 and SO₂ are common tracers for combustion sources. The organic acid concentrations are
625 poorly correlated with CO (Fig. S5, $R^2 = 0.03$ to 0.15) and SO₂ (Fig. S6, $R^2 = 0.01$ to 0.24),
626 indicating that primary emissions from combustion are a minor source of organic acids in
627 Yorkville. HNO₃ and O₃ are common photochemical tracers of urban air masses. The
628 organic acid concentrations are weakly correlated with O₃ (Fig. S7, $R^2 = 0.11$ to 0.32) and
629 HNO₃ (Fig. S8, $R^2 = 0.33$ to 0.56). In addition, there is no noticeable increase in organic
630 acid concentrations during periods of elevated CO, SO₂, O₃ and HNO₃ concentrations when
631 the site was impacted by pollution plumes. Together, these results indicate that the primary
632 sources of organic acids in Yorkville are likely not anthropogenic in nature.

633 Diurnal profiles of the measured organic acids suggest that their sources are linked
634 to higher daytime temperatures and/or photochemical processes. Figure 8 compares the
635 concentrations of organic acids against ambient temperatures measured during the study.
636 Since there was a noticeable decrease in mean ambient temperatures starting on 28 Sept
637 2016, we grouped the datasets into two time periods (3 to 27 Sept and 28 Sept to 12 Oct)
638 to better evaluate the effect of temperature on organic acid concentrations. The average
639 temperature in the first time period (3 to 27 Sept) is 24.8 °C (32.6 °C max, 18.1 °C min),
640 while the average temperature in the second time period (28 Sept to 12 Oct) is 19.5 °C
641 (28.4 °C max, 9.5 °C min). We find that organic acid concentrations are on average higher
642 and more highly correlated with temperatures in the warmer first time period ($R^2 = 0.40$ to

643 0.63) compared to the cooler second time period ($R^2 = 0.18$ to 0.59). These observations
644 can be explained by temperature-dependent emissions of organic acids and their BVOC
645 precursors. Previous studies have shown that emissions of organic acids and their BVOC
646 precursors depend strongly on light and temperature, with substantially lower
647 concentrations being emitted in the dark and/or at low temperatures (Kesselmeier et al.,
648 1997; Kesselmeier, 2001; Sindelarova et al., 2014). We find that the concentration of
649 isoprene, which was the dominant BVOC in Yorkville, has a somewhat similar diurnal
650 profile as the organic acids and decreased with temperature on 28 Sept 2016 (Fig. S9). In
651 addition, the concentrations of formic and acetic acids are moderately correlated with that
652 of isoprene ($R^2 = 0.42$ and 0.40 , respectively) (Fig. S10).

653 Multiphase photochemical aging of ambient organic aerosols can also be a source
654 of gas-phase organic acids (Eliason et al., 2003; Ervens et al., 2004; Molina et al., 2004;
655 Lim et al., 2005; Park et al., 2006; Walser et al., 2007; Sorooshian et al., 2007; Vlasenko
656 et al., 2008; Pan et al., 2009; Sorooshian et al., 2010). Organic acids may be formed in the
657 particle phase during organic aerosol photochemical aging, with subsequent volatilization
658 into the gas phase. Real-time ion chromatography measurements of aerosol composition
659 demonstrated the presence of particulate formic, acetic, oxalic, malonic, succinic and
660 glutaric acids (Nah et al., 2018). However, since the ratios of gas-phase formic and acetic
661 acid mass concentration to the total organic aerosol mass concentration are large (study
662 averages of 40 and 35 %, respectively) (Nah et al., 2018), it is unlikely that organic aerosol
663 photochemical aging is a large source of formic and acetic acids. In contrast, the ratios of
664 gas-phase oxalic, malonic, succinic and glutaric acids mass concentration to the total
665 organic aerosol mass concentration are small, suggesting that organic aerosol
666 photochemical aging may be an important source of these gas-phase organic acids.

667 In summary, the temperature dependence and diurnal profile of organic acid
668 concentrations combined with poor correlations between organic acid concentrations and
669 those of anthropogenic pollutants CO , SO_2 , O_3 and HNO_3 strongly suggest that the primary
670 sources of gas-phase organic acids at Yorkville are biogenic in nature. However, our data
671 alone does not allow us to determine if the organic acids are a result of direct emissions or
672 photochemical oxidation of other BVOC emissions and/or organic aerosols. Partitioning

673 of these organic acids between the gas and particle phases will be discussed in a
674 forthcoming paper (Nah et al., 2018).

675 4. Summary

676 SF_6^- reacted with all of the studied organic acids to produce product ions that were
677 characteristic of the individual acids (i.e., X^- or $\text{X}\cdot\text{HF}$). These reactions all occurred at less
678 than the maximum collisional rate due to significant yields of SF_5^- and SF_4^- , which reduced
679 the sensitivity of the method. For the conditions employed in this study, the sensitivities of
680 X^- and $\text{X}\cdot\text{HF}$ ions of the organic acids relative to that of the $\text{F}_2^{34}\text{SO}_2^-$ ion (study-averaged
681 sensitivity $2928 \pm 669 \text{ Hz ppb}^{-1}$) ranged from 0.04 to 2.18. The detection limits of the
682 organic acids were approximated from 3 times the standard deviation values (3σ) of the ion
683 signals obtained during background measurements. Reasonable limits of detection for 2.5
684 min integration periods (1 to 60 ppt) were obtained for all the organic acids studied. Water
685 vapor and O_3 can lead to interferences with this method but for the conditions employed in
686 this study, they were largely limited to acetic acid measurements at m/z 59. However,
687 fluctuations in ambient water vapor can also lead to changes in sensitivity for the detection
688 of some species (e.g., SO_2). Uncertainties in organic acid concentrations originate primarily
689 from calibration measurements and ranged from 9 to 22 %. Overall, the tractable mass
690 spectra obtained by the SF_6^- CIMS method coupled with reasonable limits of detection and
691 the high correlations observed between the individual organic acids demonstrated the
692 potential of this method. Obvious next steps for the SF_6^- CIMS method are to compare it
693 to other measurement methods for organic acids and to deploy the SF_6^- ion chemistry to a
694 higher resolution time-of-flight mass spectrometer to reduce the potential for interferences.

695 The SF_6^- CIMS method was deployed for measurements of gas phase organic acids
696 in a mixed forest-agricultural area in Yorkville, Georgia from Sept to Oct 2016. The
697 organic acids measured in the field study were formic and acetic acids. In addition,
698 measurements tentatively assigned to oxalic, butyric, glycolic, propionic, valeric, malonic,
699 succinic and glutaric acids were performed. Ambient concentrations of these organic acids
700 ranged from a few ppt to several ppb. All the organic acids exhibited similar strong diurnal
701 trends. Organic acid concentrations built up throughout the day, peaked between 17:30 and
702 19:30 before decreasing continuously overnight. Strong correlations between organic acid

703 concentrations indicated that these organic acids likely have the same or similar sources at
704 Yorkville. We concluded that the organic acids were likely not due to anthropogenic
705 emissions since they were poorly correlated with anthropogenic pollutants and their
706 concentrations were not elevated when the site was impacted by pollution plumes. Higher
707 organic acid concentrations were measured during warm and sunny days. Organic acid
708 concentrations were strongly correlated with temperature during the first month of the
709 study when ambient temperatures were high. Together, our results suggested that the
710 primary sources of organic acids at Yorkville were biogenic in nature. Direct biogenic
711 emissions of organic acids and/or their BVOC precursors were likely enhanced at high
712 ambient temperatures, resulting in the observed variability of organic acid concentrations.
713 Another potential source is the production of organic acids in the particle phase from the
714 multiphase photochemical aging of organic aerosols followed by evaporation to the gas
715 phase, though this source is likely not a large source of formic and acetic acids. However,
716 given the inability of current models and photochemical mechanisms to explain formic acid
717 observations in the Southeastern U.S. (Millet et al., 2015), it is unlikely that our
718 observations of formic acid and larger organic acids can be explained as well. Further work
719 (i.e., laboratory, field and modeling studies) is needed to determine how organic acids are
720 formed in the atmosphere.

721 **5. Acknowledgements**

722 The authors thank Eric Edgerton (Atmospheric Research and Analysis, Inc.) for
723 providing CO, O₃ and VOC measurements and meteorological data.

724 **6. Funding**

725 This publication was developed under US Environmental Protection Agency (EPA)
726 STAR Grant R835882 awarded to Georgia Institute of Technology. It has not been
727 formally reviewed by the EPA. The views expressed in this document are solely those of
728 the authors and do not necessarily reflect those of the EPA. EPA does not endorse any
729 products or commercial services mentioned in this publication.

730 **7. Competing financial interests**

731 The authors declare no competing financial interests.

732 **8. Data availability**

733 Data can be accessed by request (greg.huey@eas.gatech.edu).

734 **9. References**

Deleted: 8

735 Acree, W., and Chickos, J. S.: Phase Transition Enthalpy Measurements of Organic and
736 Organometallic Compounds. Sublimation, Vaporization and Fusion Enthalpies From 1880
737 to 2010, J. Phys. Chem. Ref. Data, 39, 942, 10.1063/1.3309507, 2010.

738 Aljawhary, D., Lee, A. K. Y., and Abbatt, J. P. D.: High-resolution chemical ionization
739 mass spectrometry (ToF-CIMS): application to study SOA composition and processing,
740 Atmospheric Measurement Techniques, 6, 3211-3224, 10.5194/amt-6-3211-2013, 2013.

741 Andreae, M. O., Talbot, R. W., Andreae, T. W., and Harriss, R. C.: Formic and Acetic
742 Acid over the Central Amazon Region, Brazil. 1. Dry Season, Journal of Geophysical
743 Research-Atmospheres, 93, 1616-1624, 10.1029/JD093iD02p01616, 1988.

744 Arnold, S. T., and Viggiano, A. A.: Turbulent ion flow tube study of the cluster-mediated
745 reactions of SF₆- with H₂O, CH₃OH, and C₂H₅OH from 50 to 500 torr, J. Phys. Chem.
746 A, 105, 3527-3531, 10.1021/jp003967y, 2001.

747 Baasandorj, M., Millet, D. B., Hu, L., Mitroo, D., and Williams, B. J.: Measuring acetic
748 and formic acid by proton-transfer-reaction mass spectrometry: sensitivity, humidity
749 dependence, and quantifying interferences, Atmospheric Measurement Techniques, 8,
750 1303-1321, 10.5194/amt-8-1303-2015, 2015.

751 Baboukas, E. D., Kanakidou, M., and Mihalopoulos, N.: Carboxylic acids in gas and
752 particulate phase above the Atlantic Ocean, Journal of Geophysical Research-
753 Atmospheres, 105, 14459-14471, 10.1029/1999jd900977, 2000.

754 Brophy, P., and Farmer, D. K.: A switchable reagent ion high resolution time-of-flight
755 chemical ionization mass spectrometer for real-time measurement of gas phase oxidized

757 species: characterization from the 2013 southern oxidant and aerosol study, *Atmospheric*
758 *Measurement Techniques*, 8, 2945-2959, 10.5194/amt-8-2945-2015, 2015.

759 Carlton, A. G., Turpin, B. J., Lim, H. J., Altieri, K. E., and Seitzinger, S.: Link between
760 isoprene and secondary organic aerosol (SOA): Pyruvic acid oxidation yields low volatility
761 organic acids in clouds, *Geophys. Res. Lett.*, 33, 4, 10.1029/2005gl025374, 2006.

762 Chebbi, A., and Carlier, P.: Carboxylic acids in the troposphere, occurrence, sources, and
763 sinks: A review, *Atmospheric Environment*, 30, 4233-4249, 10.1016/1352-
764 2310(96)00102-1, 1996.

765 Crounse, J. D., McKinney, K. A., Kwan, A. J., and Wennberg, P. O.: Measurement of gas-
766 phase hydroperoxides by chemical ionization mass spectrometry, *Analytical Chemistry*,
767 78, 6726-6732, 10.1021/ac0604235, 2006.

768 Daubert, T. E., and Danner, R. P.: Physical and thermodynamic properties of pure
769 chemicals: data compilation, Taylor & Francis, Washington, DC, 1989.

770 Eliason, T. L., Aloisio, S., Donaldson, D. J., Cziczo, D. J., and Vaida, V.: Processing of
771 unsaturated organic acid films and aerosols by ozone, *Atmospheric Environment*, 37, 2207-
772 2219, 10.1016/s1352-2310(03)00149-3, 2003.

773 Ervens, B., Feingold, G., Frost, G. J., and Kreidenweis, S. M.: A modeling study of aqueous
774 production of dicarboxylic acids: 1. Chemical pathways and speciated organic mass
775 production, *Journal of Geophysical Research-Atmospheres*, 109, 10.1029/2003jd004387,
776 2004.

777 Ervens, B., Carlton, A. G., Turpin, B. J., Altieri, K. E., Kreidenweis, S. M., and Feingold,
778 G.: Secondary organic aerosol yields from cloud-processing of isoprene oxidation
779 products, *Geophys. Res. Lett.*, 35, 10.1029/2007gl031828, 2008.

780 Galloway, J. N., Likens, G. E., Keene, W. C., and Miller, J. M.: The Composition of
781 Precipitation in Remote Areas of the World, *Journal of Geophysical Research-Oceans and*
782 *Atmospheres*, 87, 8771-8786, 10.1029/JC087iC11p08771, 1982.

783 Granby, K., Egelov, A. H., Nielsen, T., and Lohse, C.: Carboxylic acids: Seasonal variation
784 and relation to chemical and meteorological parameters, *Journal of Atmospheric*
785 *Chemistry*, 28, 195-207, 10.1023/a:1005877419395, 1997.

786 Grosjean, D.: Ambient Levels of Formaldehyde, Acetaldehyde, and Formic acid in
787 Southern Californic- Results of a One-year Base-line Study, *Environmental Science &*
788 *Technology*, 25, 710-715, 10.1021/es00016a016, 1991.

789 Hansen, D. A., Edgerton, E. S., Hartsell, B. E., Jansen, J. J., Kandasamy, N., Hidy, G. M.,
790 and Blanchard, C. L.: The southeastern aerosol research and characterization study: Part 1-
791 overview, *Journal of the Air & Waste Management Association*, 53, 1460-1471, 2003.

792 Hartmann, W. R., Santana, M., Hermoso, M., Andreae, M. O., and Sanhueza, E.: Diurnal
793 Cycles of Formic and Acetic Acids in the Northern Part of the Guayana Sheld, Venezuela,
794 *Journal of Atmospheric Chemistry*, 13, 63-72, 10.1007/bf00048100, 1991.

795 Hennigan, C. J., Bergin, M. H., Russell, A. G., Nenes, A., and Weber, R. J.: Gas/particle
796 partitioning of water-soluble organic aerosol in Atlanta, *Atmos. Chem. Phys.*, 9, 3613-
797 3628, 10.5194/acp-9-3613-2009, 2009.

798 Huey, L. G., Hanson, D. R., and Howard, C. J.: Reactions of SF₆- and I- with Atmospheric
799 Trace Gases, *Journal of Physical Chemistry*, 99, 5001-5008, 10.1021/j100014a021, 1995.

800 Huey, L. G., Tanner, D. J., Slusher, D. L., Dibb, J. E., Arimoto, R., Chen, G., Davis, D.,
801 Buhr, M. P., Nowak, J. B., Mauldin, R. L., Eisele, F. L., and Kosciuch, E.: CIMS
802 measurements of HNO₃ and SO₂ at the South Pole during ISCAT 2000, *Atmospheric*
803 *Environment*, 38, 5411-5421, 10.1016/j.atmosenv.2004.04.037, 2004.

804 Kawamura, K., Ng, L. L., and Kaplan, I. R.: Determination of Organic Acids (C₁-C₁₀) in
805 the Atmosphere, Motor Exhausts, and Engine Oils, *Environmental Science & Technology*,
806 19, 1082-1086, 10.1021/es00141a010, 1985.

807 Keene, W. C., Galloway, J. N., and Holden, J. D.: Measurement of Weak Organic Acidity
808 in Precipitation from Remote Areas of the World, *Journal of Geophysical Research-Oceans*
809 *and Atmospheres*, 88, 5122-5130, 10.1029/JC088iC09p05122, 1983.

810 Keene, W. C., and Galloway, J. N.: Organic Acidity in Precipitation of North America,
811 Atmospheric Environment, 18, 2491-2497, 10.1016/0004-6981(84)90020-9, 1984.

812 Kesselmeier, J., Bode, K., Hofmann, U., Muller, H., Schafer, L., Wolf, A., Ciccioli, P.,
813 Brancaleoni, E., Cecinato, A., Frattoni, M., Foster, P., Ferrari, C., Jacob, V., Fugit, J. L.,
814 Dutaur, L., Simon, V., and Torres, L.: Emission of short chained organic acids, aldehydes
815 and monoterpenes from *Quercus ilex* L. and *Pinus pinea* L. in relation to physiological
816 activities, carbon budget and emission algorithms, Atmospheric Environment, 31, 119-133,
817 10.1016/s1352-2310(97)00079-4, 1997.

818 Kesselmeier, J.: Exchange of short-chain oxygenated volatile organic compounds (VOCs)
819 between plants and the atmosphere: A compilation of field and laboratory studies, Journal
820 of Atmospheric Chemistry, 39, 219-233, 10.1023/a:1010632302076, 2001.

821 Khare, P., Kumar, N., Kumari, K. M., and Srivastava, S. S.: Atmospheric formic and acetic
822 acids: An overview, Reviews of Geophysics, 37, 227-248, 10.1029/1998rg900005, 1999.

823 Kim, S., Huey, L. G., Stickel, R. E., Tanner, D. J., Crawford, J. H., Olson, J. R., Chen, G.,
824 Brune, W. H., Ren, X., Leshner, R., Wooldridge, P. J., Bertram, T. H., Perring, A., Cohen,
825 R. C., Lefer, B. L., Shetter, R. E., Avery, M., Diskin, G., and Sokolik, I.: Measurement of
826 HO₂NO₂ in the free troposphere during the intercontinental chemical transport experiment
827 - North America 2004, Journal of Geophysical Research-Atmospheres, 112,
828 10.1029/2006jd007676, 2007.

829 Kuhn, U., Rottenberger, S., Biesenthal, T., Ammann, C., Wolf, A., Schebeske, G., Oliva,
830 S. T., Tavares, T. M., and Kesselmeier, J.: Exchange of short-chain monocarboxylic acids
831 by vegetation at a remote tropical forest site in Amazonia, Journal of Geophysical
832 Research-Atmospheres, 107, 18, 10.1029/2000jd000303, 2002.

833 Lee, B. H., Lopez-Hilfiker, F. D., Mohr, C., Kurten, T., Worsnop, D. R., and Thornton, J.
834 A.: An Iodide-Adduct High-Resolution Time-of-Flight Chemical-Ionization Mass
835 Spectrometer: Application to Atmospheric Inorganic and Organic Compounds,
836 Environmental Science & Technology, 48, 6309-6317, 10.1021/es500362a, 2014.

837 Liao, J., Sihler, H., Huey, L. G., Neuman, J. A., Tanner, D. J., Friess, U., Platt, U., Flocke,
838 F. M., Orlando, J. J., Shepson, P. B., Beine, H. J., Weinheimer, A. J., Sjostedt, S. J., Nowak,
839 J. B., Knapp, D. J., Staebler, R. M., Zheng, W., Sander, R., Hall, S. R., and Ullmann, K.:
840 A comparison of Arctic BrO measurements by chemical ionization mass spectrometry and
841 long path-differential optical absorption spectroscopy, *Journal of Geophysical Research-*
842 *Atmospheres*, 116, 10.1029/2010jd014788, 2011.

843 Lide, D. R.: *CRC handbook of chemistry and physics: a ready-reference book of chemical*
844 *and physical data*, CRC Press, Boca Raton, FL, 1995.

845 Lim, H. J., Carlton, A. G., and Turpin, B. J.: Isoprene forms secondary organic aerosol
846 through cloud processing: Model simulations, *Environmental Science & Technology*, 39,
847 4441-4446, 10.1021/es048039h, 2005.

848 Millet, D. B., Baasandorj, M., Farmer, D. K., Thornton, J. A., Baumann, K., Brophy, P.,
849 Chaliyakunnel, S., de Gouw, J. A., Graus, M., Hu, L., Koss, A., Lee, B. H., Lopez-Hilfiker,
850 F. D., Neuman, J. A., Paulot, F., Peischl, J., Pollack, I. B., Ryerson, T. B., Warneke, C.,
851 Williams, B. J., and Xu, J.: A large and ubiquitous source of atmospheric formic acid,
852 *Atmos. Chem. Phys.*, 15, 6283-6304, 10.5194/acp-15-6283-2015, 2015.

853 Molina, M. J., Ivanov, A. V., Trakhtenberg, S., and Molina, L. T.: Atmospheric evolution
854 of organic aerosol, *Geophys. Res. Lett.*, 31, 10.1029/2004gl020910, 2004.

855 Nah, T., Guo, H., Sullivan, A. P., Chen, Y., Tanner, D. J., Nenes, A., Russell, A., Ng, N.
856 L., Huey, L. G., and Weber, R. J.: Characterization of Aerosol Composition, Aerosol
857 Acidity and Organic Acid Partitioning at an Agriculture-intensive Rural Southeastern U.S.
858 Site, In *Preparation*, 2018.

859 Neuman, J. A., Ryerson, T. B., Huey, L. G., Jakoubek, R., Nowak, J. B., Simons, C., and
860 Fehsenfeld, F. C.: Calibration and evaluation of nitric acid and ammonia permeation tubes
861 by UV optical absorption, *Environmental Science & Technology*, 37, 2975-2981,
862 10.1021/es0264221, 2003.

863 Nguyen, T. B., Crouse, J. D., Teng, A. P., Clair, J. M. S., Paulot, F., Wolfe, G. M., and
864 Wennberg, P. O.: Rapid deposition of oxidized biogenic compounds to a temperate forest,
865 Proc. Natl. Acad. Sci. U. S. A., 112, E392-E401, 10.1073/pnas.1418702112, 2015.

866 Nolte, C. G., Solomon, P. A., Fall, T., Salmon, L. G., and Cass, G. R.: Seasonal and spatial
867 characteristics of formic and acetic acids concentrations in the southern California
868 atmosphere, Environmental Science & Technology, 31, 2547-2553, 10.1021/es960954i,
869 1997.

870 Nowak, J. B., Huey, L. G., Russell, A. G., Tian, D., Neuman, J. A., Orsini, D., Sjostedt, S.
871 J., Sullivan, A. P., Tanner, D. J., Weber, R. J., Nenes, A., Edgerton, E., and Fehsenfeld, F.
872 C.: Analysis of urban gas phase ammonia measurements from the 2002 Atlanta Aerosol
873 Nucleation and Real-Time Characterization Experiment (ANARChE), Journal of
874 Geophysical Research-Atmospheres, 111, 14, 10.1029/2006jd007113, 2006.

875 Orzechowska, G. E., and Paulson, S. E.: Photochemical sources of organic acids. 1.
876 Reaction of ozone with isoprene, propene, and 2-butenes under dry and humid conditions
877 using SPME, J. Phys. Chem. A, 109, 5358-5365, 10.1021/jp050166s, 2005.

878 Pan, X., Underwood, J. S., Xing, J. H., Mang, S. A., and Nizkorodov, S. A.:
879 Photodegradation of secondary organic aerosol generated from limonene oxidation by
880 ozone studied with chemical ionization mass spectrometry, Atmos. Chem. Phys., 9, 3851-
881 3865, 10.5194/acp-9-3851-2009, 2009.

882 Park, J., Gomez, A. L., Walser, M. L., Lin, A., and Nizkorodov, S. A.: Ozonolysis and
883 photolysis of alkene-terminated self-assembled monolayers on quartz nanoparticles:
884 implications for photochemical aging of organic aerosol particles, Physical Chemistry
885 Chemical Physics, 8, 2506-2512, 10.1039/b602704k, 2006.

886 Paulot, F., Wunch, D., Crouse, J. D., Toon, G. C., Millet, D. B., DeCarlo, P. F.,
887 Vigouroux, C., Deutscher, N. M., Abad, G. G., Notholt, J., Warneke, T., Hannigan, J. W.,
888 Warneke, C., de Gouw, J. A., Dunlea, E. J., De Maziere, M., Griffith, D. W. T., Bernath,
889 P., Jimenez, J. L., and Wennberg, P. O.: Importance of secondary sources in the

890 atmospheric budgets of formic and acetic acids, *Atmos. Chem. Phys.*, 11, 1989-2013,
891 10.5194/acp-11-1989-2011, 2011.

892 Seco, R., Penuelas, J., and Filella, I.: Short-chain oxygenated VOCs: Emission and uptake
893 by plants and atmospheric sources, sinks, and concentrations, *Atmospheric Environment*,
894 41, 2477-2499, 10.1016/j.atmosenv.2006.11.029, 2007.

895 Sindelarova, K., Granier, C., Bouarar, I., Guenther, A., Tilmes, S., Stavrakou, T., Muller,
896 J. F., Kuhn, U., Stefani, P., and Knorr, W.: Global data set of biogenic VOC emissions
897 calculated by the MEGAN model over the last 30 years, *Atmos. Chem. Phys.*, 14, 9317-
898 9341, 10.5194/acp-14-9317-2014, 2014.

899 Singh, H., Chen, Y., Tabazadeh, A., Fukui, Y., Bey, I., Yantosca, R., Jacob, D., Arnold,
900 F., Wohlfrom, K., Atlas, E., Flocke, F., Blake, D., Blake, N., Heikes, B., Snow, J., Talbot,
901 R., Gregory, G., Sachse, G., Vay, S., and Kondo, Y.: Distribution and fate of selected
902 oxygenated organic species in the troposphere and lower stratosphere over the Atlantic,
903 *Journal of Geophysical Research-Atmospheres*, 105, 3795-3805, 10.1029/1999jd900779,
904 2000.

905 Slusher, D. L., Pitteri, S. J., Haman, B. J., Tanner, D. J., and Huey, L. G.: A chemical
906 ionization technique for measurement of pernitric acid in the upper troposphere and the
907 polar boundary layer, *Geophys. Res. Lett.*, 28, 3875-3878, 10.1029/2001gl013443, 2001.

908 Slusher, D. L., Huey, L. G., Tanner, D. J., Chen, G., Davis, D. D., Buhr, M., Nowak, J. B.,
909 Eisele, F. L., Kosciuch, E., Mauldin, R. L., Lefer, B. L., Shetter, R. E., and Dibb, J. E.:
910 Measurements of pernitric acid at the South Pole during ISCAT 2000, *Geophys. Res. Lett.*,
911 29, 10.1029/2002gl015703, 2002.

912 Sorooshian, A., Ng, N. L., Chan, A. W. H., Feingold, G., Flagan, R. C., and Seinfeld, J.
913 H.: Particulate organic acids and overall water-soluble aerosol composition measurements
914 from the 2006 Gulf of Mexico Atmospheric Composition and Climate Study (GoMACCS),
915 *Journal of Geophysical Research-Atmospheres*, 112, 16, 10.1029/2007jd008537, 2007.

916 Sorooshian, A., Murphy, S. M., Hersey, S., Bahreini, R., Jonsson, H., Flagan, R. C., and
917 Seinfeld, J. H.: Constraining the contribution of organic acids and AMS m/z 44 to the
918 organic aerosol budget: On the importance of meteorology, aerosol hygroscopicity, and
919 region, *Geophys. Res. Lett.*, 37, 5, 10.1029/2010gl044951, 2010.

920 Souza, S. R., and Carvalho, L. R. F.: Seasonality influence in the distribution of formic and
921 acetic acids in the urban atmosphere of Sao Paulo City, Brazil, *Journal of the Brazilian
922 Chemical Society*, 12, 755-762, 2001.

923 Spaulding, R. S., Talbot, R. W., and Charles, M. J.: Optimization of a mist chamber (cofer
924 scrubber) for sampling water-soluble organics in air, *Environmental Science &
925 Technology*, 36, 1798-1808, 10.1021/es011189x, 2002.

926 Talbot, R. W., Beecher, K. M., Harriss, R. C., and Cofer, W. R.: Atmospheric
927 Geochemistry of Formic and Acetic Acids at a Mid-latitude Temperate Site, *Journal of
928 Geophysical Research-Atmospheres*, 93, 1638-1652, 10.1029/JD093iD02p01638, 1988.

929 Talbot, R. W., Mosher, B. W., Heikes, B. G., Jacob, D. J., Munger, J. W., Daube, B. C.,
930 Keene, W. C., Maben, J. R., and Artz, R. S.: Carboxylic Acids in the Rural Continental
931 Atmosphere over the Eastern United States during the Shenandoah Cloud and
932 Photochemistry Experiment, *Journal of Geophysical Research-Atmospheres*, 100, 9335-
933 9343, 10.1029/95jd00507, 1995.

934 Talbot, R. W., Dibb, J. E., Scheuer, E. M., Blake, D. R., Blake, N. J., Gregory, G. L.,
935 Sachse, G. W., Bradshaw, J. D., Sandholm, S. T., and Singh, H. B.: Influence of biomass
936 combustion emissions on the distribution of acidic trace gases over the southern Pacific
937 basin during austral springtime, *Journal of Geophysical Research-Atmospheres*, 104, 5623-
938 5634, 10.1029/98jd00879, 1999.

939 Veres, P., Roberts, J. M., Warneke, C., Welsh-Bon, D., Zahniser, M., Herndon, S., Fall, R.,
940 and de Gouw, J.: Development of negative-ion proton-transfer chemical-ionization mass
941 spectrometry (NI-PT-CIMS) for the measurement of gas-phase organic acids in the
942 atmosphere, *Int. J. Mass Spectrom.*, 274, 48-55, 10.1016/j.ijms.2008.04.032, 2008.

943 Veres, P., Roberts, J. M., Burling, I. R., Warneke, C., de Gouw, J., and Yokelson, R. J.:
944 Measurements of gas-phase inorganic and organic acids from biomass fires by negative-
945 ion proton-transfer chemical-ionization mass spectrometry, *Journal of Geophysical*
946 *Research-Atmospheres*, 115, 10.1029/2010jd014033, 2010.

947 Veres, P. R., Roberts, J. M., Cochran, A. K., Gilman, J. B., Kuster, W. C., Holloway, J. S.,
948 Graus, M., Flynn, J., Lefer, B., Warneke, C., and de Gouw, J.: Evidence of rapid production
949 of organic acids in an urban air mass, *Geophys. Res. Lett.*, 38, 10.1029/2011gl048420,
950 2011.

951 Vlasenko, A., George, I. J., and Abbatt, J. P. D.: Formation of volatile organic compounds
952 in the heterogeneous oxidation of condensed-phase organic films by gas-phase OH, *J. Phys.*
953 *Chem. A*, 112, 1552-1560, 10.1021/jp0772979, 2008.

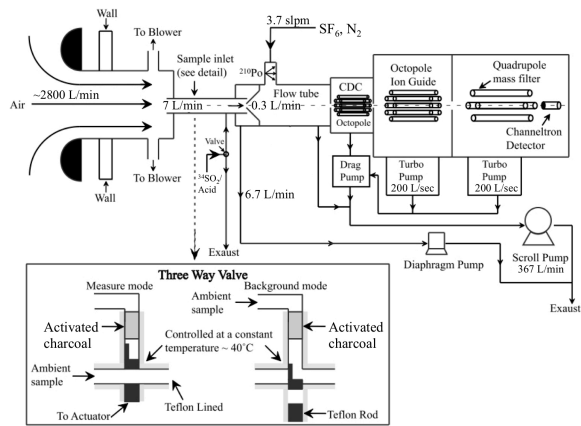
954 Walser, M. L., Park, J., Gomez, A. L., Russell, A. R., and Nizkorodov, S. A.:
955 Photochemical aging of secondary organic aerosol particles generated from the oxidation
956 of d-limonene, *J. Phys. Chem. A*, 111, 1907-1913, 10.1021/jp0662931, 2007.

957 Xu, L., Guo, H. Y., Weber, R. J., and Ng, N. L.: Chemical Characterization of Water-
958 Soluble Organic Aerosol in Contrasting Rural and Urban Environments in the Southeastern
959 United States, *Environmental Science & Technology*, 51, 78-88, 10.1021/acs.est.6b05002,
960 2017.

961 Yatavelli, R. L. N., Mohr, C., Stark, H., Day, D. A., Thompson, S. L., Lopez-Hilfiker, F.
962 D., Campuzano-Jost, P., Palm, B. B., Vogel, A. L., Hoffmann, T., Heikkinen, L., Aijala,
963 M., Ng, N. L., Kimmel, J. R., Canagaratna, M. R., Ehn, M., Junninen, H., Cubison, M. J.,
964 Petaja, T., Kulmala, M., Jayne, J. T., Worsnop, D. R., and Jimenez, J. L.: Estimating the
965 contribution of organic acids to northern hemispheric continental organic aerosol,
966 *Geophys. Res. Lett.*, 42, 6084-6090, 10.1002/2015gl064650, 2015.

967 Zhang, R. Y., Suh, I., Zhao, J., Zhang, D., Fortner, E. C., Tie, X. X., Molina, L. T., and
968 Molina, M. J.: Atmospheric new particle formation enhanced by organic acids, *Science*,
969 304, 1487-1490, 10.1126/science.1095139, 2004.

970



971

972 **Figure 1:** The CIMS instrument and inlet configuration used in the field study. The
 973 automated three-way sampling valve is shown in the inset. The figure was adapted from
 974 Liao et al. (2011).

975

976

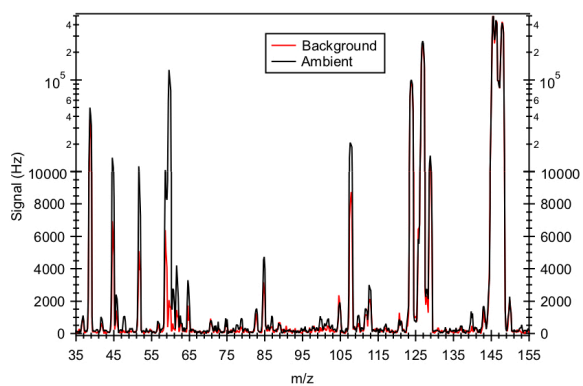
977

978

979

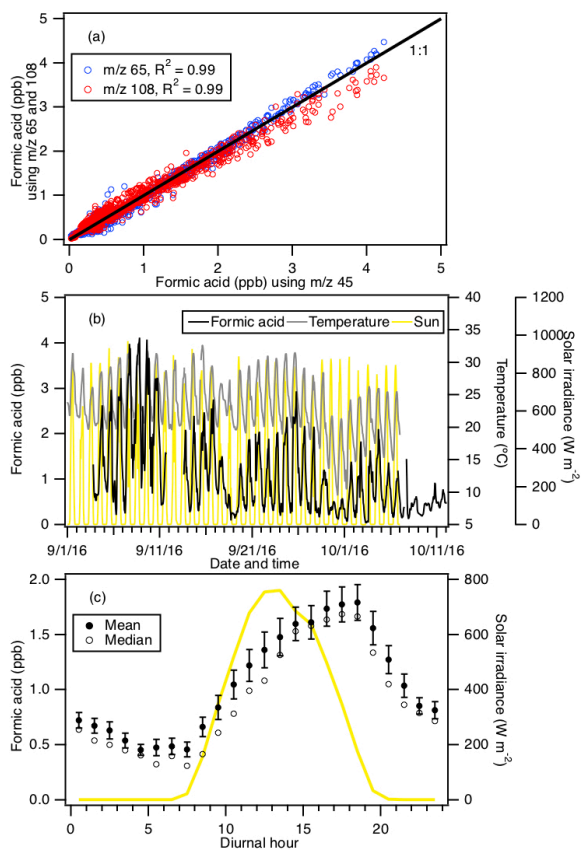
980

981



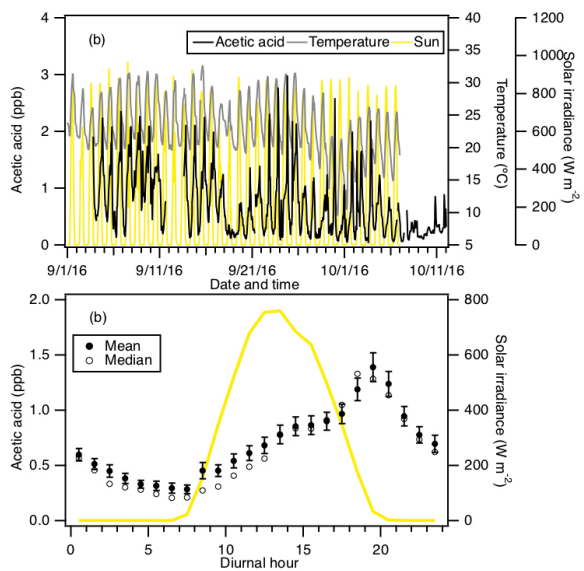
982

983 **Figure 2:** Mass spectrum of ambient air and background measured in Yorkville, Georgia
 984 on 8 Sept 2016 using SF₆⁻. Note that the ³²SF₆⁻ reagent ion signal (at m/z 146) is saturated,
 985 causing the sharp drop in its signal. As a result, the ion signal of its isotope ³⁴SF₆⁻ (at m/z
 986 150) was monitored to determine if the reaction of SF₆⁻ with ambient water vapor and O₃
 987 depleted SF₆⁻ reagent ions.



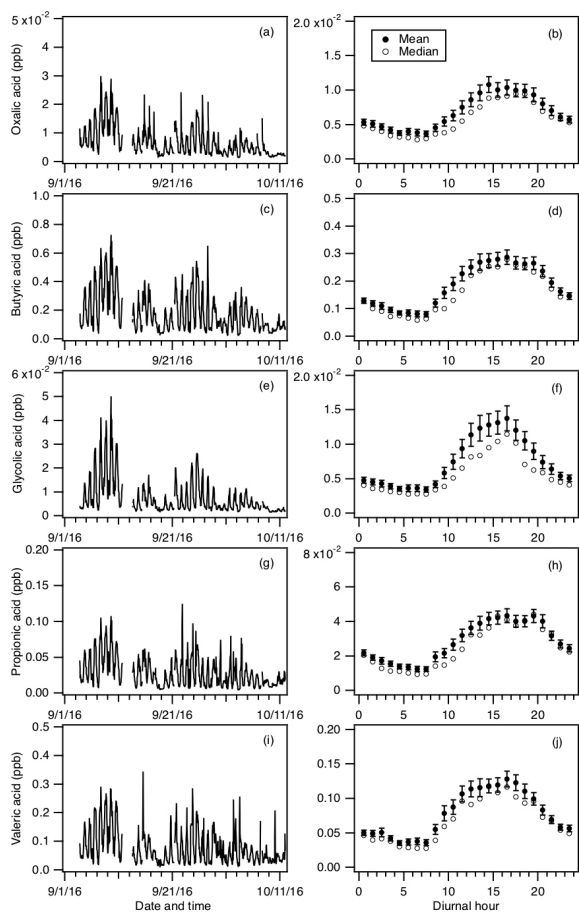
988

989 **Figure 3:** (a) Scatter plot comparison of ambient formic acid concentrations determined
 990 using mass peaks m/z 45, 65 and 108. The three datasets correlated well with one another
 991 ($R^2 = 0.99$). Linear regression of the data gave slopes of 1 (for m/z 65) and 0.95 (for m/z
 992 108), indicating that all three mass peaks can be used to determine the formic acid
 993 concentration. (b) Time series of formic acid concentration, temperature and solar
 994 irradiance. All the data are displayed as 1-hour averages. (c) Diurnal profiles of formic acid
 995 concentration (symbols) and solar irradiance (yellow line). All the concentrations represent
 996 averages in 1-hour intervals and the standard errors are plotted as error bars.



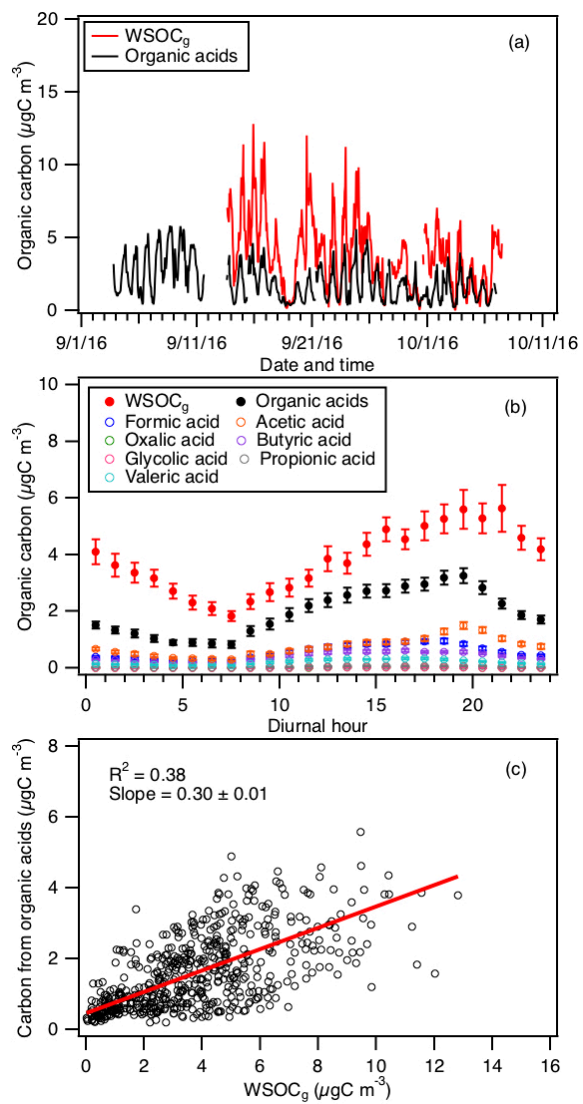
997

998 **Figure 4:** (a) Time series of acetic acid concentration, temperature and solar irradiance.
 999 All the data are displayed as 1-hour averages. (c) Diurnal profiles of acetic acid (symbols)
 1000 and solar irradiance (yellow line). All the concentrations represent averages in 1-hour
 1001 intervals and the standard errors are plotted as error bars.



1002

1003 **Figure 5:** Time series of concentrations of (a) oxalic, (c) butyric, (e) glycolic, (g) propionic,
 1004 and (i) valeric acids measured during the field study. All the data are displayed as 1-hour
 1005 averages. Their corresponding diurnal profiles are shown in (b), (d), (f), (h) and (j),
 1006 respectively. The diurnal profile concentrations represent averages in 1-hour intervals and
 1007 the standard errors are plotted as error bars.



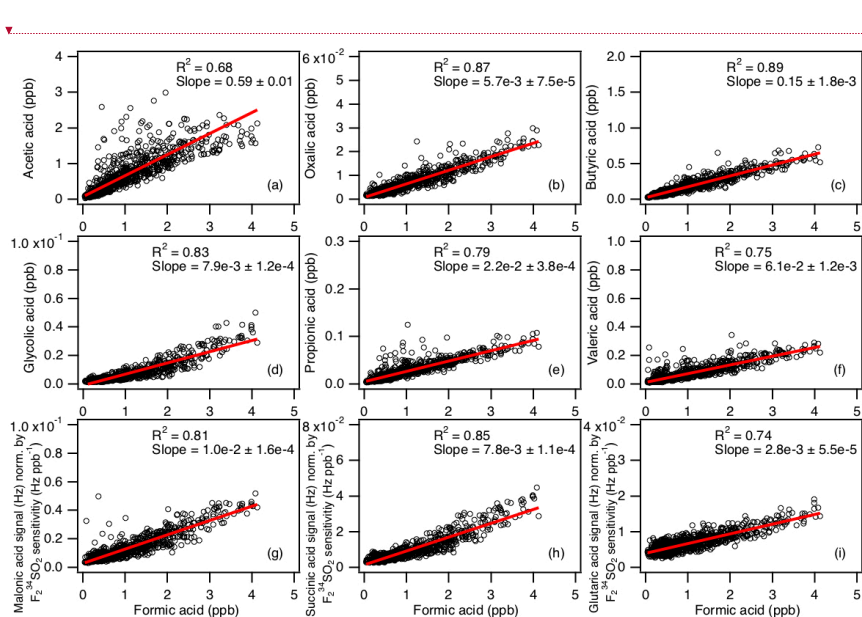
1008

1009 **Figure 6:** (a) Time series of WSOC_g and the total organic carbon contributed by the
 1010 measured organic acids. All the data are displayed as 1-hour averages. (b) Diurnal profiles
 1011 of WSOC_g and the total organic carbon contributed by the measured organic acids. Also
 1012 shown are the diurnal profiles of the organic carbon contributed by the individual measured

Deleted: (i.e., formic, acetic, oxalic, butyric, glycolic, propionic and valeric acids)

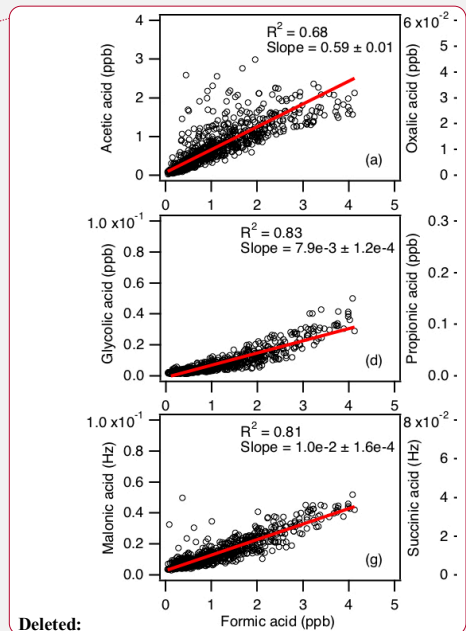
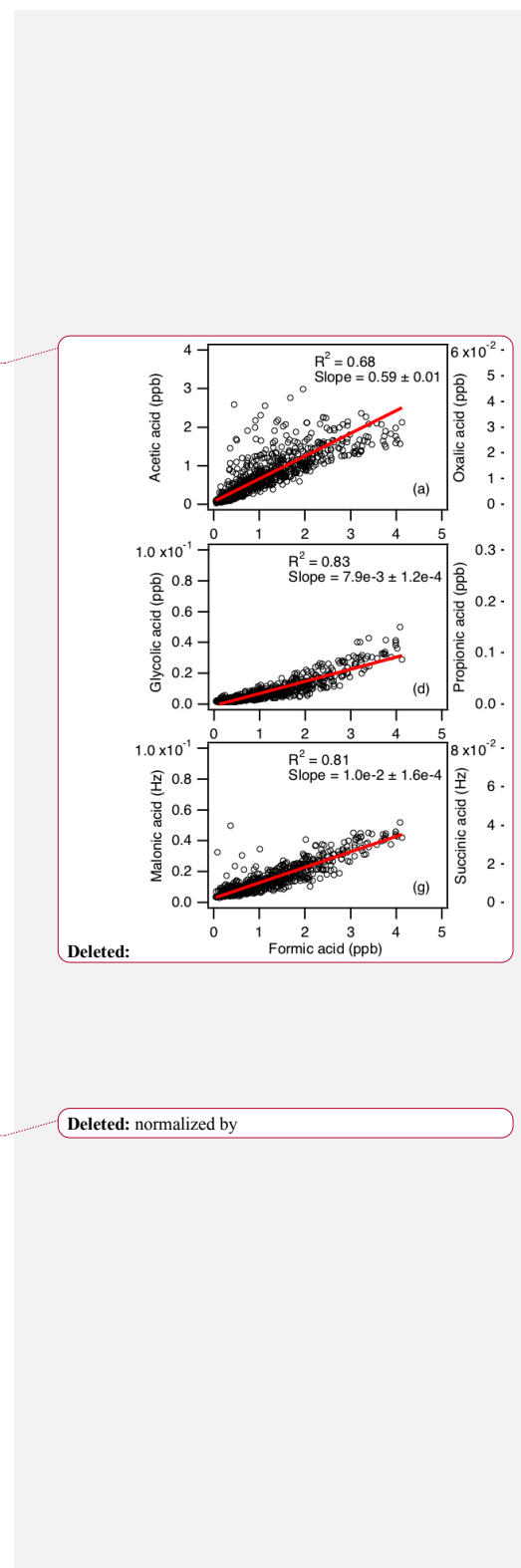
1015 organic acids. All the concentrations represent the mean hourly averages and the standard
 1016 errors are plotted as error bars. (c) Scatter plot of total organic carbon contributed by the
 1017 measured organic acids with WSOC_g. *Note that the ion peak assignment to some of these*
 1018 *organic acids are speculative.*

1019



1020

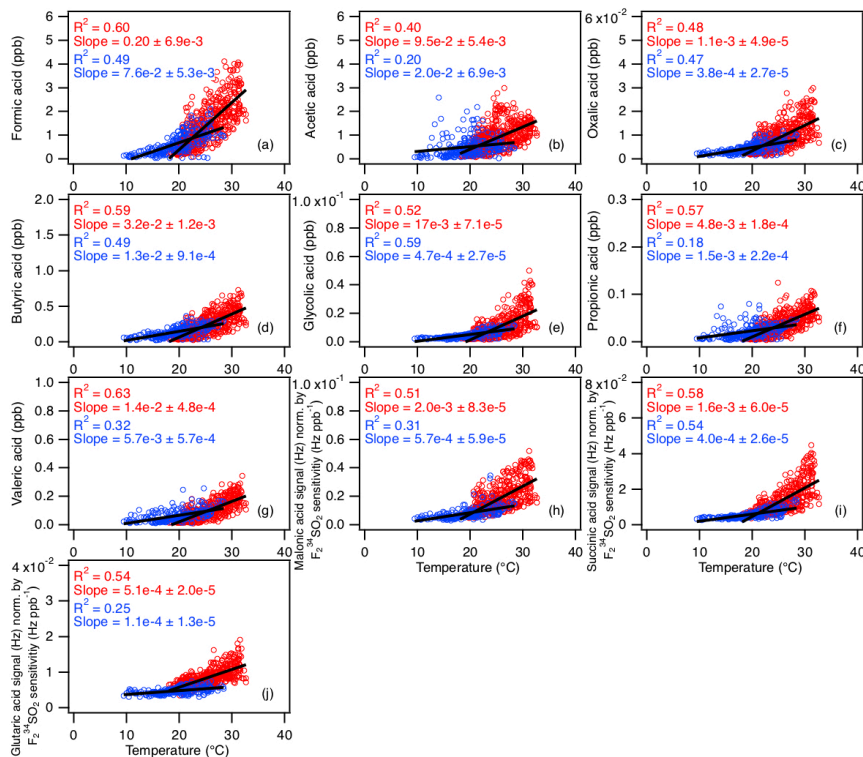
1021 **Figure 7:** Scatter plots of concentrations (or signals) of (a) acetic, (b) oxalic, (c) butyric,
 1022 (d) glycolic, (e) propionic, (f) valeric, (g) malonic, (h) succinic, and (i) glutaric acids with
 1023 formic acid concentration. All the data are displayed as 1-hour averages. The data for
 1024 malonic, succinic and glutaric acids are presented as *the ratio of their ion signals (Hz) to*
 1025 *the instrument's sensitivity to F₂³⁴SO₂ (Hz ppb⁻¹)* since these organic acids were not
 1026 calibrated. Red lines shown are linear fits to the data.



Deleted:

Deleted: normalized by

1029

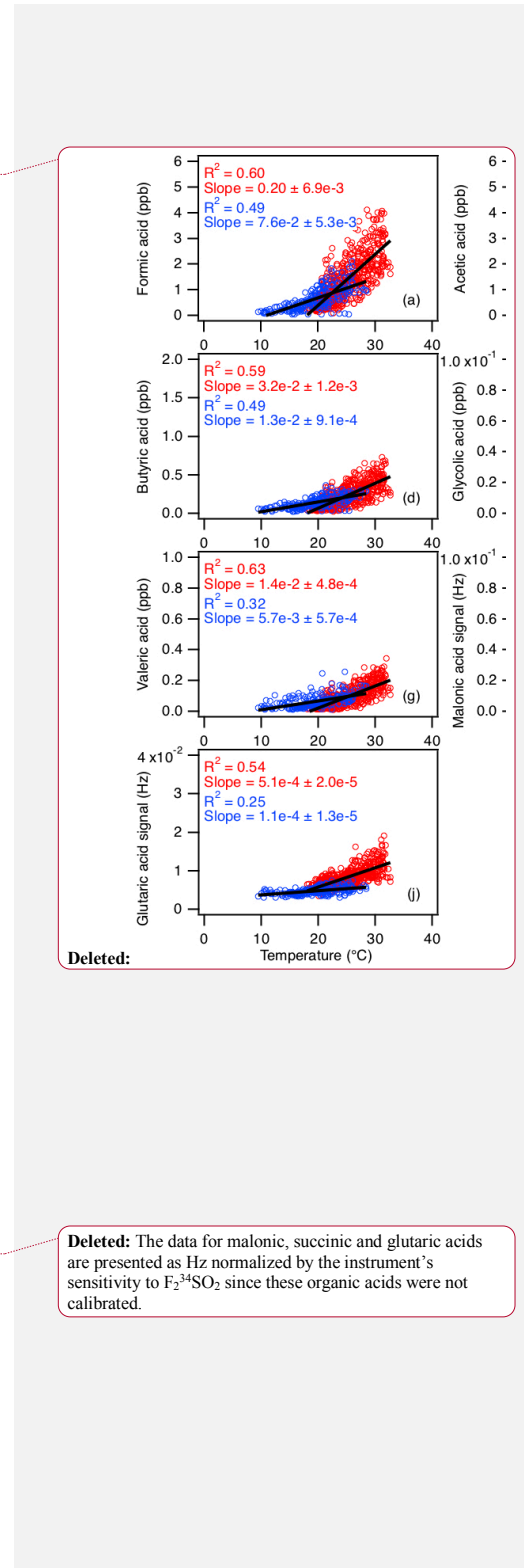


1030

1031 **Figure 8:** Scatter plots of concentrations (or signals) of (a) formic, (b) acetic, (c) oxalic,
 1032 (d) butyric, (e) glycolic, (f) propionic, (g) valeric, (h) malonic, (i) succinic, and (j) glutaric
 1033 acids with ambient temperature. The red symbols are data collected from 3 to 27 Sept,
 1034 while the blue symbols are data collected from 28 Sept onwards. All the data are displayed
 1035 as 1-hour averages. The data for malonic, succinic and glutaric acids are presented as the
 1036 ratio of their ion signals (Hz) to the instrument's sensitivity to $F_2^{34}SO_2$ (Hz ppb⁻¹) since
 1037 these organic acids were not calibrated. Black lines shown are linear fits to the datasets.

1038

1039



1045 **Table 1:** Summary of organic acids of interest, their detection limits and sensitivities of
 1046 their X⁻ and X⁻•HF ions^a

Organic Acid	Detection limit (ppt) ^b	Sensitivity (Hz ppt ⁻¹)	
		X ⁻	X ⁻ •HF
Formic acid	30	1.29 ± 0.22	0.29 ± 0.05
Acetic acid	60	1.46 ± 0.29	0.30 ± 0.06
Oxalic acid	1	6.38 ± 0.32	0.97 ± 0.05
Butyric acid	30	0.41 ± 0.01	0.12 ± 0.004
Glycolic acid	2	5.53 ± 0.11	1.64 ± 0.03
Propionic acid	6	2.05 ± 0.02	1.26 ± 0.01
Valeric acid	10	0.76 ± 0.008	0.35 ± 0.004

1047 ^aOnly organic acids with calibration measurements are shown.

1048 ^bDetection limits are approximated from 3 times the standard deviation values (3σ) of the
 1049 ion signals measured during background mode. Shown here are the average detection limits
 1050 of the organic acids for 2.5 min averaging periods which corresponds to the length of a
 1051 background measurement at a 4% duty cycle for each mass.

- Deleted: relative to the F₂³⁴SO₂⁻ ion
- Deleted: °
- Deleted: 0.44
- Deleted: 0.10
- Deleted: 0.50
- Deleted: 0.10
- Deleted: 2.18
- Deleted: 0.33
- Deleted: 0.14
- Deleted: 0.04
- Deleted: 1.89
- Deleted: 0.56
- Deleted: 0.70
- Deleted: 0.43
- Deleted: 0.26
- Deleted: 0.12
- Deleted: integration
- Deleted: 0.04
- Deleted: s
- Deleted: ¶
- Study-averaged sensitivity of the F₂³⁴SO₂⁻ ion = 2928 ± 669 Hz ppb⁻¹

1 **Supplementary Information:**

2 **Real-time measurements of gas-phase organic acids using SF₆⁻ chemical ionization**
3 **mass spectrometry**

4

5 Theodora Nah,¹ Yi Ji,^{1,2} David J. Tanner,¹ Hongyu Guo,¹ Amy P. Sullivan,³ Nga Lee Ng,^{1,2}
6 Rodney J. Weber¹ and L. Gregory Huey^{1*}

7

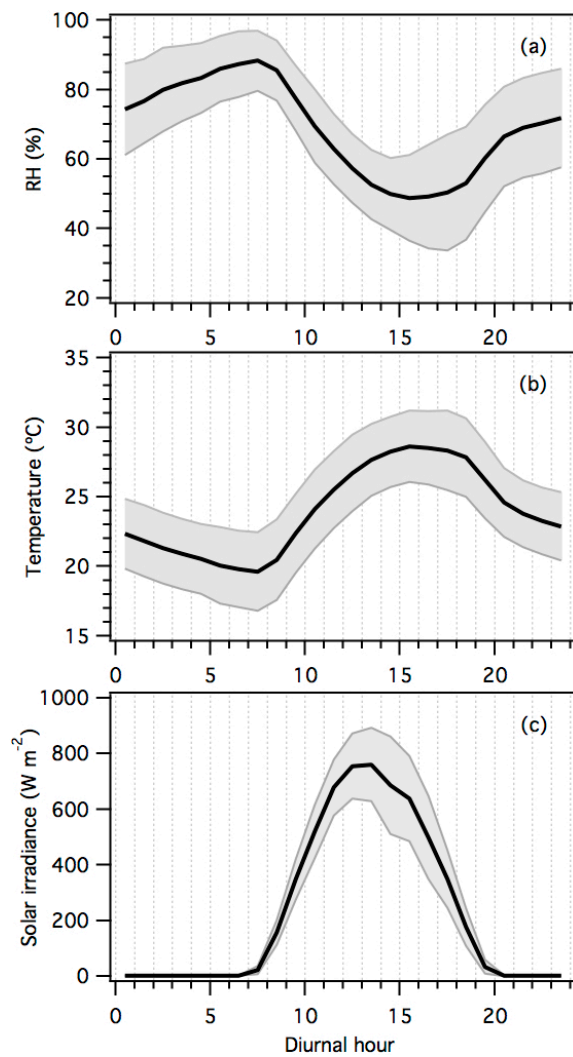
8 ¹*School of Earth and Atmospheric Sciences, Georgia Institute of Technology, Atlanta, GA, USA*

9 ²*School of Chemical and Biomolecular Engineering, Georgia Institute of Technology, Atlanta, GA, USA*

10 ³*Department of Atmospheric Science, Colorado State University, Fort Collins, CO, USA*

11

12 * *To whom correspondence should be addressed: greg.huey@eas.gatech.edu*

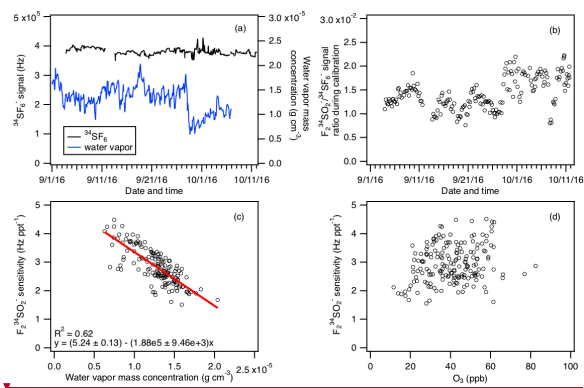


13

14 **Figure S1:** Diurnal trends of (a) relative humidity, (b) temperature, and (c) solar radiance.

15 The lines within the shaded area represents the average values. The upper and lower

16 boundaries of the shaded areas mark one standard deviation.



17

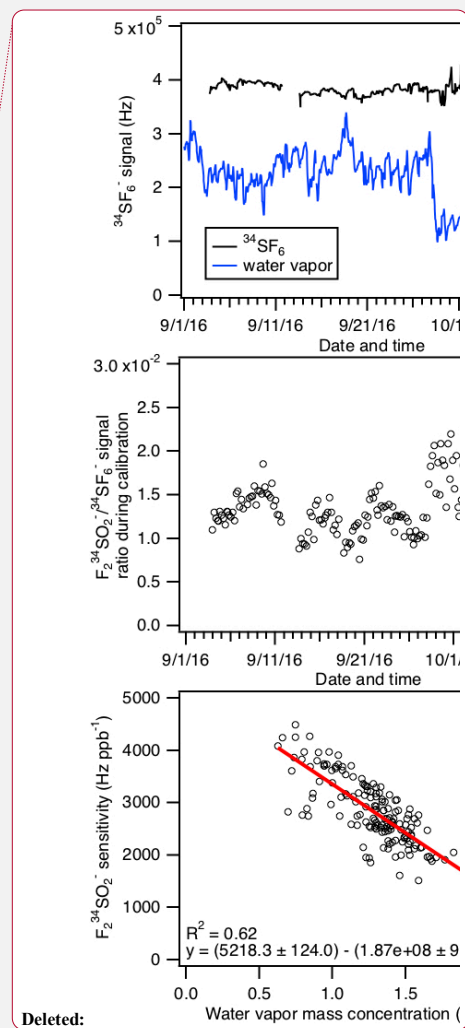
18 **Figure S2:** (a) Time series of $^{34}\text{SF}_6^-$ reagent ion signal and ambient water vapor
 19 concentration for the entire field study. The ambient water vapor mass concentrations are
 20 determined from ambient relative humidities and temperatures. (b) Time series of $\text{F}_2^{34}\text{SO}_2^-$
 21 $/^{34}\text{SF}_6^-$ ion signal ratio obtained during calibration measurements. **Panels (c) and (d) show**
 22 **the $\text{F}_2^{34}\text{SO}_2^-$ ion sensitivity obtained from calibration measurements as a function of**
 23 **ambient water vapor and O_3 concentrations.** Data in panels (a) to (d) are displayed as 1-
 24 hour averages.

25

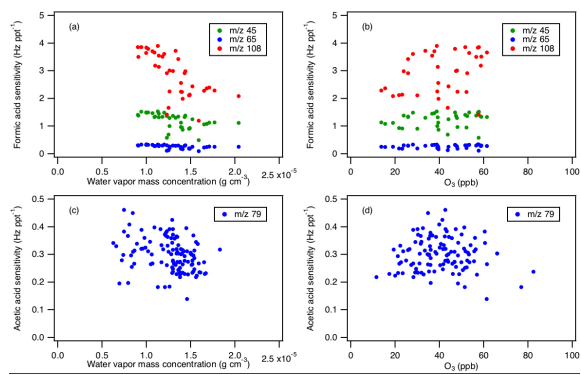
26

27

28



Deleted:



30

31 **Figure S3:** Panels (a) and (b) show the sensitivities of formic acid ions (HCOO^- at m/z 45,
 32 $\text{HCOO}\cdot\text{HF}$ at m/z 65, and SF_4^- at m/z 108) obtained from calibration measurements as a
 33 function of ambient water vapor and O_3 concentrations. Panels (c) and (d) show the acetic
 34 acid sensitivity ($\text{CH}_3\text{COO}\cdot\text{HF}$ at m/z 79) obtained from calibration measurements as a
 35 function of ambient water vapor and O_3 concentrations.

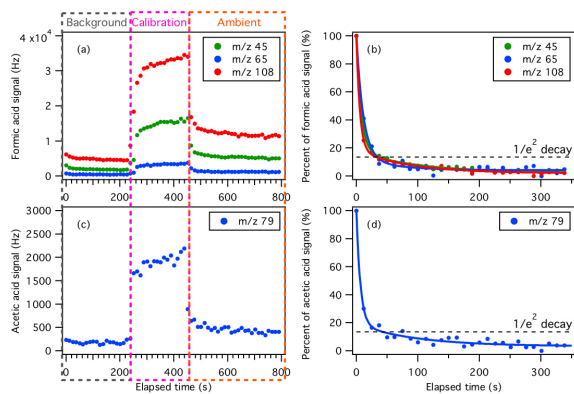
36

37

38

39

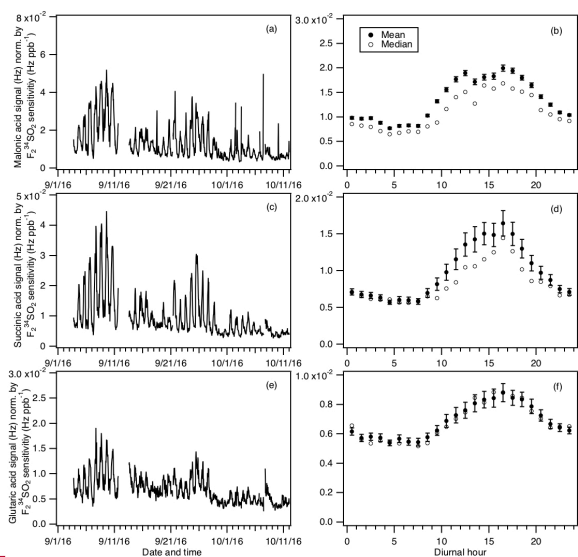
40



41

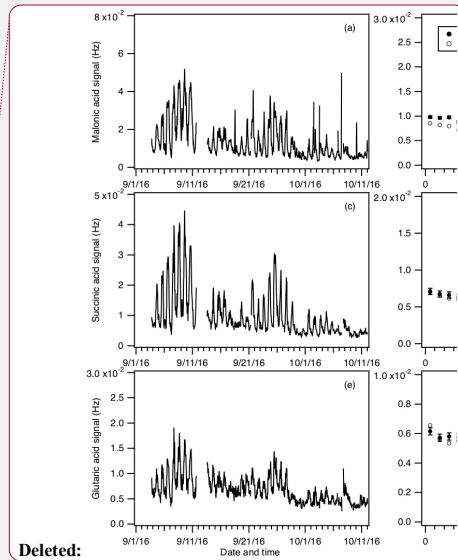
42 **Figure S4:** Example of the CIMS instrument response during switches between
 43 background, calibration and ambient measurements of (a) formic, and (c) acetic acids.
 44 Panels (b) and (d) show the percent of formic and acetic acid ion signals after the removal
 45 of a 6.75 ppb of formic acid and 5.87 ppb of acetic acid standard addition calibration as a
 46 function of time. The data shown here is 13 s time resolution data. Double exponential fits
 47 to each m/z ion are shown as colored solid lines. Black dashed lines show the times for the
 48 ions to decay to $1/e^2$.

49



50

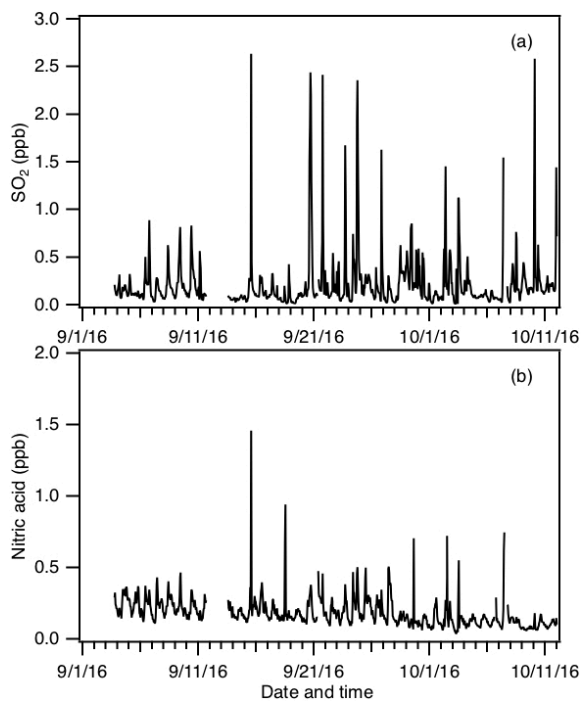
51 **Figure S5:** Time series of signals of (a) malonic, (c) succinic, and (e) glutaric acids
 52 measured during the field study. The data are displayed as 1-hour averages. Their
 53 corresponding diurnal profiles are shown in (b), (d) and (f), respectively. All the signals
 54 represent averages in 1-hour intervals and the standard errors are plotted as error bars.
 55 These organic acids were not calibrated so all the signals are presented here as Hz
 56 normalized by the instrument's sensitivity to $F_2^{34}SO_2$ ($Hz\ ppb^{-1}$), which was the primary
 57 calibrant used in the field study.



Deleted:

Deleted: S3

Deleted: ,

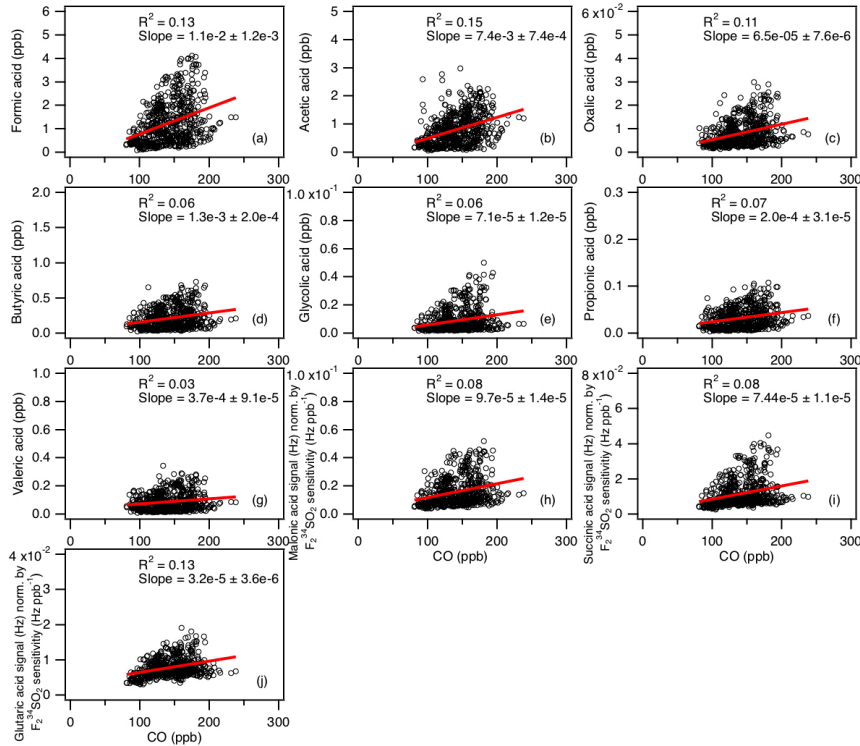


61

62 **Figure S6:** Time series of (a) SO₂ and (b) HNO₃ concentrations measured during the field
 63 study. All the data are displayed as 1-hour averages.

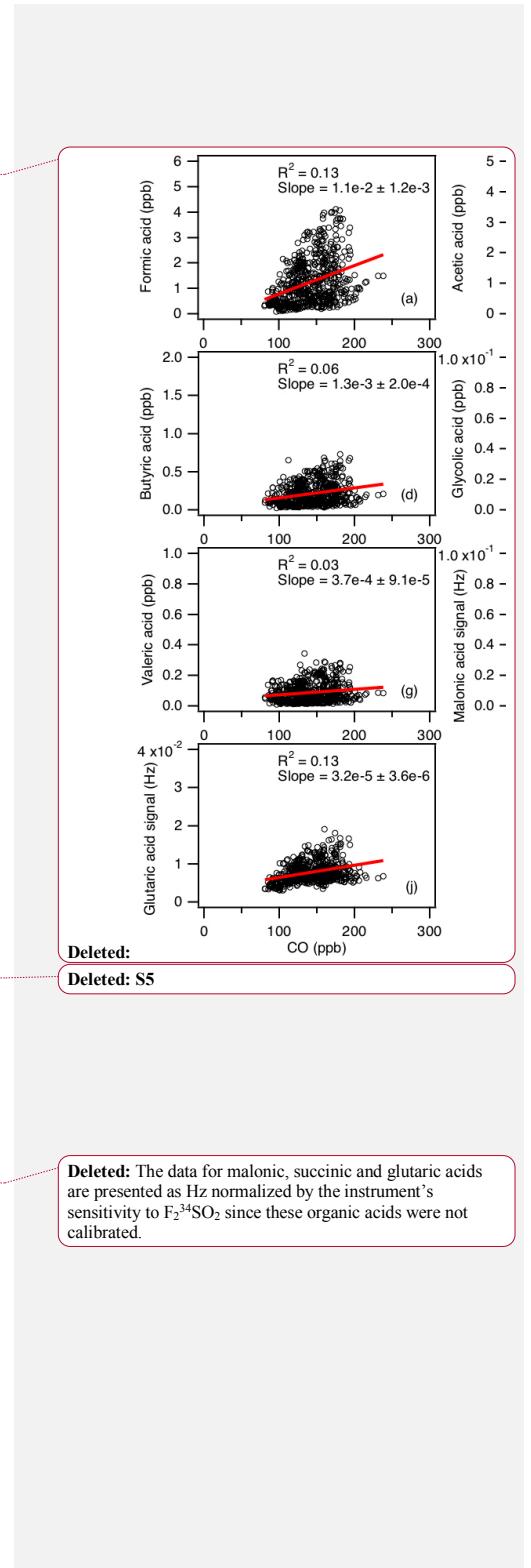
Deleted: S4

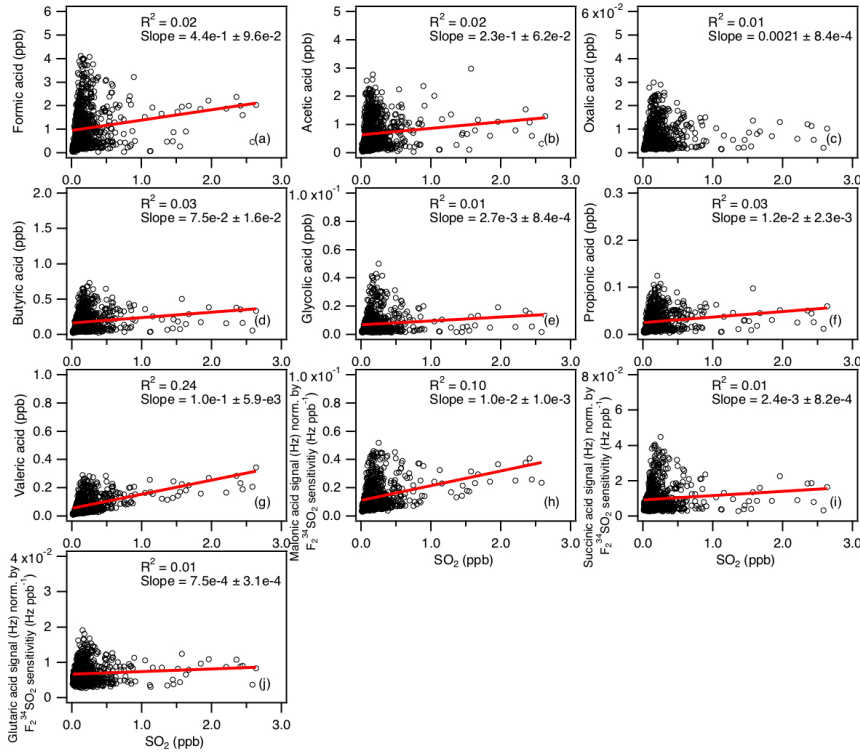
65



66

67 **Figure S7:** Scatter plots of concentrations (or signals) of (a) formic, (b) acetic, (c) oxalic,
 68 (d) butyric, (e) glycolic, (f) propionic, (g) valeric, (h) malonic, (i) succinic, and (j) glutaric
 69 acids with CO concentration. All the data are displayed as 1-hour averages. The data for
 70 malonic, succinic and glutaric acids are presented as the ratio of their ion signals (Hz)
 71 to the instrument's sensitivity to F₂³⁴SO₂ (Hz ppb⁻¹) since these organic acids were not
 72 calibrated. Red lines shown are linear fits to the data.





80

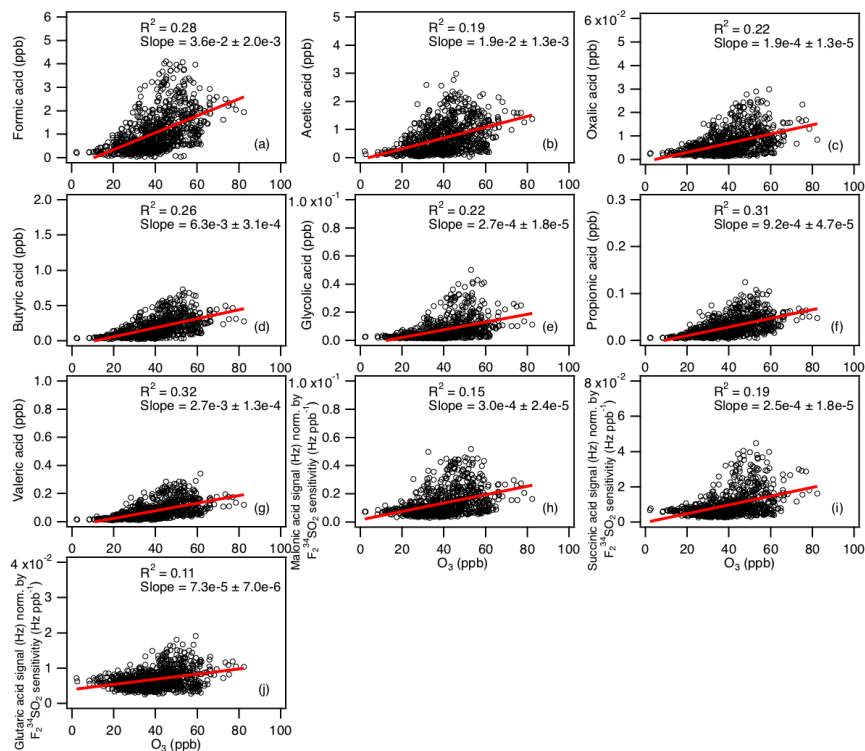
81 **Figure S8:** Scatter plots of concentrations (or signals) of (a) formic, (b) acetic, (c) oxalic,
 82 (d) butyric, (e) glycolic, (f) propionic, (g) valeric, (h) malonic, (i) succinic, and (j) glutaric
 83 acids with SO₂ concentration. All the data are displayed as 1-hour averages. The data for
 84 malonic, succinic and glutaric acids are presented as the ratio of their ion signals (Hz) to
 85 the instrument's sensitivity to F₂³⁴SO₂ (Hz ppb⁻¹) since these organic acids were not
 86 calibrated. Red lines shown are linear fits to the data.

Deleted:

Deleted: S6

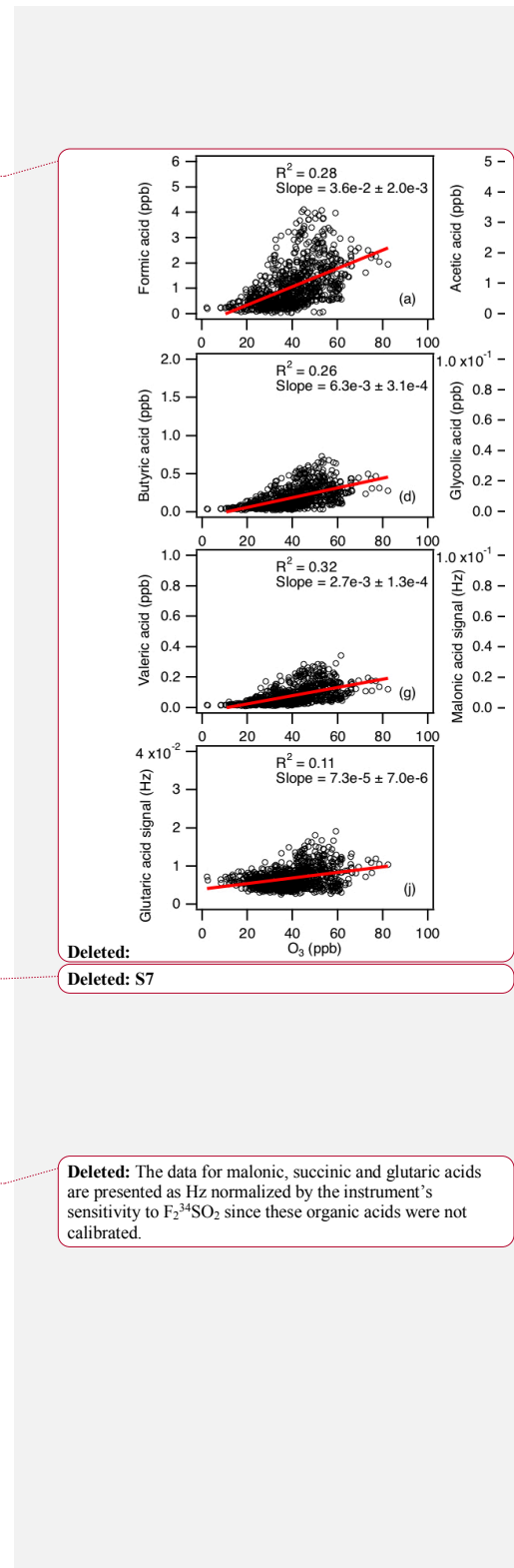
Deleted: The data for malonic, succinic and glutaric acids are presented as Hz normalized by the instrument's sensitivity to F₂³⁴SO₂ since these organic acids were not calibrated.

93



94

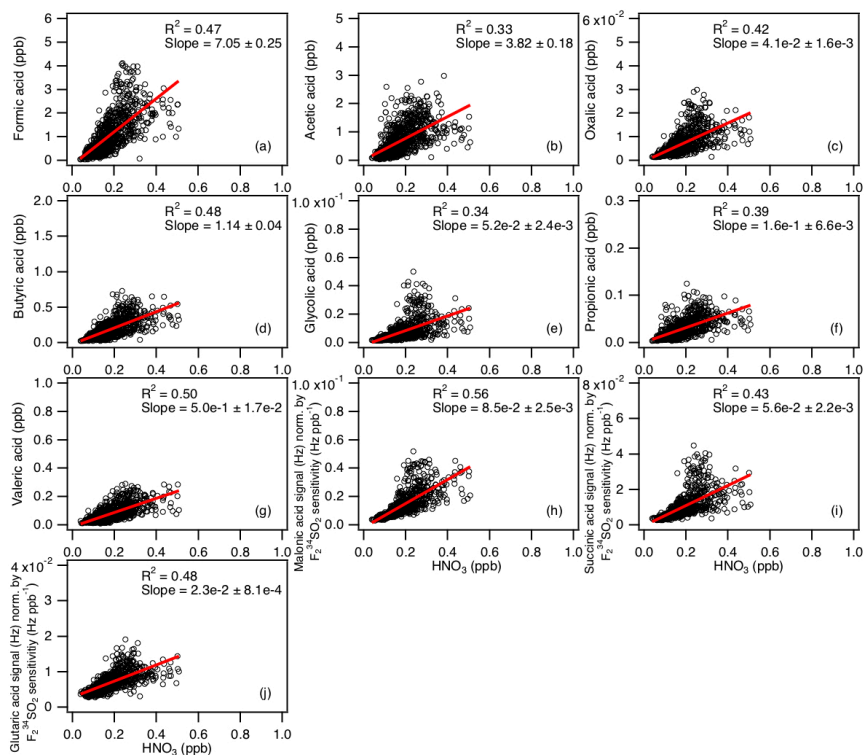
95 **Figure S9:** Scatter plots of concentrations (or signals) of (a) formic, (b) acetic, (c) oxalic,
 96 (d) butyric, (e) glycolic, (f) propionic, (g) valeric, (h) malonic, (i) succinic, and (j) glutaric
 97 acids with O₃ concentration. All the data are displayed as 1-hour averages. The data for
 98 malonic, succinic and glutaric acids are presented as the ratio of their ion signals (Hz)
 99 to the instrument's sensitivity to F₂³⁴SO₂ (Hz ppb⁻¹) since these organic acids were not
 100 calibrated. Red lines shown are linear fits to the data.



Deleted:
 Deleted: S7

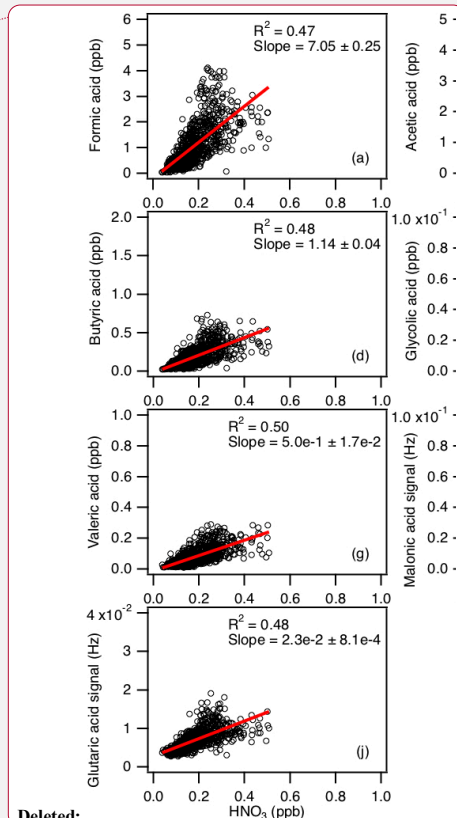
Deleted: The data for malonic, succinic and glutaric acids are presented as Hz normalized by the instrument's sensitivity to F₂³⁴SO₂ since these organic acids were not calibrated.

107



108

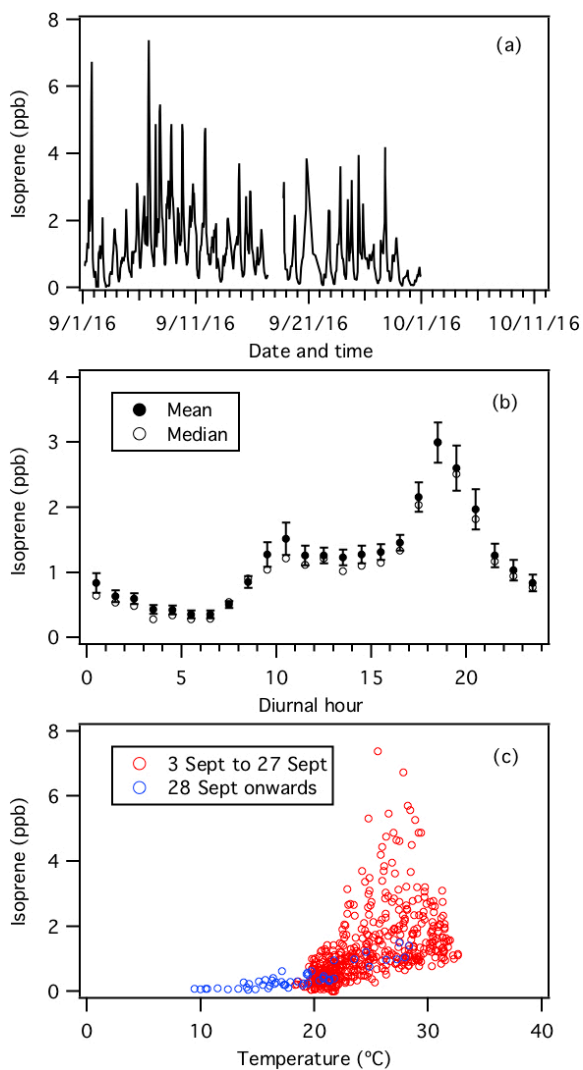
109 **Figure S10:** Scatter plots of concentrations (or signals) of (a) formic, (b) acetic, (c) oxalic,
 110 (d) butyric, (e) glycolic, (f) propionic, (g) valeric, (h) malonic, (i) succinic, and (j) glutaric
 111 acids with HNO_3 concentration. To exclude periods when the site was affected by urban or
 112 power plant emissions, data where $HNO_3 > 0.5$ ppb are excluded from these scatter plots.
 113 All the data are displayed as 1-hour averages. The data for malonic, succinic and glutaric
 114 acids are presented as the ratio of their ion signals (Hz) to the instrument's sensitivity to
 115 $F_2^{34}SO_2$ (Hz ppb⁻¹) since these organic acids were not calibrated. Red lines shown are linear
 116 fits to the data.



Deleted:

Deleted: S8

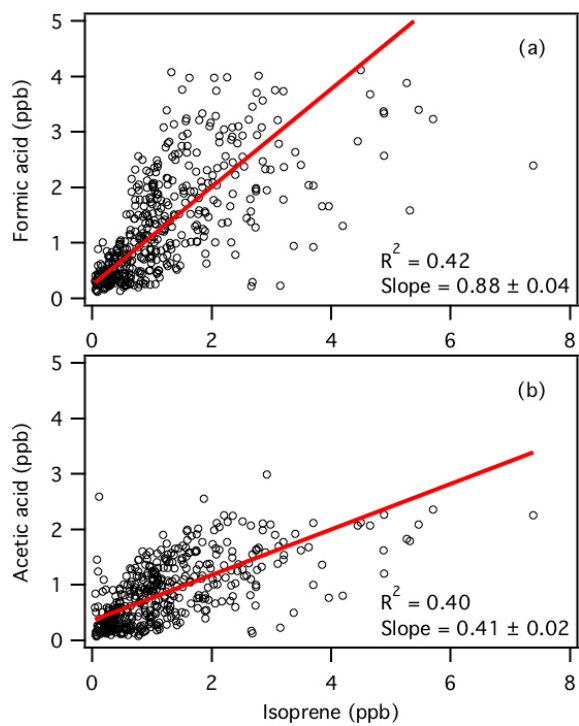
Deleted: The data for malonic, succinic and glutaric acids are presented as Hz normalized by the instrument's sensitivity to $F_2^{34}SO_2$ since these organic acids were not calibrated.



123

124 **Figure S11:** (a) Time series of isoprene concentration during the field study. (b) Diurnal
 125 profile of isoprene. All the concentrations represent averages in 1-hour intervals and the
 126 standard errors are plotted as error bars. (c) Scatter plot of isoprene concentration with
 127 ambient temperature. All the data are displayed as 1-hour averages.

Deleted: S9



129

130 **Figure S12:** Scatter plots of concentrations of (a) formic and (b) acetic acids with isoprene
131 concentration. All the data are displayed as 1-hour averages. Red lines shown are linear
132 fits to the data.

Deleted: S10